MICROSCOPIC THEORY OF FERROELASTIC PHASE TRANSITIONS IN ALKALI CYANIDES

By

Devaraj Sahu

A DISSERTATION

Submitted to
Michigan State University
in partial fulfillment of the requirements
for the degree of

DOCTOR OF PHILOSOPHY

Department of Physics

1983

ABSTRACT

MICROSCOPIC THEORY OF FERROELASTIC PHASE TRANSITIONS IN ALKALI CYANIDES

By

Devaraj Sahu

Alkali cyanides are classic examples of ionic molecular solids which show anomalous elastic and phonon softening in their high temperature pseudo-cubic phases. As the temperature is decreased, there is a critical temperature at which they order ferroelastically via a first order phase transition. In this work we have developed a microscopic theory based on a translation-rotation (TR) model, originally proposed by Michel and Naudts, to explain the above mentioned properties of both the disordered and the ordered phases.

We use Zubarev's Green's function technique and an RPA-type approximation to obtain the phonon frequencies in the disordered phase. We find important competing mechanisms in these solids which had been missed in previous works. These are (i) competition between short range repulsion and quadrupole electric field gradient contribution to TR coupling, (ii) competition between short range single site

potential and direct quadrupolar interaction, and (iii) competition between direct quadrupolar interactions and lattice mediated interactions. To explain the observed elastic properties we have to assume that the quadrupole moment of the anion in the crystal environment is considerably reduced from its free ion value. This conclusion agrees with the results of molecular dynamics simulations on orientational correlation functions in KCN. However, in contrast to molecular dynamics simulations for CsCN our calculation predicts a strong dependence of elastic properties on the quadrupole moment of the anion.

To study the ordering in the ferroelasic phase, we use a canonical transformation to eliminate the linear TR coupling and derive an effective orientational Hamiltonian. We use this Hamiltonian to obtain the free energy in terms of five orientational order parameters. We find that the form of this free energy has all the necessary third order terms to account for the first order nature of the transitions and the symmetries of the ordered phases. As a concrete example we apply our theory to CsCN. We point out the difficulties associated with explaining simultaneously the properties of both the disordered and ordered phases in terms of a single microscopic Hamiltoninan. Finally we suggest improvements which can give better results.

To My Parents

ACKNOWLEDGEMENTS

It is a great pleasure to acknowledge my debt to Dr. S.D. Mahanti for suggesting the problem in this dissertation to me and for his guidance throughout the course of this work. His intuition and meticulous attention to details have greatly contributed to my learning process. I am particularly thankful to him for allowing me to interrupt his work at my convenience and for listening patiently to my questions.

I would like to express my sincere thanks to Dr. T.A.Kaplan for his easy accessibility and for clarifying my doubts at great length and depth. I am thankful to Dr. M.F.Thorpe for allowing me to take part in his Tuesday seminars. I am quite grateful to Dr. J.S.Kovacs for his help and cordiality. My warmest thanks are also due to Dr. P.K.Misra for his constant encouragement. It is a delight to express my gratitude to Dr. Rasik H. Raythatha for his extremely friendly interaction with me and for his genuine concern for me.

I am quite grateful to Mr. Balan Chenera, an unselfish friend, but for whom my stay in East Lansing would

have been a whole lot tougher.

I would like to thank my friends in the solid state theory group, Mr. Hong Xing He, Mr. Edward J. Garboczi and Mr. J. Marshall Thomsen for their cordiality in discussing physics with me. I am grateful to Dr. R.F.Stein for letting me use his editor and printer and to Dr. J.B.Hoffer for his assistance in using the editor.

It is my greatest pleasure to thank my wife Urmila for her love, patience and understanding during my graduate studies and for bearing ungrudgingly the pains of long hours of absence from home. I would like to thank my son Ashutosh whose smiles have meant so much for our happiness. Words cannot convey my gratitude to my father Mr. Narasimha Sahu and my mother Mrs. Radha Devi for the love and support they have given me in such abundance. I would also like to thank Mrs. Joyasree (Ranoo) Mahanti for her help during my stay in East Lansing.

Finally I am grateful to Michigan State University and the National Science Foundation, through grant number DMR 81-17297, for financial assistance.

TABLE OF CONTENTS

APPENDICES

LIST OF TABLES

LIST OF FIGURES

LIST OF ABBREVIATIONS

AD	anistropic dispersion
BKM	Bounds, Klein and McDonald
BZ	Brillouin Zone
CF	crystal field
c.m.	center of mass
d	dimension
dBM	deRaedt, Binder and Michel
efg	electric field gradient
FE	ferro elastic
MD	molecular dynamics
MF	molecular field
MN	Michel and Naudts
nn	nearest neighbor
Q	quadrupole moment
R	short range repulsion
RPA	random phase approximation
s.p.	saddle point
SR	short range
T	temperature
TR	translation-rotation

CHAPTER 1

INTRODUCTION

The theory of phase transitions has been a very active area of research in recent years. Understanding the nature of phase transitions in a variety of physical systems such as fluids, magnets, superconductors, molecular solids and so forth has been quite challenging. In the study of phase transitions in these systems one can ask several interesting questions, for example: what drives the phase transitions? Is there any universal behavior in the phase transitions in spite of the diversity of the systems? What are the origins of the observed macroscopic properties? Eventhough we do not attempt to answer all these questions in this thesis, we would like to point out two main directions in which theories of phase transitions have proceeded to answer some of these questions.

The first approach has been to concentrate on the universal aspects of the phase transitions. In this approach one uses the fact that a physical system is characterized by its spatial dimensionality (D), the dimensionality of its order parameter (d), and the symmetry of its order parameter. Systems otherwise distinct, but having the same D, d and symmetry of its order parameter are said to belong to the same universality class. Such systems exhibit identical critical behavior in spite of the fact that the interactions which give rise to this behavior are entirely distinct. In particular, one can add terms to the Hamiltonian consistent with a given universality class and yet leave the critical behavior unchanged. The details of the interactions are relatively unimportant in such an approach (Fis 79, Fle 81).

On the other hand, in a different approach, one identifies the physical mechanisms that drive the phase transitions and studies the relative importance of various competing processes that contribute to the phase transitions. In particular one likes to know whether the parameters that enter the theory have a microscopic justification and if not, whether they are even plausible from a microscopic point of view. In this approach the emphasis is on the details of interactions, their sources and microscopic origin.

The work in this thesis is based on the latter approach. The motivation for pursuing such an approach is due to the fact that not much emphasis has been given in recent years to develop microscopic theories of structural phase transitions. On the other hand, phenomenological theories of structural phase transitions have been reasonably successful in explaining soft mode behavior, order-disorder transitions etc. in terms of adjustable parameters. One can ask several pertinent questions regarding such phenomenological theories. Do these theories convey any information as to the details of the interactions? Are there any competing processes on which the observed properties depend sensitively? A proper microscopic theory can address and shed light on some of these questions.

R.A.Cowley has formulated stringent criteria (Cow 81) to find out whether a theory is microscopic or not. According to Cowley a proper microscopic theory of phase transition should be able to predict parameters such as transition temperature, soft mode wave vector, the symmetry of the soft mode etc. If one has to introduce extra parameters to explain the above properties, then one should be also able to predict other properties such as phonon dispersion relation, optical reflectivity of a metal and so on. On the basis of these criteria Cowley points out that there has been little progress in so far as the microscopic theory of structural phase transitions is concerned. It is therefore clear that developing a proper microscopic theory has been a challenge to theorists. Hence we have chosen such an approach.

The outline of this thesis is as follows. In chapter 2 we summarize the experimental observations pertinent to the systems under investigation, viz. the alkali cyanides. In chapter 3 we review the earlier theoretical works in the literature that attempt to explain soft mode behavior in these systems. In chapter 4 we present our theory of phonon softening and discuss the different sources that contribute to translation-rotation (TR) coupling in these solids: short range repulsion and anisotropic electrostatic interaction. The latter has not been taken into account in previous works (except in recent molecular dynamics simulations, see Bou 81, Kle 81,82) and is shown to play a significant role in understanding the physics of these solids. In chapter 5 we present the results of our elastic and phonon softening calculations and show that the two effects mentioned above compete against each other. In chapter 6 we review an earlier theory (deR 81) which tried to explain the ferroelastic order in the cyanides in a semi-phenomenological way. We point out some of the inadequacies of this work and present our microscopic theory starting from Bogolyubov's variational principle for the free energy. As a concrete example we apply the theory to understand the ferroelastic order in CsCN. In the last chapter we summarize our results and point out some of the unresolved problems which should be taken up in a future investigation.

CHAPTER 2

SUMMARY OF EXPERIMENTAL DATA

In this chapter we summarize some of the experimental data on the alkali cyanides $M^+(CN)^-$, where M=Na,K,Rb and Cs. The high temperature (high T) solid phase in these compounds is denoted as phase I (pseudo-cubic phase) while the low T non-cubic phases are denoted as phases II and III respectively. Many of the phase transformation properties of the alkai cyanides can be traced to properties of the cyanide ion. For example, eventhough the alkali cyanides are structural kins of the alkali halides, the two families show remarkably different physical properties. In the latter, phases II and III are absent (Nor 58), while in phase I the isothermal elastic constants C_{44} and C_{11} harden with decrease of T (e.g. Figure 2.1). Over a range of T from 300K to 4K, C_{44} and C_{11} increase by 5% and 19% respectively for KCl. This is due to the fact that at low T, absence of lattice anharmonicities renders the alkali halide lattice hard. On the other hand, in alkali cyanides precisely the opposite effect happens: C_{44} and C_{11} dramatically soften (in phase I) with decrease of T. It is clear that this softening is due to the interactions of the CN^- molecular ions (Hau 73) with the lattice and with themselves. Thus it is

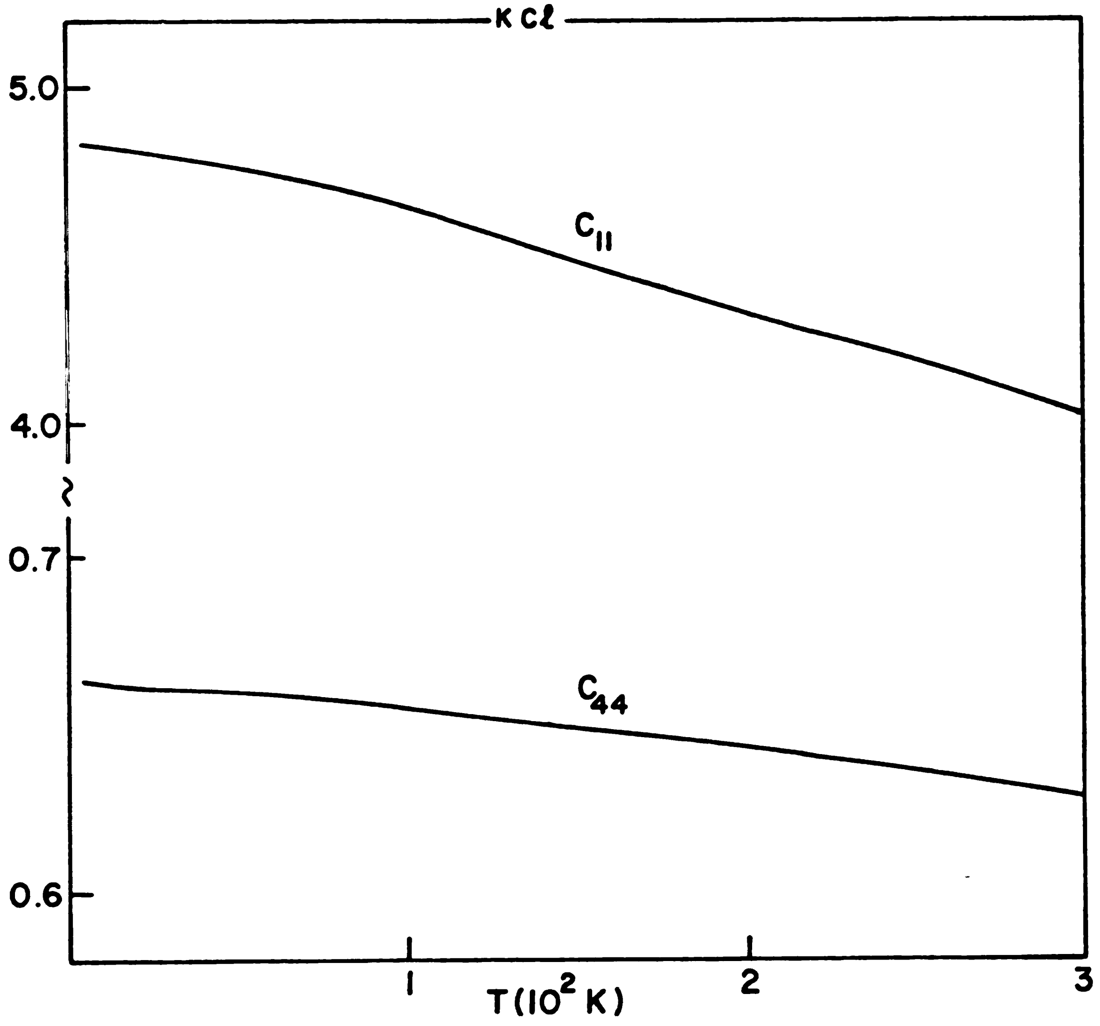

FIGURE 2.1 Elastic constants for KCl (in units of 10^{11} dyn/cm^2) see (Nor 58).

appropriate to discuss some of the properties of the CN$^-$ ion before summarizing the properties of the cyanide crystals.

(a)The Free CN$^-$ Ion

The free CN$^-$ ion has a nonspherical shape. Its properties are characterized by the following parameters (Bou 81): total charge $q_0=-e_0$ (e_0 is the charge on a proton), dipole moment $p_z=0.318$ Debye, quadrupole moment $Q_0=-4.51$ Debye×Å. Taking a typical lattice distance r, the energy scale of the direct dipole-dipole (d-d) interaction $E_{dd}=p^2/r^3\simeq10K$ while the energy scale of direct quadrupole-quadrupole (Q-Q) interaction is ten times larger i.e. $E_{QQ}=Q^2/r^5\simeq100K$. Thus to a first approximation Q-Q interactions dominate over d-d interactions. The two nuclear centers of the molecule are separated by a distance of 2d=1.19Å. Bound et al. (Bou 81, also referred to as BKM) have assumed a dumbbell model of the CN$^-$ ion for their molecular dynamics (MD) calculations with the following charge distribution: $q_N=-1.28e_0$, $q_C=-1.37e_0, q_{c.m.}=1.65e_0$. Recently LeSar and Gordon (LeS 82) have constucted a seven charge model of the anion which takes into account the higher multipole moments of the anion. Another quantity of interest is the rotational frequency of the free CN$^-$

molecule: τ_0^{-1}=3x10^{10} 1/sec (Lut 81,83). In phase II of the solid, imaginary part of the dielectric response measurements (Lut 81) show that $\tau^{-1}(T)$=a.exp(-b/kT)<τ_0^{-1}, whereas in phase I, $\tau^{-1}(T) \approx \tau_0^{-1}$. This suggests that in phase I the CN^- ions undergo quick molecular reorientations whereas in the ferroelastically ordered phase, the reorientation rate is thermally activated.

(b) Crystal Structure and Orientational Probability in the Disordered Phase

In phase I the alkali cyanides have pseudo-cubic structure (see Figures 2.2 and 2.3). Powder X-ray diffraction measurements (Ver 38, Bij 40) show that NaCN, KCN and RbCN have NaCl-type structure whereas CsCN has CsCl-type structure (Lel 42). In this phase the CN^- ions are randomly oriented so that the crystal symmetry is effectively cubic. However the probabilities of orientations are not the same for all directions and they change with T. Single crystal neutron scattering data (Row 75) in NaCN and KCN suggest that the CN^- orientation probability is large along (111) and (100) directions. We have made plots of the T-independent single site steric potential $V_0(\mathbf{n})$ to find out the maximum and the minimum of the potentials, on the basis of a simple Born-Mayer form of the potential. For KCN (e.g.

Figure 2.4) it is found that the orientation probability, $P \simeq \exp[-\beta V^0(n)]$ is a maximum for the eight (111) directions, minimum for the six (100) directions and saddle points (s.p.) for the twelve (110) directions. The discrepancy between experiment and theory as regards the orientational probability distribution could be due to the fact that experimentally it is hard to isolate the single site effects, whereas the theoretical plot is a plot of the single site potential. In contrast, for CsCN (e.g. Figure 2.5) the maxima and minima are along (100) and (111) respectively whereas (110) is still the saddle point. The form of the single site potential plays a very important role in determining the bare orientational susceptibilities in the paraelastic phase. In the lowest order, there are five such susceptibilities for the pseudo-cubic phase, two of which have E_g symmetry (for example $<(3\cos^2\theta-1)^2>$), and the rest have T_{2g} symmetry (for example$<(\sin\theta\cos\phi\sin\theta\sin\phi)^2>$), where the angular brackets indicate thermal averaging with respect to the single site potential.

(c) Some Physical Properties

Single crstals of Na,K and Rb cyanides are transparent in phase I (Hau 73,77; Kon 79). As the temperature is lowered, there is a first order ferroelastic phase transition at $T=T^*$ to a non-cubic phase (phase II).

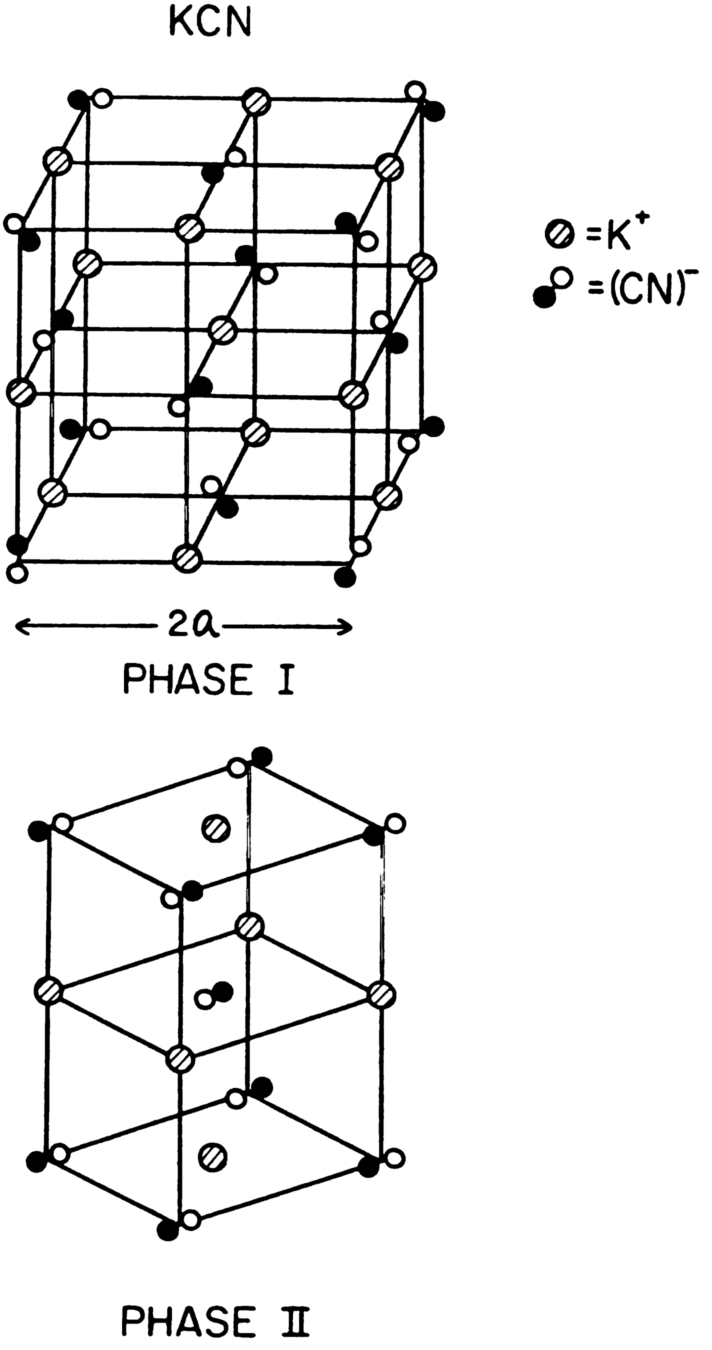

FIGURE 2.2 Crystal structure of KCN

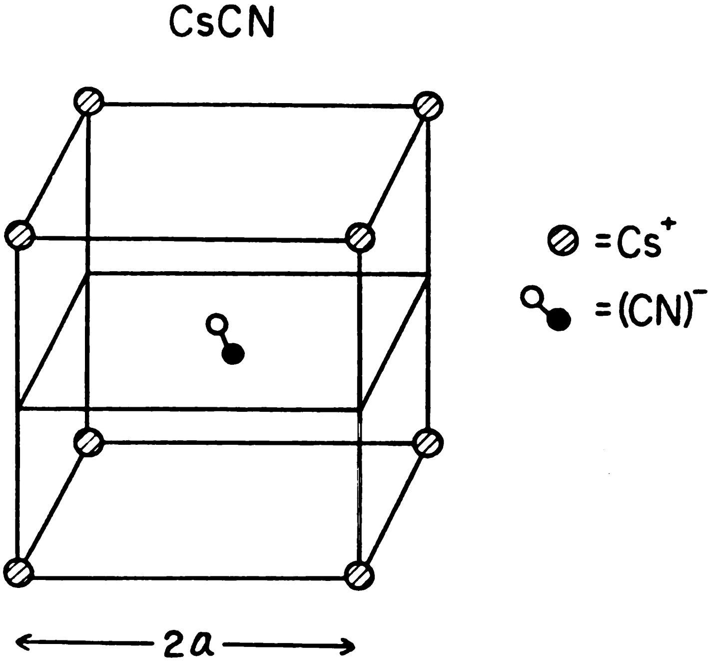

PHASE I

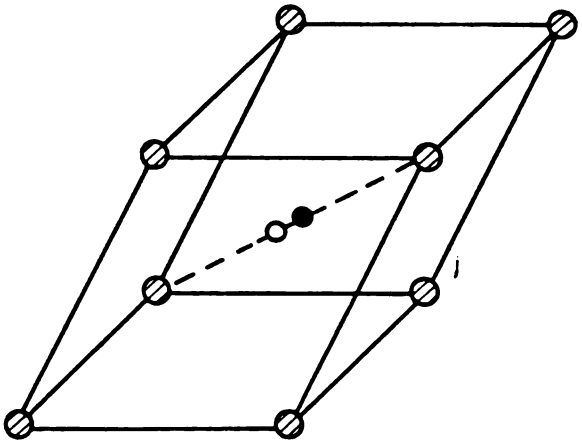

PHASE II

FIGURE 2.3 Crystal structure of CsCN

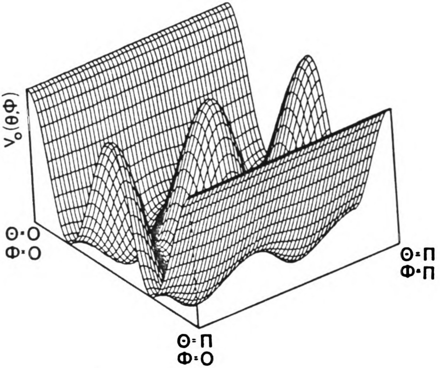

FIGURE 2.4 Single site short range repulsion potential for KCN; V_{max}=9914K, V_{min}=8350K and $V_{s.p.}$=8687K.

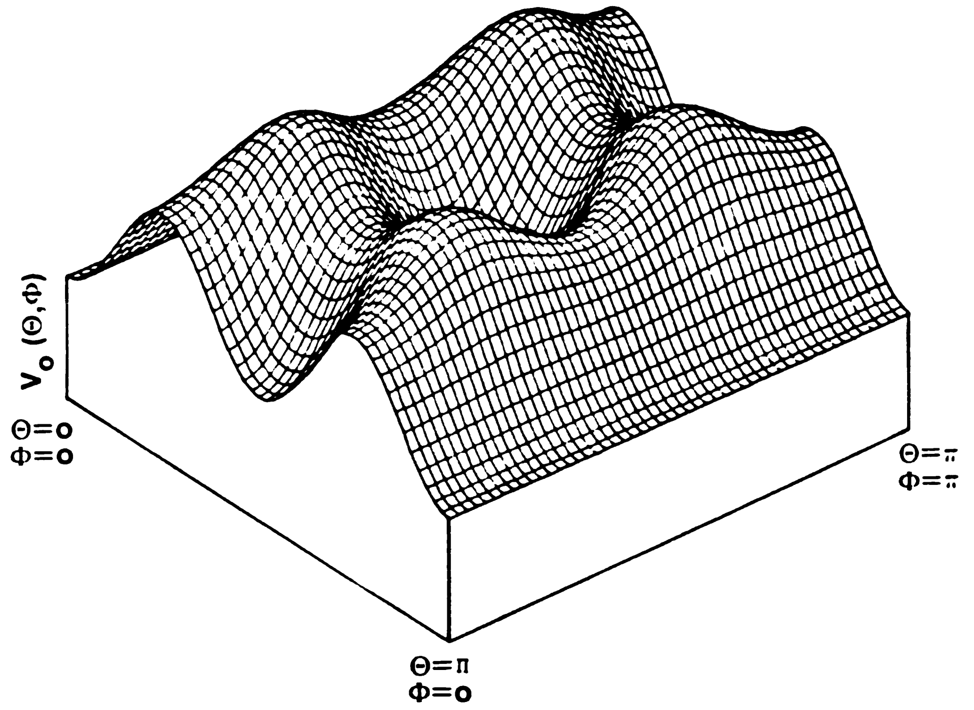

FIGURE 2.5 Single site short range repulsion potential for CsCN; V_{max}=6082K, V_{min}=5578K, $V_{s.p.}$=5919K.

In the ferroelastic (FE) phase all the CN$^-$ ions orient along some definite fixed direction in the crystal. It has been pointed out in the case of KCN (Sto 81) that there is evidence of some elastic disorder in phase II, which however averages out to zero. In the FE phase there is still a head to tail randomness of the anions, so that there is no electric dipole order. We list below some of the changes in the properties of the crystal in the I-II transition. (i) The changes in the crystal symmetry and the directions of the FE ordering of the anions are given in Table 2.1. (ii) The single crystals of phase I give rise to multiple domains upon transition to phase II. Typically the domains have a mean size of 80 microns and because of strong light scattering from the domains the crystal becomes opaque upon transition. (iii) The phase transition is first order and accompanied by changes in the configurational entropy (ΔS), the dielectric constant ($\Delta\varepsilon$) and enthalpy (ΔH) (see Table 2.2). Experimental measurement of specific heat (Lut 81) in the neighborhood of the FE phase transition indicates the existence of hysteresis effects. (iv) The most dramatic consequence of the transition is a strong pre-transitional softening of the (001) TA phonons and to a less remarkable extent that of the (001) LA phonons. Ultrasonic (Hau 73,77,79), Brillouin (Kra 79; Boi 78,80;Sat 77;Reh 77) and inelastic neutron scattering (Loi 80a,b;82) experiments show that the elastic constants C_{44} and C_{11} decrease with decrease of T. The extrapolated temperatures T_{44} and T_{11} where the respective elastic constants vanish are such that $T_{44}>T_{11}$. Since the actual transition is first order, the experimental transition temperature T^{*} is higher than the extrapolated temperature $T_c=T_{44}$ where the elasic constant C_{44} vanishes. The numerical values of the actual and the extrapolated transition temperatures are given in Table 2.2. (v) A plot of $\ln(T^{*})$ vs. the lattice constant 2a shows that $T^{*}\simeq a^{-3}$ (Lut 81). Since there is no electric dipole order in phase II, this has lead to suggest (LUt 81) that the FE ordering in phase II is due to elastic dipole interaction. (vi) Apart from the changes in the static properties, there are changes in the dynamic properties. Eventhough we will not be concerned directly with these properties, we mention two of these properties briefly. (a) In the high-T phase the Raman spectrum is liquid like and structureless, whereas in the low-T phase, the Raman spectrum shows well defined lines. In stress aligned samples in the low-T phase, there is a prominent Raman scattering peak due to the CN^- stretching vibration. (b) In the high-T phase, the dielectric response is loss free, whereas in the low-T phase there is a frequency dependent dielectric loss.

TABLE 2.1 Symmetry changes in I-II transition in alkali cyanides.

System	NaCN & KCN	RbCN	CsCN
Phase I	fcc	fcc	sc
Phase II	body-centerd orthorhombic	monoclinic	trigonal
FE order	(110) dir of phase I	(111)	(111)
Reference	Kon 79	Kon 79	deR 81

In addition to phases I and II, there is a phase III which is realised in some systems as the temperature is further lowered. In this phase there is evidence for electric dipole ordering (Lut 81). In NaCN and KCN this ordering is antiferroelectric in nature while in RbCN the

TABLE 2.2 Transition temperatures,entropy,enthalpy, and dielectric constant changes in I-II transition in alkali cyanides.

System	NaCN	KCN	RbCN	CsCN
T_c(K)	255.4	156	130	150
T^*(K)	288	168	132	193
ΔS(erg/K/mole)	Rln4	Rln2.7	Rln2	Rln3.7
ΔH(cal/mol)	783.7	339	177	461
$\Delta\varepsilon/\varepsilon$	15%	5%	3%	-
Reference	Kon 79	Kon 79	Kon 79	deR 81, Sug 68

electric ordering is perhaps that of a dipolar glass. In CsCN on the otherhand, no electric ordering has been reported upto 14K. In this work we shall not be concerned with the low-T electrically ordered phases of the alkali cyanides.

CHAPTER 3

REVIEW OF EARLIER THEORIES OF ELASTIC AND PHONON SOFTENING IN ALKALI CYANIDES

In this chapter we review the earlier theories on elastic and phonon softening in the alkali cyanides. The soft phonon frequencies, in which we are interested in, depend on two quantities: (a) the phonon frequencies of the bare lattice and (b) the corrections arising from the translation-rotation (TR) coupling. Since the calculation of bare phonon frequencies for ionic solids is by itself a complex problem and has been exhaustively studied (Har 79), we will not deal with such theories in the present chapter. We will only review the earlier theories which take into account the corrections to bare phonon frequencies. We categorize these theories as (a) purely phenomenological, (b) semi-phenomenological, and (c) microscopic. In a purely phenomenological theory the coupling of the lattice strains to the other degrees of freedom is written down in a form that is consistent with the symmetry of the high-T phase, but the coupling constants themselves are obtained by fitting the theory to experimental data. In a microscopic theory the coupling constants are calculated from interactions which have been obtained independently. A semi-phenomenological theory is a combination of the former and the latter. In the following we review these theories.

(a)Purely Phenomenological Theories:

(i) The phenomenology of elastic softening and coupled order- parameter dynamics was given by Courtens (Cou 76) in a work relating to succinonitrile. In this compound the molecule has an anisotropic polarizability P_i which gives rise to a polarizability-polarizability interaction of the form $(1/2)B_{ij}P_iP_j$ and a strain(ε_i)-polarizability interaction of the form $D_{ij}P_i\varepsilon_j$. In addition, the lattice has the usual harmonic strain energy terms. A canonical transformation leads to the appearance of an extra strain-strain term which in the low frequency limit leads to the renormalization of the elastic constants.

(ii) Boissier et al. (Boi 78,80) explain the elastic softening in KCN and NaCN, the phonon line shapes, and address the question of orientational order in phase II. They expand the free energy upto second order in the orientational order parameters η_1, η_2 and η_3 (having T_{2g} symmetry). These second order terms correspond to a pseudo-spin exchange energy. They also include a linear coupling between the order parameters and the strains. For TA phonons with wave vectors along (110) direction and with polarization vector e=(001) the free energy is

$$F_1=(1/2)C_{44}{}^0(\varepsilon_5{}^2+\varepsilon_6{}^2)+g(\varepsilon_5\eta_2+\varepsilon_6\eta_3)+(1/2)(T-T_0)J(\eta_2{}^2+\eta_3{}^2)$$

where JT_0 is the pseudo-spin exchange energy and ε's are the strains. Note that $\eta_1{}^2$ has been dropped in the above equation because it does not lead to any softening. Assuming further that the spin dynamics is diffusive, Boissier et al. obtain the equations for softening of the elastic constant C_{44} and the line shapes for the corresponding phonons. For LA phonons, however, the coupling of strains can be through order parameters of E_g symmetry only (due to symmetry reasons) and these strains cannot couple directly to the order parameters of T_{2g} symmetry. But the LA phonons can couple to the squares of the order parameters of T_{2g} symmetry. This fact gives rise to the softening and line broadening of the LA phonons in the theory of Boissier et al.

This phenomenological theory of Boissier et al. gives good fits for the elastic constants and for phonon life times (in the small wave vector regime) for KCN. However it fails to explain the C_{44} softening in NaCN because for this system the experimental softening of C_{44} goes linearly with $(T-T_0)$. Moreover there is usually a wide range of values of T_0 over which C_{11} and phonon line widths could be fitted equally well. Besides, one serious drawback of the theory is that these authors neglect the fact that the strains corresponding to LA phonons can couple linearly to the order parameter of E_g symmetry.

(iii) Rehwald et al. (Reh 77) expand the free energy of phase I upto second order in terms of a different set of order parameters which are assumed to be the six discrete <110> orientations of the cyanide ions. Linear combinations of these six orientations are taken to obtain orientations of following symmetry: one of A_{1g} symmetry, two of E_g symmetry (ξ_1,ξ_2) and three of T_{2g} symmetry (η_1,η_2 and η_3). The strains ε's couple linearly to the order parameters so that

$$F_c=\beta_t(\eta_1\varepsilon_4+\eta_2\varepsilon_5+\eta_3\varepsilon_6)+\beta_e[\xi_1(\varepsilon_1+\varepsilon_2-2\varepsilon_3)+\xi_2(\varepsilon_2-\varepsilon_3)]$$

This gives rise to

$$C_{44}=C_{44}{}^0(T-T_{2_g}{}^*)/(T+T_0)$$

and

$$C=C_0(T-T_{e_g}{}^*)/(T+T_0)$$

Here T_0 is positive and the quantities $T_{2_g}{}^*$ and $T_{e_g}{}^*$ are related to the coupling strengths β_t and β_e respectively, and $C=(1/2)(C_{11}-C_{12})$.

One of the drawbacks of this theory is that in the high T phase, all orientations are possible, not just the six discrete ones chosen in the model. In fact the most probable orientation is not along <110>, but along <111>. In addition in the Landau expansion third and fourth order terms have been neglected in the works of both Boissier et al. and Rehwald et al. Since the actual transition is first order, these terms are extremely important and should be included to have a proper understanding of the first order nature of the transition.

(b) Semi-phenomenological Theory:

Loidl et al. (Loi 80a,b;83) apply the theory of magneto-elastic coupling in rare-earth solids to the molecular solids and map the electronic degrees of freedom into the rotational degrees of freedom of the molecular species. In presence of TR coupling and three phonon anharmonic processes, the frequencies of phonons are given by the equation:

$$\omega(\mathbf{k})^2=\omega_0(\mathbf{k})^2+2\omega_0(\mathbf{k})\pi(\mathbf{k},\omega)-2A^2\omega_0{}^2(\mathbf{k})\chi(\mathbf{k},\omega)$$

where ω_0 is the bare phonon frequency; π is an anharmonicity parameter, A is a TR coupling constant and χ is the rotational susceptibility in presence of direct anion-anion interaction. By taking the long wave length limit of the above equation Loidl et al. obtain the renormalization of the elastic constants, similar in form to that obtained by (Reh 77).

The following limitations of the equation used by Loidl et al. should be noted. First, there is a single coupling constant A for both LA and TA phonons. Second, it is not clear from the above equation, the role, for any general k, of the off-diagonal elements of the susceptibility matrix in phonon softening. Moreover, the parameters of the phonon Green's function which give rise to the excitation frequencies given above, have well-defined microscopic origin. However Loidl et al. donot obtain these parameters from independent sources, instead they fit their theory with experimental data in cyanides to obtain these numbers. In addition this theory does not explore the interesting competition between various physical effects, which we show are crucial to have a proper understanding of phase transition in these systems.

(c) Microscopic Theories:

(1) Elastic Softening:

A microscopic theory for anomalous thermoelastic behavior in the alkali cyanides with NaCl type structure in phase I was first given by Michel and Naudts (Mic 77a,77b). We will review their theory in some detail because the present work is similar in spirit to theirs. They start from a model in which the anion is taken to be a dumbbell with two repulsion centers at the positions of the two nuclei. Each molecule is surrounded by an octahedral cage of six alkali ions. The single site repulsive potential on a given molecule due to its nearest neighbors (nn) is given by

$$V_0(i)=\sum_{j=1}^{6} V_0(\mathbf{R}_{ij},\mathbf{n}_i) \qquad (3.1a)$$

with
$$V_0(\mathbf{R}_{ij},\mathbf{n}_i)=\sum_{s=+,-} C_1 \exp[-C_2|\mathbf{R}_{ij}+sd\mathbf{n}_i|] \qquad (3.1b)$$

and $\mathbf{n}_i$ is a unit vector specifying the orientation of the ith molecule. The lowest order term in the crystal field potential is a Devonshire potential involving spherical harmonics of order l=4. However as the cations move from their average positions, the potential does not have cubic symmetry. This instantaneous noncubic potential as given by (3.1b) is then expanded upto terms linear in the displacements $\mathbf{u}_{ij}$

$$V_0(\mathbf{R}+\mathbf{u},\mathbf{n})=V_0(\mathbf{R},\mathbf{n})-\mathbf{P}(\mathbf{R},\mathbf{n}).\mathbf{u}+.....$$

Here $\mathbf{R}=\mathbf{R}_{ij}{}^0$, and $\mathbf{u}=\mathbf{u}_{ij}$. The coefficient of the linear term $\mathbf{P}(R,\mathbf{n})$ is again expanded in spherical harmonics. If one retains only l=2 terms, one obtains the leading order contribution to the TR Hamiltonian:

$$H_{TR}(i)=\sum_{j\alpha} Y_\alpha(\mathbf{n}_i)\mathbf{v}_\alpha{}^R(\mathbf{R}_{ij}{}^0).\mathbf{u}_j \qquad (3.2)$$

Here and in the following two chapters the five symmetry adapted spherical harmonics (not all normalized) of order l=2 are defined by:

$$Y_1(\mathbf{n})=(5/4\pi)^{1/2}(1/2)(3ct^2-1)$$

$$Y_2(\mathbf{n})=(1.5)(5/4\pi)^{1/2}st^2(cp^2-sp^2)$$

$$Y_3(\mathbf{n})=-c.st^2.sp.cp \qquad (3.3)$$

$$Y_4(\mathbf{n})=-c.st.ct.cp$$

$$Y_5(\mathbf{n})=-c.st.ct.sp$$

where $c=(15/2\pi)^{1/2}$, $ct=\cos\theta$, $st=\sin\theta$, $cp=\cos\phi$, $sp=\sin\phi$, θ and ϕ being the angles associated with the unit vector **n**. It is well known that Y_1 and Y_2 have E_g symmetry whereas Y_3, Y_4, and Y_5 have T_{2g} symmetry.The TR coupling matrix due to repulsion, $v_{\mu\alpha}$, are calculated from:

$$v_{\mu\alpha}(\mathbf{l})=c_\alpha{}^2\int P_\mu(\mathbf{l},\Omega)Y_\alpha(\Omega)d\Omega \ ; \quad (\mathbf{l}=\text{nn vector})$$

where

$$c_\alpha{}^{-2}=\int Y_\alpha{}^2 d\Omega \qquad (3.4)$$

For NaCl type structures the 3x5 coupling matrix **v** has only two independent coefficients which we will denote as A_R and B_R, where the subscript R stands for repulsion contribution. The non-spherical shape of the cyanide ion, therefore leads to a TR coupling which leads to an effective indirect orientation-orientation interaction of the form

$$(1/2)\sum_{\alpha\beta\mathbf{k}} Y_\alpha{}^*(\mathbf{k})I_{\alpha\beta}(\mathbf{k})Y_\beta(\mathbf{k})$$

where the indirect interaction matrix I is given by

$$I_{\alpha\beta}(\mathbf{k})=-\sum_{ij} v_{\alpha i}(\mathbf{k})R_{ij}(\mathbf{k})v_{j\beta}(\mathbf{k})$$

and $R^{-1}(\mathbf{k})=M^0$ is the bare dynamical matrix. $Y_\alpha(\mathbf{k})$ is defined by

$$Y_\alpha(\mathbf{k})=(1/N)^{1/2}\sum_i \exp(i\mathbf{k}.\mathbf{R}_i)Y_\alpha(\mathbf{n}_i)$$

The TR coupling not only introduces an effective orientational interaction, but also changes the dynamical matrix from M^0 to M such that

$$M=[1+F.R]^{-1}M^0 \qquad (3.5a)$$

where

$$F=v\chi v^t \qquad (3.5b)$$

In presence of the indirect interaction I, the rotational susceptibility $\chi=\chi(\mathbf{k})$ is given in the molecular field approximation by the solution to the matrix equation

$$\chi=\chi^0-\chi^0 I(\mathbf{k})\chi \qquad (3.6)$$

where

$$\chi_{\alpha\beta}{}^0=(1/kT)\int\exp(-\beta V_0)Y_\alpha(\Omega)Y_\beta(\Omega)d\Omega/Z \qquad (3.7a)$$

with

$$Z=\int\exp(-\beta V_0)d\Omega \qquad (3.7b)$$

It should be pointed out that the TR coupling matrices enter not only in equation (3.5) but also in equation (3.6) through indirect interaction I. Such a treatment leads to the correct equations for the elastic and phonon softening. In contrast, in our theory (see section (e) of Chapter 4) when the renormalized phonon frequencies are calculated in RPA (Random Phase Approximation), it is not necessary to include the indirect interaction in the expression for the susceptibility χ, because it will lead to overcounting of interactions. The equivalence between the approach of this thesis and that of MN (Mic 77a) is proved in Appendix A.

Taking the elastic limit in equation (3.5) and (3.6) Michel and Naudts (MN) obtain the softening of the elastic constants:

$$C_{44}=C_{44}^{0}[1-(2B_R^{2}\chi_t^{0})/(aC_{44}^{0})] \qquad (3.8a)$$

$$C_{11}=C_{11}^{0}[1-(8A_R^{2}\chi_e^{0})/(aC_{11}^{0})] \qquad (3.8b)$$

where 2a is the lattice constant (see Figures 2.2 and 2.3), χ^{0}'s are susceptibilities of appropriate symmetries.

The parameters A_R and B_R in equation (3.8) depend on: the strength C_1 and inverse range C_2 of the Born-Mayer potential; on a and on the bond length 2d. They are given in Appendix B of (Sah 82,enclosed with this thesis) and were first derived by MN (Mic 77a).

For KCN the above theory for elastic softening gave good agreement with experiment. However while checking the orientational susceptibility curves of E_g and T_{2g} symmetry given in Figures 1 and 2 of (Mic 77a,b) we were unable to reproduce these curves. We also noted that a different choice of the repulsion strength C_1, viz. $C_1=2C^{MN}$ could easily reproduce their curves. However since A_R and B_R are proportional to C_1 it is clear that doubling C_1 should also double the coupling constants A_R and B_R and as such will spoil the agreement between theory and experiment. In other words a simple rescaling of the parameters would not give the reported (Mic 77a) agreement between theory and experiment. Therefore it is clear that in order to obtain agreement of the theory with experimental data one has to invoke additional physical processes. We outline such a physical process in section (d).

(2)Phonon Softening Over the Entire Brillouin Zone (BZ):

The original microscopic theory of MN was primarily focused on calculating elastic properies. However there have been several attempts to apply the theory to calculate phonon dispersion relations. We review these theories below.

(i) Strauch et al. (Str 79) start from the basic TR coupling matrix discussed above and write the dynamical matrix as $M=M^0+\delta M$, where δM is a 6x6 matrix which can be partitioned into sub-matrices of order 3x3. The upper left hand side sub-matrix in δM is then given in terms of the TR coupling matrix v and the bare susceptibilities χ^0. Strauch et al. find that the use of v as given by MN does not give good agreement between theory and experiment for the systems NaCN and KCN. Hence they chose different constants that give good fits to the experiment. It is clear that there is no microscopic justification for the choice of parameters used in this work [but see (Sah 82)].

(ii) Ehrhardt et al. (Ehr 80,83) obtain the phonon dispersion relations for RbCN basing their theory again on the microscopic model of MN. Their dynamical matrix is identical to that given in equation (3.5) where the rotational susceptibilities are calculated in the presence of lattice mediated interaction, i.e. according to equation (3.6). Note that the dynamical matrices of (i) above and that of (Ehr 80) are different from each other. Whereas in (i) the upper right hand side submatrix in δM is a 3x3 null matrix, in (Ehr 80) the corresponding quantity is a non-null matrix.

It should be pointed out that in both the works (i) and in (ii) the rotational susceptibilities have been assumed to be frequency independent. This certainly breaks down when the time scales of orientational motion are comparable to phonon time scales. For a proper dynamical calculation involving projection operators, we refer the reader to the later work of MN (Mic 78).

(d) Suggestions for Improvement:

As mentioned earlier, the model due to MN (Mic 77a) which had only SR contribution to TR coupling, failed to account for the observed thermoelastic softening in KCN.

Moreover the theory of Loidl et al. (Loi 80a,b), in which the phonon frequencies were calculated from the poles of phonon Green's function, were ultimately fitted to the experiments to obtain the parameters, thus revealing no information at the microscopic level. Our aim in the next chapter is to develop a microscopic theory similar in spirit to the work of MN, but uses the Green's function formalism to derive an equation similar to that used by Loidl et al. (Loi 80a,b). The combination of the two approaches and the inclusion of a physical mechanism mentioned below, leads to a theory that brings out the essential physics of the softening in the alkali cyanides in a straight forward manner.

One of the major contribution of this work was to realize that an improved agreement theory and experiment could be obtained by incorporating TR coupling due to quadrupole moment (Q) of the anion interacting with the fluctuating electric field gradient (efg) at the site of the anion. Since Q happens to be negative, the TR coupling contributions due to SR repulsion and Q-efg interaction compete against each other. To see the physics of this competition, consider a $(CN)^-$ ion oriented along the z-axis and a positive charge also on the positive z-axis, at a distance a from the c.m. of the anion. If one moves the positive charge towards the anion along the z-axis, then the short range repulsion energy increases, whereas the electrostatic energy decreases because of the charge distribution associated with the anion. Thus we see that there is a competition between these two effects in their contribution to TR coupling which is important in understanding the observed elastic softening in the alkali cyanides. The details of this and other competing processes are presented in the next chapter.

CHAPTER 4

MICROSCOPIC THEORY OF ELASTIC AND PHONON SOFTENING IN IONIC MOLECULAR SOLIDS

In this chapter we present a microscopic theory of elastic and phonon softening in ionic molecular solids in general, with particular application to solids with NaCl and CsCl structures. We show that our theory reproduces the earlier microscopic theory of MN (Mic 77a) in the appropriate limiting cases. Improvements over the earlier microscopic theory which takes into account the non-vanishing electric quadrupole moment Q of the molecular ion are presented. These improvements are two fold: (i) there is a non-zero contribution to TR coupling arising due to Q-efg interaction, (ii) there is a modification of the rotational susceptibility arising from direct Q-Q interaction between the anions. We show that the presence of (i) drastically modifies the conclusions of earlier works. We find that in the contribution (i) it is inadequate to retain just the nn contributions because contributions from other neighbors may be of opposite in sign to nn contributions. It is also found that going upto third nn is usually adequate. However for direct Q-Q interaction nn approximation is adequate because the contributions fall off as $1/R^5$.

We divide this chapter into seven sections. Details of some of the results given in this chapter can be found in Appendix B of this thesis.

(a) Model and Crystal Field (CF) Potential

We treat the CN^- ion as a rigid dumbbell which has two identical centers separated by a distance 2d. The alkali ion M^+ on the other hand is represented by a spherically symmetric charge distribution. The short range (SR) repulsion between a given $(CN)^-$ and an M^+ ion is characterized by two constants C_1 and C_2 which represent the strength and the inverse range of the repulsion potential respectively. Since we are treating the two centers of the anion as identical, there is only one set of atom-atom potential parameters C_1 and C_2 for each cyanide crystal. Since the short range potential falls off exponentially with distance, we will ignore the SR interaction beyond the first nn. With these assumptions, the orientation dependent single site CF potential is easily obtained from equation (3.1).

(b) Hamiltonian

The Hamiltonian H consists of three parts $H=H_T + H_R + H_{TR}$. The translational part H_T is obtained by treating the ions as spherical charge distributions and keeping the harmonic terms

$$H_T=(1/2)\sum_{\mathbf{k}\kappa\mu}\Big[(1/m_\kappa)p_\mu^*(\kappa,\mathbf{k})p_\mu(\kappa,\mathbf{k})+$$

$$\sum_{\lambda\nu}C_{\mu\nu}(\kappa,\lambda,\mathbf{k})u_\mu^*(\kappa,\mathbf{k})u_\nu(\lambda,\mathbf{k})\Big] \qquad (4.1)$$

where m_κ is the mass of the κth ion (+,-) in a unit cell, $\mathbf{k}$ is the wave vector, μ is the cartesian component x,y,z; $C_{\mu\nu}(\kappa,\lambda,\mathbf{k})$ is the dynamical matrix (note that the matrix M^0 introduced in Chapter 3 gives only the acoustic modes), and $\mathbf{u}$,$\mathbf{p}$ are the fourier transforms of the displacements (from the appropriate cubic structure) and momentum respectively.

The rotational part of the Hamiltonian is obtained by fixing the c.m. of the $(CN)^-$ ions at cubic lattice sites:

$$H_R=\sum_{\mathbf{k}\lambda}[1/(2I)]L(\lambda,\mathbf{k})^*L(\lambda,\mathbf{k})+\sum_i V_0(\mathbf{n}_i)+\sum_{<ij>}V_d(ij) \qquad (4.2)$$

where I is the moment of inertia of the dumbbell about each of its two principal axes (i.e. $\lambda=1,2$) and $L(\lambda,\mathbf{k})$ is the fourier transform of the angular momentum $L(\lambda,i)$, $V_0(\mathbf{n}_i)$ is the CF potential energy term already discussed in the previous section. The term $V_d(ij)$ represents the direct interaction between two molecules at sites i and j and oriented arbitrarily with respect to crystal axes.

The TR coupling term H_{TR} represents a coupling between the orientational degrees of freedom $Y_\alpha(\mathbf{n}_i)$ of a molecular ion and the translational degrees of all the other ions. Following MN we write

$$H_{TR}=i\sum_{\alpha\mu\kappa\mathbf{k}} Y_\alpha^*(\mathbf{k})v_{\alpha\mu}(\kappa,\mathbf{k})u_\mu(\kappa,\mathbf{k}) \tag{4.3}$$

This term is obtained by displacing the c.m.s from their equilibrium positions and keeping terms linear in the displacements. Equation (4.3) is a fourier space representation of equation (3.2) after summing over all lattice sites i. The coupling matrix v will be discussed in detail in section (f).

If we describe the translational degrees of freedom in terms of phonons, then H_T and H_{TR} can be rewritten in terms of phonon creation and destruction operators b^* and b respectively. Let $\mathbf{k}$ and j denote the wave vector and the polarization index respectively. Then

$$H_T=\sum_{j\mathbf{k}}\omega_{j\mathbf{k}}^0(b_{j\mathbf{k}}^*b_{j\mathbf{k}}+1/2) \tag{4.4}$$

where the bare phonon frequencies $\omega_{j\mathbf{k}}^0$ are obtained by solving a secular equation involving the dynamical matrix C in equation (4.1). For detailed description about the calculation of bare phonon frequencies in ionic solids with long range interactions but without TR coupling we refer the reader to the book by Hardy and Karo (Har 79). We can express the displacements $u_\mu(\kappa,\mathbf{k})$ as a sum over the normal modes of vibration:

$$u_\mu(\kappa,\mathbf{k})=\sum_j (2\omega_0 m_\kappa)^{-1/2} e_\mu(\kappa,\mathbf{k}j)(b_{j\mathbf{k}}+b_{j-\mathbf{k}}^*) \qquad (4.5)$$

where $e_\mu(\kappa,\mathbf{k}j)$ is the polarization vector of a κ type ion for the phonon mode $j\mathbf{k}$. One then obtains

$$H_{TR}=i\sum_{j\alpha\mathbf{k}} Y_\alpha^*(\mathbf{k})V_{\alpha j}(\mathbf{k})(b_{j\mathbf{k}}+b_{j-\mathbf{k}}^*) \qquad (4.6)$$

where $V_{\alpha j}(\mathbf{k})=(2\omega_{j\mathbf{k}}^0)^{-1/2}\sum_{\mu\kappa}(m_\kappa)^{-1/2}e_\mu(\kappa\mathbf{k}j)v_{\mu\alpha}(\kappa,\mathbf{k}) \qquad (4.7)$

(c) Direct Interaction

Direct interaction between two molecules at sites R_i and R_j can arise due to (a) Q-Q interaction, (b) anistropic dispersion (AD) interaction and (c) short range repulsion (R) interaction. One can write this interaction as (Koh 60)

$$V_d(ij)=\sum_m A_m Y_{2,m}(\omega_i)Y_{2,-m}(\omega_j) \qquad (4.8)$$

where the unit vectors ω_i and ω_j are the orientations of the molecules i and j respectively with respect to the line joining their c.m. taken as the polar axis. The coefficients A_m can be written as

$$A_m = A_m(QQ) + A_m(AD) + A_m(R) \qquad (m=-2,2)$$

and $$A_{-m} = A_m$$

The individual contributions to the direct interaction from the various sources are given in Table 4.1 (Goo 71, Dun 77, deB 42). As seen from this Table, the QQ interaction falls off as $1/R^5$, while the AD interaction falls off as $1/R^6$. In Table 4.1, ε and σ are parameters of the Lenard-Jones potential and κ is the anistropic polarizability. To obtain the anionic repulsion interaction that is listed in Table 4.1 a power law potential of the form $4A/R^{12}$ between the anion centers was assumed. In this work we neglect the effects of AD and R contributions. Because of the large quadrupole moment of the $(CN)^-$ anion, and large intermolecular separation, this assumption is justified. Estimates of p,q and r give the following values (for nn anions): q=1146K, p=-41K and r=1K where we have used the following parameters ε=118K, σ=3.46Å, κ=.25 and $A=8\times10^7 K(Å)^{12}$. Moreover since the dipole moment of the $(CN)^-$ ion is small, we ignore the direct dipole-dipole interaction. The direct interaction between the anions arising due to their quadrupole moments can be written as (using 4.8):

$$H_d = 1/2 \sum_{\alpha\beta\mathbf{k}} D_{\alpha\beta}(\mathbf{k}) Y_\alpha(\mathbf{k})^* Y_\beta(\mathbf{k}) \qquad (4.9)$$

TABLE 4.1 Strengths of direct interaction between a pair of molecules

	QQ	AD	R
A_0	q	p	$8.41r$
A_1	$(2/3)q$	$(2/3)p$	$(5/3r)$
A_2	$(1/6)q$	$(1/3)p$	$37.33r$
where	$q=24\pi Q^2/5R^5$	$p=-48\pi\varepsilon\sigma^6\kappa^2/5R^6$	$r=24\pi 336Ad^4/5R^{16}$

The form of the interaction term $D_{\alpha\beta}(\mathbf{k})$ is explicitly given in (Sah 82), attached to this thesis as Appendix B. In evaluating the direct interaction terms above one has to sum over the Euler angles of the lattice vectors joining a given anion to its nn anions (see Figures 2.2 and 2.3). These

Euler angles are given in Tables 4.2 and 4.3 for NaCl and CsCl structures respectively.

The **k**-dependence of the direct interaction matrix D(**k**) for various symmetry directions will be given in chapter 5 and will be discussed in that chapter.

TABLE 4.2 Euler angles of nn intermolecuar axis for NaCl structure

position(units of a)	$-\beta,-\gamma$(units of π)
1,1,0	1/2,1/4
1,-1,0	1/2,7/4
-1,-1,0	1/2,5/4
-1,1,0	1/2,3/4
0,1,1	1/4,1/2
0,-1,1	1/4,3/2
0,-1,-1	3/4,3/2
0,1,-1	3/4,1/2
1,0,1	1/4,0
-1,0,1	1/4,1
-1,0,-1	3/4,1
1,0,-1	3/4,0

TABLE 4.3 Euler angles for nn intermolecular axis for CsCl structure

position(units of 2a)	$-\beta,-\gamma$(units of π)
1,0,0	1/2,0
-1,0,0	1/2,1
0,1,0	1/2,1/2
0,-1,0	1/2,3/2
0,0,1	0,0
0,0,-1	1,0

(d) Renormalization of Phonon Frequencies

In alkali cyanides the bare phonon frequencies of the high-T phase are renormalized because of the TR coupling given by equation (4.6). To obtain these modified phonon frequencies we use Zubarev's Green's function technique (Zub

60). We define the time- and temperature-dependent retarded Green's function G by

$$G_{j\mathbf{k}}(t-t')=(1/i)\langle[\phi_{j\mathbf{k}}(t),\phi_{j\mathbf{k}}^{*}(t')]\rangle\theta(t-t') \qquad (4.10)$$

For simplicity of notation if we drop the jk's for the moment, then $\phi(t)=b(t)+b^{*}(t)$ is the phonon field operator in the Heisenberg representation. The square bracket is the commutator, < > stands for the average over a canonical ensemble and $\theta(t-t')$ is the step function. The equation of motion for G is

$$i(d/dt)G(t-t')=\delta(t-t')\langle[\phi(t),\phi^{*}(t')]\rangle$$

$$+(1/i)\theta(t-t')\langle[[\phi(t),H],\phi^{*}(t')]\rangle$$

The fourier transform of $G(t-t')$ is given by

$$\omega\langle\langle\phi;\phi^{*}\rangle\rangle_{\omega}=\langle[\phi,\phi^{*}]\rangle+\langle\langle[\phi,H];\phi^{*}\rangle\rangle_{\omega} \qquad (4.11)$$

where

$$\langle\langle\phi;\phi^{*}\rangle\rangle_{\omega}=G(\omega)=\int_{-\infty}^{\infty}G(t)\exp(i\omega t)dt \qquad (4.12)$$

The Hamiltonian H appearing in the above equation is the sum of rotational, translational and TR parts. Following the treatment given in Appendix B, we obtain the renormalized phonon frequencies in RPA as:

$$\omega_{j\mathbf{k}}^{2}=(\omega_{j\mathbf{k}}^{0})^{2}-2\omega_{j\mathbf{k}}^{0}\sum_{\alpha\beta}V_{\alpha j}(\mathbf{k})\chi_{\alpha\beta}(\mathbf{k}\omega)V_{\beta j}(\mathbf{k}) \qquad (4.13)$$

where the rotational susceptibility is defined as the time fourier transform of the angle-angle Green's function:

$$\chi_{\alpha\beta}(\mathbf{k},\omega)=-\langle\langle Y_\alpha(\mathbf{k});Y_\beta^*(\mathbf{k})\rangle\rangle_\omega \qquad (4.14)$$

We would like to point out the assumptions under which equation (4.13) has been derived. One assumption is that the rotational dynamics is determined by H_R alone, i.e. the rotational dynamics has a faster time scale compared to translational dynamics. In the elastic regime this is a reasonable approximation. For higher phonon frequencies, one has to consider the retardation effects in an adequate fashion. Another assumption in obtaining equation (4.13) has been that a Green's function involving two orientational operators and two phonon operators has been replaced by the average value of orientational operators times the Green's function of the phonon operators.

(e) Rotational Susceptibility

For calculation of elastic constants it is sufficient to consider the $\omega=0$ limit of the rotational susceptibility. We will further assume that $\chi_{\alpha\beta}(\mathbf{k})$, which we define to be the zero frequency limit of the susceptibility, can be replaced by the isothermal susceptibility $\chi_{\alpha\beta}{}^T(\mathbf{k})$. We calculate this latter susceptibility in presence of direct interaction between the molecules within a MF approximation. We have also neglected fluctuation effects in our calculations. As we have shown (Sah 82) this susceptibility in the paraelastic phase is obtained by solving the matrix equation

$$\chi(\mathbf{k})=[1+\chi^0 D(\mathbf{k})]^{-1}\chi^0 \qquad (4.15)$$

where χ^0 is the bare susceptibility given by equation (3.7) and is calculated by taking the thermal average over the single site potential V_0. Because of cubic symmetry $\chi_{\alpha\beta}{}^0$ is diagonal in α,β and has only two independent elements $\chi_e{}^0$ and $\chi_t{}^0$:

$$\chi_{\alpha\alpha}{}^0=(\chi_e{}^0, 3\chi_e{}^0, \chi_t{}^0, \chi_t{}^0, \chi_t{}^0) \qquad (4.16)$$

Similarly in the elastic limit ($\mathbf{k}\to0$), the direct interaction matrix is diagonal with

$$D_{\alpha\alpha}(\mathbf{k}=0)=(f, f/3, g, g, g) \qquad (4.17)$$

where $f=D_{11}{}^0$, $g=D_{33}{}^0$. Note that the factors 3 and 1/3 in equations (4.16) and (4.17) respectively appear because the symmetry adapted spherical harmonic Y_2 is unnormalized (see equation 3.3). From equations (4.15) to (4.17) it follows that for $\mathbf{k}=0$, χ is diagonal with

$$\chi_{\alpha\alpha}=(m, 3m, n, n, n) \qquad (4.18)$$

where $m=\chi_{11}$, and $n=\chi_{33}$. In the absence of single site potential, i.e. for a free rotator, one has $\chi_e{}^0=(1/kT)(1/4\pi)$ and $\chi_t{}^0=(1/kT)(1/2\pi)$. Clearly these values will be modified when the single site potential is non-zero, the precise nature of the modification will depend on the type of lattice considered. The completeness relation of the spherical harmonics allows one to write down a sum rule on the bare susceptibilities:

$$2\chi_e{}^0+1.5\chi_t{}^0=(1/kT)(5/4\pi) \tag{4.19}$$

Next we quote, for the sake of completeness, how equation (4.15) is modified if we include self-interaction (Geh 75) effects. Self-interactions can alter the single site susceptibility in two ways: (1) by changing the single site potential and (2) by changing the effective indirect interaction between the molecular ions. In presence of self-interactions the new single site potential is V_T:

$$V_T(\Omega)=V_0(\Omega)+V_S(\Omega)$$

where V_0 is defined in equation (3.1) and

$$V_S(\Omega)=\sum_{\alpha\beta\mathbf{k}} I_{\alpha\beta}(\mathbf{k})Y_\alpha(\Omega)Y_\beta(\Omega) \tag{4.20}$$

with the indirect interaction between the molecules given by

$$I_{\alpha\beta}(\mathbf{k})=-\sum_j 2V_{\alpha j}{}^*(\mathbf{k})V_{\beta j}(\mathbf{k})/(\omega_{j\mathbf{k}}{}^0) \tag{4.21}$$

One has then to calculate the bare susceptibility given by equation (3.7) with respect to the total single site potential $V_T(\Omega)$. In addition the matrix equation for the susceptibility (4.15) becomes

$$\chi(\mathbf{k})=[1+\chi^0(D(\mathbf{k})-\sum_{\mathbf{k}} I_{\alpha\beta}(\mathbf{k}))]^{-1}\chi^0 \qquad (4.22)$$

Note that equation (4.22) has been obtained by defining the self-interaction contribution to the single-site potential through equation (4.20). One could as well define pV_S (where p is an arbitrary number) as the self-interaction contribution to single site potential with the consequence that in equation (4.22) one obtains $-pI_{\alpha\beta}(\mathbf{k})$ instead of $-I_{\alpha\beta}(\mathbf{k})$. In an exact calculation such arbitrariness (through the number p) is expected to have no effect. However since we are using a meanfield approximation, the nature of this arbitrariness might affect the final results.

(f) Rotation Translation Coupling Coefficients

In this section we discuss in detail the different contributions to the TR coupling matrix that appears in equation (4.6). These coefficients can be written as a sum of two parts:

$$v(\kappa,\mathbf{k})=v^R(\kappa,\mathbf{k})+v^{efg}(\kappa,\mathbf{k}), \quad (\kappa=+,-)$$

where R indicates SR repulsion contribution and efg indicates the contribution coming from the interaction between the Q of the anion and the fluctuating efg produced at its site by all the other ions (taken to be point charges). Here κ indictes the sign of the charges and could be + or - depending on the type of neighbor considered. For SR repulsion, it is sufficient to retain contributions from nn's only (κ=+), while for efg terms we include contributions upto third nn's.

(1) Repulsion Contribution

The TR coupling matrix due to repulsion, in coordinate space, is calculated from equation (3.4) with the help of equation (3.2). We discuss two cases:

(i)NaCl structure:

This case has already been discussed by MN (Mic 77b) and the corresponding results for the **k** space is also discussed by them. It should be noted that there are only two constants A_R and B_R in this coupling matrix. These constants depend on the parameters C_1,C_2,d and a which are given in Section (a) of Chapter 5 which deals with the calculation of parameters (see Table 5.1).

(ii)CsCl structure:

We will evaluate the coupling matrix for this case in the coordinate space for the nn lattice vector **l**=(a,a,a) (see Figure 2.3). Let N be an operator such that N**l**=**l** and

$Nn=n'$, where n is a unit vector specifying the direction of the molecule. From equation (3.4) we obtain

$$v_{\mu\alpha}(l)=c_\alpha^2\int[NP_\mu(l,n)][NY_\alpha(n)]dn \qquad (4.23)$$

Choosing $N=S_{xy}$, an operator for reflection along the [110] direction and also choosing $N=R_3$, an operator for 3-fold rotation about the [111] axis, we find that there are three independent constants A_R, B_R and C_R. In contrast, for NaCl structure the SR coupling matrix has only two constants A_R and B_R. The coupling matrix for CsCl structure in direct space and in momentum space are given in Tables 4.4 and 4.5 respectively.

(2) Q-efg Contribution

As the lattice vibrates, there is a deviation from local cubic symmetry at the positions of the molecules and the resulting efg couples to Q. To the lowest order in displacements this leads to an additional coupling between rotation and translation. Depending on the sign of Q the net TR coupling will be either enhanced or suppressed.

The Q-efg interaction is given by (Coh 57)

$$H'=(1/6)\sum_{ilj}Q_{lj}(i)U_{lj}(i) \qquad (4.24)$$

where the Cartesian components of the Quadrupole and field gradient tensors at site i are:

$$Q_{lj}(i)=\int[3r_{il}r_{ij}-\delta_{lj}r_i^{2}]\rho(r_i)dr \quad (r_i=r-R_i) \qquad (4.25)$$

$$U_{lj}(i)=(\partial/\partial x_l)(\partial/\partial x_j)\sum_n{}' q_n/|R_i-R_n|, \quad (x\varepsilon R_i) \qquad (4.26)$$

TABLE 4.4 The transpose of the coupling matrix $v^R(a,a,a)$ for CsCl structure. $p=A_R/4, q=B_R/4, r=C_R/4$.

	x	y	z
1	p	p	-2p
2	-p	p	0
3	q	q	r
4	q	r	q
5	r	q	q

TABLE 4.5 The transpose of the coupling matrix $(1/8)v^R(\mathbf{k})$ for CsCl structure, where si=Sin(k_ia),ci=Cos(k_ia), i=x,y,z.

	x	y	z
1	p.sx.cy.cz	p.cx.sy.cz	-2p.cx.cy.sz
2	-p.sx.cy.cz	p.cx.sy.cz	o
3	q.cx.sy.cz	q.sx.cy.cz	-r.sx.sy.sz
4	q.cx.cy.sz	-r.sx.sy.sz	q.sx.cy.cz
5	-r.sx.sy.sz	q.cx.cy.sz	q.cx.sy.cz

Here $\rho(\mathbf{r}_i)$ is the charge density at site i and $U_{lj}(i)$ is the second derivative of the electrostatic potential at the ith site due to all the other charges. We can express the Cartesian quadrupole moment tensor as a linear combination of spherical quadrupole moment tensors of rank 2:

$$Q_{2m}(i)=\int r_i{}^2 Y_{2m}(i)\rho(\mathbf{r}_i)d\mathbf{r} \qquad (4.27)$$

so that

$$H'=\sum_{i,m} Q_{2m}(i)U_2^{-m}(i) \tag{4.28}$$

where $U_2^{-m}(i)$'s are appropriate linear combinations of $U_{lj}(i)$'s. Now we can express Q_{2m}, which is defined with respect to lab axes, in terms of Q which is measured with respect to the molecular axes. Let (θ_i,ϕ_i) be the polar coordinates of the principal axis of the molecule i with respect to the lab axes. Then an Euler angle transformation gives:

$$Q_{2m}(i)=Y_{2m}(\theta_i,\phi_i)Q \tag{4.29}$$

Equations (4.28) and (4.29) can then be rewritten as

$$H'=Q\sum_{i\alpha} Y_\alpha(i)U_\alpha(i) \tag{4.24'}$$

where the $U_\alpha(i)$'s are appropriate linear combinations of the second derivatives of the electric potential given in equation (4.26), and are given in the reference (Sah 82, see Appendix B). Finally, one can take the fourier transform of the Q-efg interaction term and express it as:

$$H'=i\sum_{\mathbf{k}\kappa\mu} Y_\alpha^{*}(\mathbf{k})v_{\mu\alpha}^{efg}(\kappa,\mathbf{k})u_\mu(\kappa,\mathbf{k}) \tag{4.30}$$

We now discuss the coupling constant matrix $v_{\mu\alpha}^{efg}(\kappa,\mathbf{k})$ for the two types of lattices that we are interested in.

The explicit expressions for the coupling matrices coming from Q-efg interaction are given in Appendix A of (Sah 82) for NaCl-structure.

The coupling matrix for Q-efg interaction for the CsCl structure are easily obtained from those of the NaCl structure by making use of the correspondence shown in Table 4.6. Note that the factors p, q and r defined in that Table take care of the different signs and different distances of the neighbors of the CsCl-structure as compared to that of NaCl-structure.

(g) Elastic Constants

The elastic constants can be obtained from the $\mathbf{k}=0$ limit of $\omega_{j\mathbf{k}}$. We define:

$$A_{eff}=A_R+\alpha A_Q$$

$$B_{eff}=B_R+\alpha B_Q$$

$$\alpha=1+1/(4\sqrt{2})-8/(27\sqrt{3})-1/16=0.943 \text{ (NaCl)} \qquad (4.31)$$

$$\alpha=8/(27\sqrt{3})+1/16-1/(64\sqrt{2})=.2225 \text{ (CsCl)} \qquad (4.32)$$

$$A_Q=\pm\sqrt{(9\pi/4)}Qe_0/(a^5), \text{ (+ NaCl, - CsCl)} \qquad (4.33)$$

$$B_Q=-A_Q\sqrt{(2/3)} \qquad (4.34)$$

TABLE 4.6 The correspondence for obtaining $v_{i\alpha}^{efg}(\kappa,\mathbf{k})$ for CsCl-structure from that of NaCl-structure, where $p=1/16$, $q=1/64\sqrt{2}$ and $r=8/27\sqrt{3}$.

NaCl	CsCl
2a	2a
1st nn	2nd nn
2nd nn	3rd nn
3rd nn	1st nn
A_Q	$-pA_Q$
$\bar{A}_Q$	qA_Q
$\bar{\bar{A}}_Q$	$-rA_Q$

Case 1:

For a wave along (001) direction we take $k_x=0$, $k_y=0$ and $k_z=k$ and consider LA and TA phonon frequencies. The LA frequency in the limit **k**=0 is

$$\omega_{LA}^2=(C_{11}/\rho)k^2$$

and the corresponding polarization vector is

$$\mathbf{e}(\kappa,\mathbf{k})=\surd(m_\kappa/m)(0,0,1)$$

where m_κ is the mass of the κ-type ion, $m=m_+ + m_-$ and ρ is the mass density: $\rho=m/(2a^3)$ for NaCl structure and $\rho=m/(8a^3)$ for CsCl structure. From equation (4.13) one then obtains

$$C_{11}=C_{11}^0-a_{11}A_{eff}^2\chi_{e_g}(T) \qquad (4.35)$$

where $a_{11}=8/a$ for NaCl structure and $a_{11}=2/a$ for CsCl structure. Similarly for the TA phonon branch one has

$$\omega_{TA}^2=(C_{44}/\rho)k^2$$

$$\mathbf{e}(\kappa,\mathbf{k})=\surd(m_\kappa/m)(1,0,0)$$

and

$$C_{44}=C_{44}^0-a_{44}B_{eff}^2\chi_{t_{2g}}(T) \qquad (4.36)$$

where $a_{44}=2/a$ (NaCl) and $a_{44}=1/(2a)$ (CsCl)

Case 2:

For a wave propagating along (110) direction we take $k_x=k_y=k/\surd 2$ and $k_z=0$. For a TA wave in the xy plane one has

$$\omega_{TA}^2=(k^2/2)(C_{11}-C_{12})/\rho,$$

$$e(\kappa,\mathbf{k})=\surd(m_\kappa/2m).(1,-1,0)$$

so that

$$C_{12}=C_{12}^0+a_{12}A_{eff}^2\chi_{e_g}(T) \qquad (4.37)$$

where $a_{12}=4/a$ (NaCl) and $a_{12}=1/a$ (CsCl)

Equations (4.35) to (4.37) are in agreement with the results of Michel and Naudts (Mic 77a) although they have been derived in a completely different and straight forward way. Note also that the rotational susceptibilities in these equations have to be calculated in presence of direct interactions. The numerical results of our calculations will be discussed in the next chapter.

The summary of the final results of elastic softening are given in Table 4.7 (see next page).

TABLE 4.7 Summary table.

quantity	NaCl	CsCl
a_{11}	8/a	2/a
a_{44}	2/a	1/2a
a_{12}	4/a	1/a

$$C_{11}=C_{11}^0-a_{11}A_{eff}^2\chi_{e_g}(T)$$

$$C_{44}=C_{44}^0-a_{44}B_{eff}^2\chi_{t_{2g}}(T)$$

$$C_{12}=C_{12}^0+a_{12}A_{eff}^2\chi_{e_g}(T)$$

CHAPTER 5

RESULTS AND DISCUSSIONS ON THE DISORDERED PHASES

In the previous chapter we developed a theory of elastic and phonon softening for the orientationally disordered phase of the alkali cyanides. In this chapter we indicate how the various parameters appearing in the theory are calculated and then discuss our results. We then make comparision with experiment and comment on various aspects of the theory.

(a) Calculation of Parameters

We calculate the atom-atom parameters C_1 and C_2 of equation (3.1b) from the data of Fumi and Tosi (Fum 64) and of Hirshfeld and Mirsky (Hir 79). The former work lists the repulsion parameters between identical pairs of alkali ions while the latter work lists the repulsion parameters between C-C and N-N atoms. The parameters for the alkali cyanides are then obtained by applying simple averaging schemes. For example, for calculating C_1 for a dissimilar pair of atoms we take the geometric mean of the constituent pairs while for calculating C_2 we take the arithmatic mean of the values of the pairs. For simplicity we further assume that C and N ends of the anion are identical. For the alkali cyanides we found that this turns out to be not too bad an assumption. We indicate below the calculation of C_1 and C_2 for KCN as a concrete example. The repulsion energy between a pair of K^+ ions is

$$V(r)=C_1(K^+-K^+)\exp[-C_2(K^+-K^+)r]$$

so that following the notation of equation 3 of (Fum 64)

$$C_1(K^+-K^+)=c_{++}b_+^2 \text{ and } C_2(K^+-K^+)=1/\rho$$

Here $b_+^2=(46.92)^2$ erg/molecule and $\rho=0.3394$ Å, and the Pauling constant $c_{++}=1.25$. In a similar fashion we obtain the atom-atom parameters for C-C and N-N repulsion. Then we use

$$C_1(K\text{-}CN)=[C_1(K\text{-}K)^2.C_1(C\text{-}C).C_1(N\text{-}N)]^{1/4}$$

and $$C_2(K\text{-}CN)=(1/4)[2C_2(K\text{-}K)+C_2(C\text{-}C)+C_2(N\text{-}N)]$$

The parameters obtained in this way are listed in Table 5.1. It should be noted that there are two sets of parameters for C_1 nd C_2 given in Table 2 of (Fum 64). Our final results are not very sensitive to choosing either of these two sets. This agrees with the observation of Bound, Klein and McDonald (BKM) (Bou 81) that modest changes of atom-atom potentials do not affect their MD results in the disordered phase to any appreciable extent. Moreover the parameters for NaCN obtained by us agree with those listed by Klein and adopted by Raich and Huller (Rai 79) in their work on the azides. In the MD study of KCN, BKM (Bou 81) found that f approximately equal to 0.5 gave good agreement between their MD calculations on the orientational probability distribution functions and the experimental results. Our calculations also suggest that $f<1$. For cyanides having NaCl-type structure we found that $f=0.6$ gave reasonable agreement of our theory with experimental softening of the elastic constants C_{11} and C_{44}. For CsCN on the other hand we found that f is less than 0.15. This should be contrasted with the MD simulations for CsCN by Klein et al. (Kle 82) who found that the orientational probability distribution functions and phonon dispersion relations (for a few $\mathbf{k}$ points) are not affected appreciably by choosing different f values. Our calculations, on the other hand suggest that the phonon dispersion relations are sensitively dependent on f for both type of structures (for all $\mathbf{k}$).

Next we discuss about the constants A_R, B_R, C_R, A_Q and B_Q which play an important role in elastic and phonon softening. These constants are calculated from a knowledge of C_1, C_2 and Q about which we have already mentioned. For an NaCl type structure with short range repulsion between the nearest neighbors $C_R=0$ and for a CsCl-type crystal eventhough $C_R\neq0$, it does not appear in the calculation of elasic constants. We have listed values of these constants in Table 5.2. The quadrupolar contributions in this table have been calculated by taking into account the reduction factor f that is indicated in the table.

TABLE 5.2 Repulsion and quadrupolar contributions to TR coupling

quantity	NaCN	KCN	RbCN	CsCN
f	0.6	0.6	0.6	0.15
A_R(K/Å)	5578	4379	3323	-706.5
B_R(")	-1390	-988	-713	3261.7
C_R(")	x	x	x	4127.2
A_Q(")	-3065	-2064	-1693	2822
B_Q(")	2503	1685	1382	-2304
B_R/A_R	-0.249	-0.226	-0.215	-4.617
B_Q/A_Q	-0.816	-0.816	-0.816	-0.816

Another set of parameters that enter our calculations are the bare elastic constants $C_{11}{}^0$, $C_{44}{}^0$, and $C_{12}{}^0$. MN (Mic 77a) obtained the bare elastic constant $C_{44}{}^0$ by fitting the experimental value of the extrapolated transition temperature to their theoretical value. Another procedure is to use the high T elastic constants of the alkali bromides as the bare elastic constants because Br^- and $(CN)^-$ ions are roughly of the same size (deR 81). Both these fitting schemes have some limitations. For example it is well known that near but above the transition, fluctuations become very large and can in cases reduce the transition temperature significantly. Since the present theory does not incorporate fluctuation effects the first fitting procedure is unreasonable. The second procedure, though less unsatisfactory, has the limitation that it refers to a crystal other than the one under investigation. We have, therfore, followed a different procedure. We have obtained the bare elastic constants by fitting to the experimental values of the elastic constants of the cyanides at a temperature T_{fit} far above the transition temperature. In fact we choose T_{fit} as the highest temperature at which the elastic constants have been measured. The values of the bare elastic constants and T_{fit} are given in Table 5.3.

In our calculations we have incorporated the effects of anharmonicity on elastic constants by supposing-ing that there is an additional renormalization of elastic constants which decrease linearly with T, at the temperatures of interest, i.e. $\delta C_{ii}{}^{an}=-\gamma_i T$. The reason for this assumption is that experimentally anharmonicity effects in the alkali halides show a similar variation. To find γ_i we have further assumed that $\gamma_i(MCN)=\gamma_i(MBr)$. These values are given in Table 5.3 and have been obtained from (Nor 58, Gha 70, Ove 51, Rei 61). The elastic constant can now be expressed as

$$C_{ij}(T)=C_{ij}{}^{0}+\delta C_{ij}{}^{an}(T)+\delta C_{ij}{}^{TR}(T) \quad (i,j=1,\ 2, \text{or } 4) \quad (5.1)$$

where the TR coupling contributions to the renormalization of the elastic constants are given by equations (4.35) to (4.37). The importance of the anharmonic terms is discussed at the end of section (c).

(b) Isothermal Rotational Susceptibility

The isothermal rotational susceptibility $\chi_{\alpha\beta}(\mathbf{k})$ can be calculated with a knowledge of the bare susceptibilities and the direct interaction between the anions (see section (e) of Chapter 4). The bare susceptibilities were calculated using equation (3.7) by numerical techniques. We used the 16-point Gaussian quadrature formula of Fehlner and Vosko (Feh 76) to calculate the bare susceptibilities. For temperatures T>100K, this interpolation formula gives the paraelastic susceptibilities quite accurately. For lower temperatures, though, one should use an interpolation

TABLE 5.3 Bare elastic constants, T_{fit} and anharmonicity parameters in units of 10^{11} dyn/cm^2, K and 10^9 dyn/cm^2/K respectively

quantity	NaCN	KCN	RbCN	CsCN
C_{11}^0	5.749	5.115	4.022	2.548
C_{44}^0	0.752	0.470	0.411	1.190
T_{fit}	473	453	380	300
γ_1	0.26	0.27	0.28	0.120
γ_4	0.019	0.013	0.008	0.106

formula of still greater accuracy. The susceptibilities of the paraelastic phase are plotted in Figures 5.1 and 5.2 over the temperature range of about 150 to 500K. In the long wave length limit we have

$$\chi_{ii}(\mathbf{k}=0)=\chi_{ii}^0/[1+D_{ii}(\mathbf{k}=0)\chi_{ii}^0] \quad (i=1 \text{ or } 4) \qquad (5.2)$$

where $\chi_{11}^0=\chi_{e_g}^0$ and $\chi_{44}^0=\chi_{t_{2g}}^0$. The T-dependence of the bare susceptibilities can be written as $\chi_{ii}^0(T)=S_{ii}(T)/T$, so that the total susceptibility can be expressed in a Curie-

Weiss form with a T-dependent 'Curie Constant', i.e.

$$\chi_{ii}(\mathbf{k}=0)=S_{ii}(T)/[T+T_{cw}{}^{i}] \qquad (5.3)$$

From equation (5.3) it is clear that the direct interactions, depending on their sign, can either enhance or suppress the susceptibilities from their bare values. We have plotted, for the sake of illustration, the enhancement factors $R_1=\chi eg/\chi eg^0$ and $R_4=\chi t2g/\chi t2g^0$ for KCN in Figure 5.1. Note that in our theory the Curie-Weiss temperatures are not only functions of T but also different for E_g and T_{2g} symmetries. We list these quantities for two temperatures in Table 5.4 and compare them with other works. We would like to point out that in our work the Curie-Weiss temperatures for susceptibilities of E_g and T_{2g} symmetries are of opposite sign and of different magnitude, whereas in the other works they are of the same sign and of equal magnitude. Note also that the Curie-Weiss temperatures for CsCN are very close to zero which is a consequence of the fact that quadrupole moment of the anion in the solid environment is reduced by about 85% of its free ion value.

The short range potential strongly affects the bare rotational susceptibilities. In the limit T approaching ∞, the anions tend to be more like free rotators so that S_1 is about 0.08 and S_4 is about 0.16. In the presence of a CF potential, though, the anions prefer to orient along some

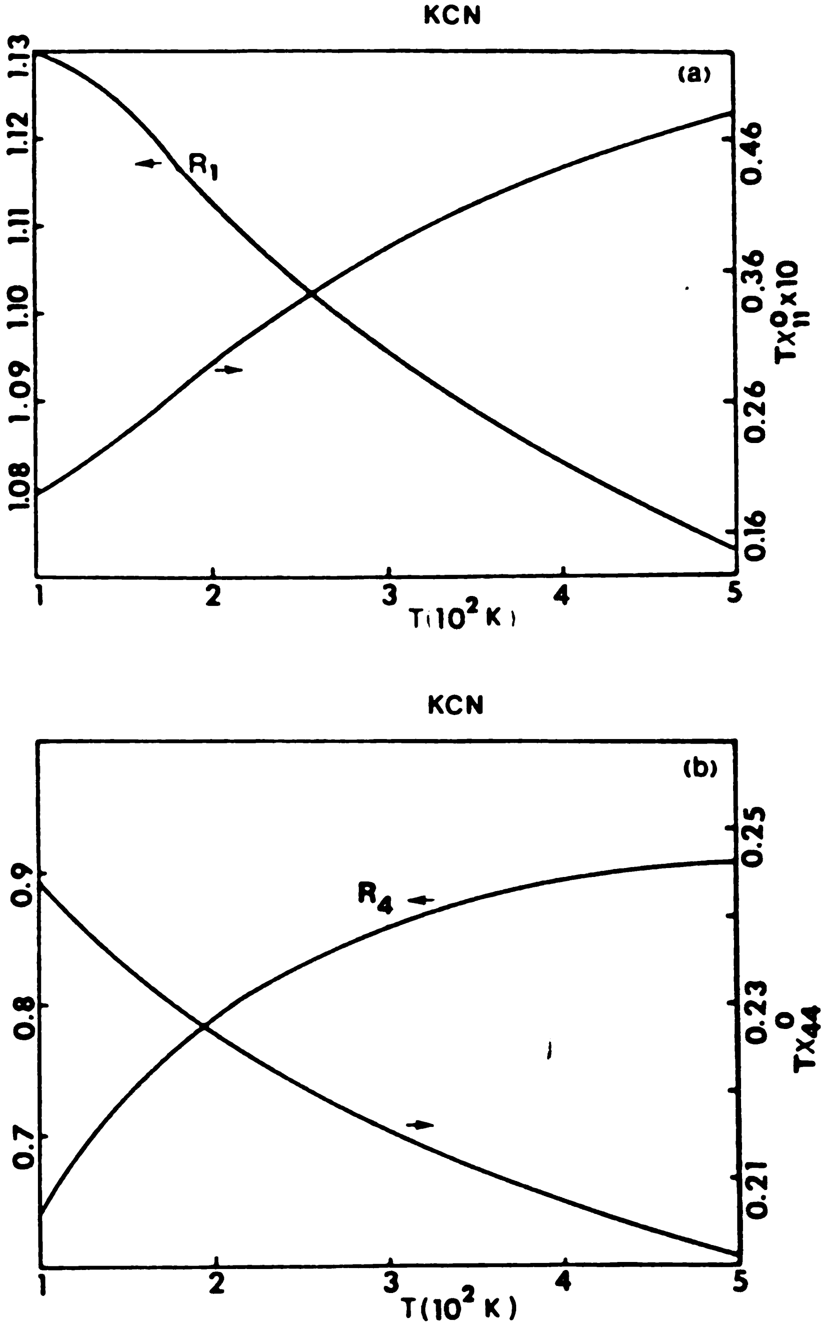

FIGURE 5.1 Single site susceptibilities $T\chi_{ii}^{0}$ and enhancement factors $R_i=\chi_{ii}(T)/\chi_{ii}^{0}(T)$ for KCN. (a) $i=1$ (e_g) (b) $i=4$ (t_{2g})

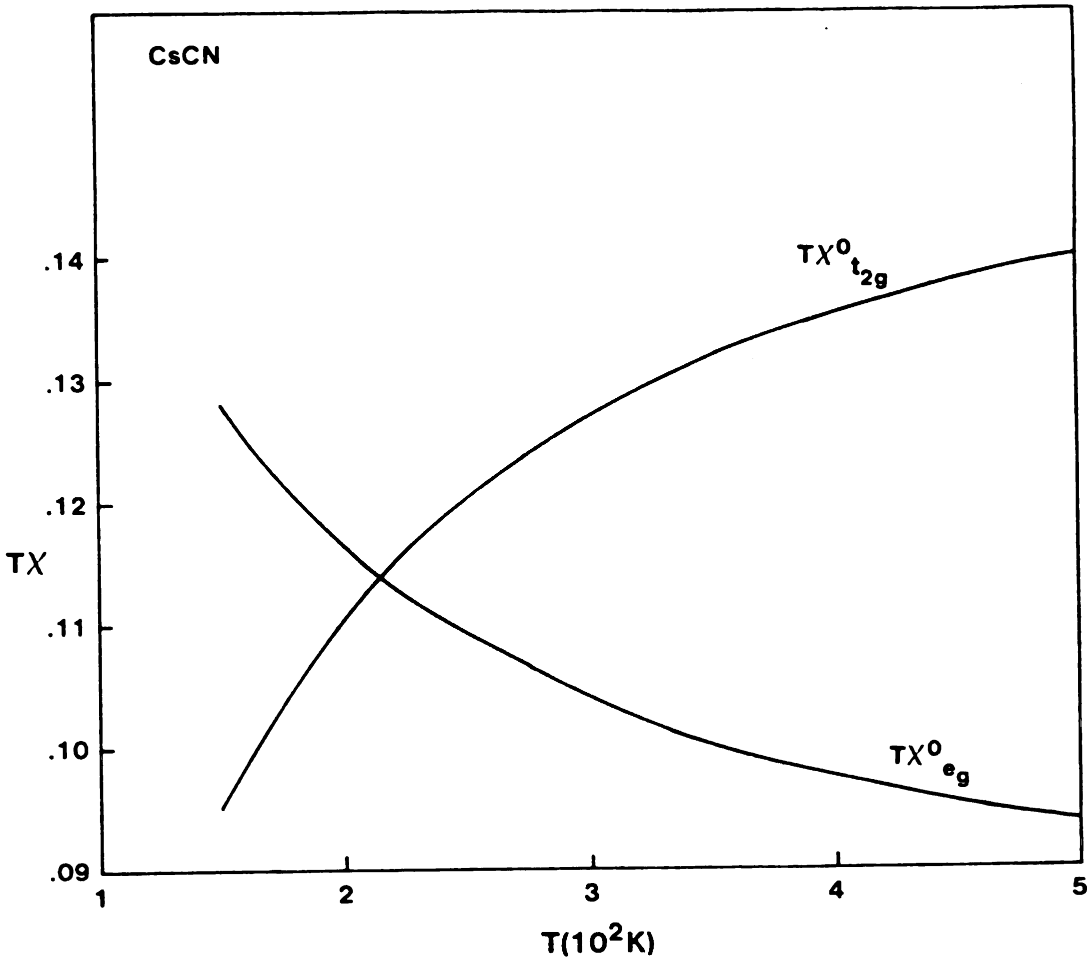

FIGURE 5.2 Single site susceptibilities of e_g and t_{2g} symmetries for CsCN.

specific directions of the crystal. For NaCl structure, there are strong repulsion centers along the principal crystal axes, whereas no such centers exist along the body diagonal directions. Hence for NaCl structure $S_4 > S_1$. In fact from Figure 5.1 it is found that S_4/S_1 is about 10 for the temperature range of 100 to 500 K. However as T becomes very large, this ratio tends to the free rotator value of 2. On the other hand for CsCl structure, it is found from Figure 5.2 that S_4/S_1 is of the order of 1 in the same temperature range. For CsCl structure S_1 is large in the low-T regime because orientations with E_g symmetry reduce the repulsion energy. With increase of temperature, however, S_1 decreases and S_4 increases. In contrast in the NaCl structure the opposite happens. These differences strongly affect the nature of elastic and phonon softenings in the alkali cyanides with different crystal structures.

Next we examine the effect of direct interactions on the rotational susceptibilities and hence on the elastic softening. We discuss two cases:(i) KCN and (ii) CsCN. For KCN, taking $f=0.6$, we find that $D_{11}(0)=-704K$ and $D_{44}(0)=235K$. From equation (5.2) it follows that $R_1>1$ and $R_4<1$ which indicate that direct intermolecular interactions

TABLE 5.4 'Curie-Weiss' temperatures for KCN(f=.6) and CsCN(f=.15) for k=0

	Ref	T(K)	$T_{cw}(e_g)$	$T_{cw}(t_{2g})$
KCN	this work	100	-13	212
	"	500	-34	47
	Boi 78	x	86	86
	Reh 77	x	231	230
	Loi 80	200	-42	-42
CsCN	this work	150	17	-4
	"	500	13	-6
	Loi 83	x	0.	0.

enhance C_{11} softening and suppress C_{44} softening. Since S_4/S_1 is about 10 in the temperature range of interest we have $1.08<R_1<1.13$ and $0.6<R_4<0.9$. For CsCN, the susceptibilities and enhancement factors show a completely different behavior. Taking, for example, a value of f=0.4 we find that $D_{11}(0)=947K$ and $D_{44}(0)=-316K$. Hence over a temperature range of 100-500K, $0.42<R_1<0.85$ and $1.28>R_4>1.09$, so that $D_{44}(0)$ tends to enhance C_{44} softening. Since S_4/S_1 is about 1, direct interactions are important for both types of susceptibilities. In the limit f=1 and $\gamma_i=0$, direct interaction produces most dramatic effect on elastic softening. In this limit B_R is approximately $-\alpha B_Q$, and therefore $B_{eff}=0$. So C_{44} shows a very gradual softening in the range 300-500K. However since $T_{cw}{}^4<0$, the denominator in equation (5.2) enhances C_{44} softening. Hence as $T\rightarrow|T_{cw}{}^4|$, the rotational susceptibility of T_{2g} symmetry diverges. From equation (4.13) we find that there is an abrupt softening of the elastic constant C_{44} (see Figure 5.6b) in the neighborhood of $T_{cw}{}^4$.

For the sake of completeness we have plotted the **k**-dependence of $D_{\alpha\beta}(\mathbf{k})$ for the three symmetry directions (001), (110) and (111) in figures (5.3) through (5.5). Some of the direct interaction strengths show quite a bit of dispersion for some of the directions considered. Also notice that the direct interaction strengths change sign in some cases as one goes from the zone center to the zone boundary. We will discuss more about phonon softening at non-zero **k** for KCN later in section (d) of this chapter.

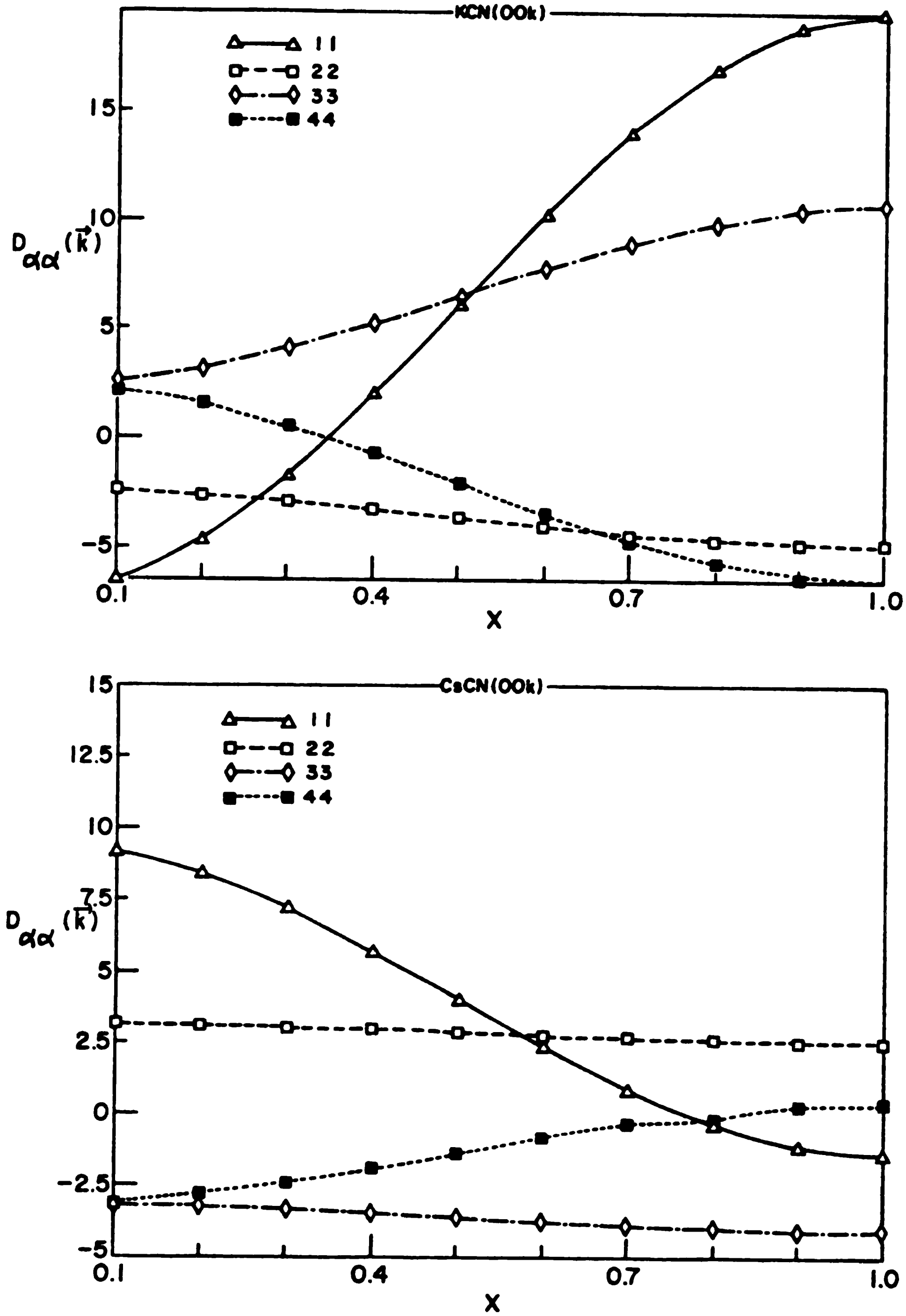

FIGURE 5.3 Direct interaction strengths D(00k) (in units of 100K) as a function of the reduced wave vector x; KCN (f=.6), CsCN (f=.4)

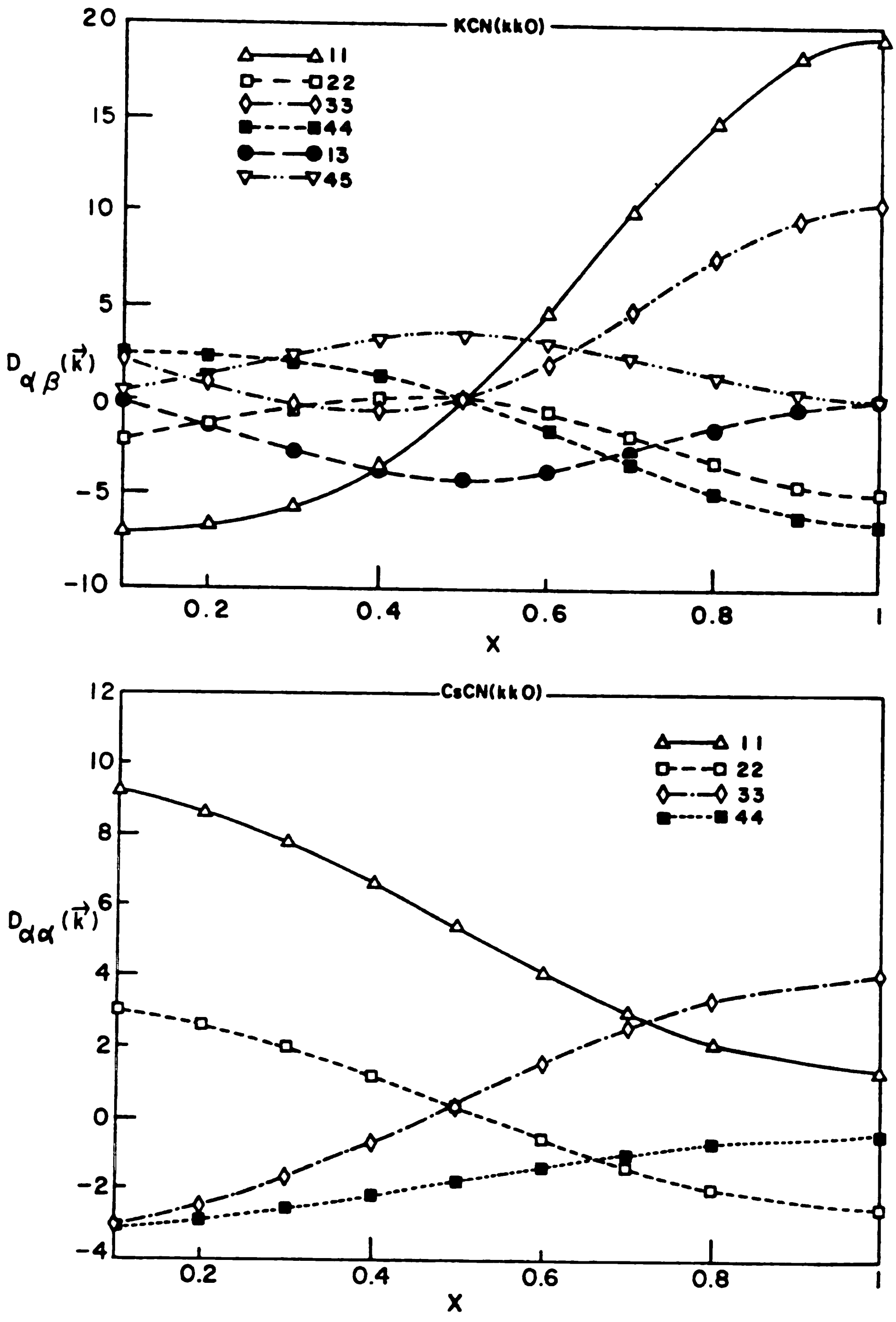

FIGURE 5.4 Direct interaction strengths D(kk0) (in units of 100K) as a function of the reduced wave vector x; KCN (f=.6), CsCN (f=.4)

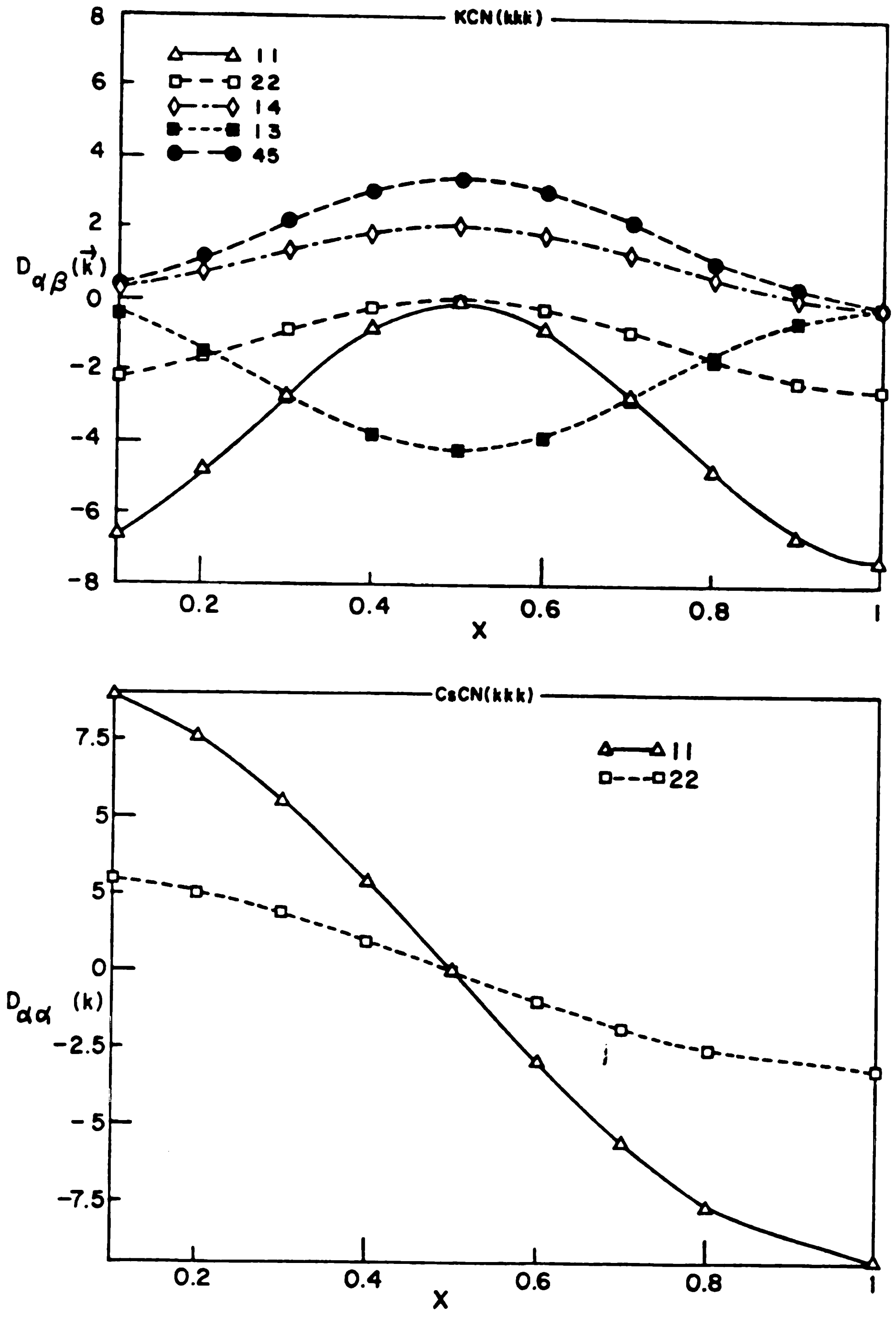

FIGURE 5.5 Direct interaction strengths D(kkk) (in units of 100K) as a function of the reduced wave vector x; KCN (f=.6), CsCN (f=.4)

(c) Elastic Softening and Transition Temperatures

As seen from equations (4.35) to (4.37), the elastic softening due to TR coupling depends on A_i and B_i (i=R,Q) and the rotational susceptibilities of E_g and T_{2g} symmetries. First we discuss the effect of the coupling constants. The relevant quantities that determine the elastic softening are the squares of A_{eff} and B_{eff}. Eventhough the signs of the coupling constants are not relevant for elastic softening, diffuse inelastic neutron scattering can probe the signs of these quantities. For KCN Rowe has found that our sign of B_{eff} (which is positive) agrees with his experimental findings (Row 82). The second point to notice is that A_R and A_Q are opposite in sign as are B_R and B_Q. Thus there is a cancellation effect in A_{eff} and B_{eff} and this arises due to the fact that Q is negative. The nature of this cancellation is quite different for the two types of structures that we have studied. For the NaCl structure, the 2nd and 3rd neighbors of a given anion have opposite charges and it turns out that they very nearly cancel out each others contributions to Q-efg coupling thus making α about 1 (equation 4.31). In contrast for the CsCl structure, in spite of the opposite signs of the charges of the second and third neighbors, they donot cancel each other's contribution appreciably, so that α is about 0.2225 (equation 4.32). Thus the exact nature of the cancellation depends not only on the sign and value of Q, but also sensitively on the structure.

Next we discuss the results of our calculations in various limiting cases.

(i)Anharmonicity Absent

In the limit Q=0, for KCN $B_{eff}/A_{eff}=-0.226$. The large value of A_{eff} leads to a very strong C_{11} softening and a relatively weak C_{44} softening. In this limit one expects to recover the results of MN (Mic 77a) who only considered SR repulsion contribution to TR coupling. However we donot recover their numerical results because of a factor-of-two error in their calculation of rotational susceptibilities. For a brief discussion on this point we refer the reader to the papers (Mah 82 ,page 938 reference 10; Sah 82 ,page 2993). In the other limit where repulsion is small (or T is large) and f=1, B_{eff}/A_{eff} is about -0.8 and S_4/S_1 is about 2, so that the TA phonons soften appreciably leading to a vanishing of C_{44}. In realistic cases both repulsion and quadrupolar effects are important and we have found that f=0.6 gives a good fit to the experiment (see Figure 5.6a and Figures 5.7 to 5.9).

For CsCN the situation is completely different. In the limit Q=0, $B_{eff}/A_{eff}=-4.62$ so that there is a strong C_{44}

softening (Figure 5.6b) and a weak C_{11} softening. In the limit f=1, B_R and αB_Q are comparable in magnitude but opposite in sign. Hence B_{eff} is small. Thus for large T , C_{44} doesnot soften appreciably whereas C_{11} shows a pronounced softening due to the large difference in the values of A_R=-706.5K/Å and αA_Q=4186K/Å. With decrease of T, though, the susceptibility of T_{2g} symmetry becomes important and shows a very sharp drop off (Figure 5.6b). To obtain a good fit to the experiments (Loi 83) f=0.4 seems a good choice provided anharmonicity effects are neglected.

(ii)Anharmonicity Present

The combined effects of TR coupling and anharmonicity are given in equation (5.1) and the anharmonicity parameters in Table 5.3. It is clear from that table that for NaCl structure γ_4/γ_1 is about .1 so that anharmonicities affect C_{11} more strongly than C_{44}. For NaCN and KCN the overall agreement of C_{11} with experiment (Figures 5.7 and 5.8) seems to be very good. In particular the peak in $C_{11}(T)$ is understood in terms of a competition between the TR coupling and anharmonicity affect. For RbCN inclusion of anharmonicity gives a peak, but the agreement (Figure 5.9) is not as good. This might be due to the mean field nature of the theory. The temperatures T_{44} where the elastic constants C_{44} would extrapolate to zero are given in Table 5.5 . For NaCl structure the affect of including anharmoni-

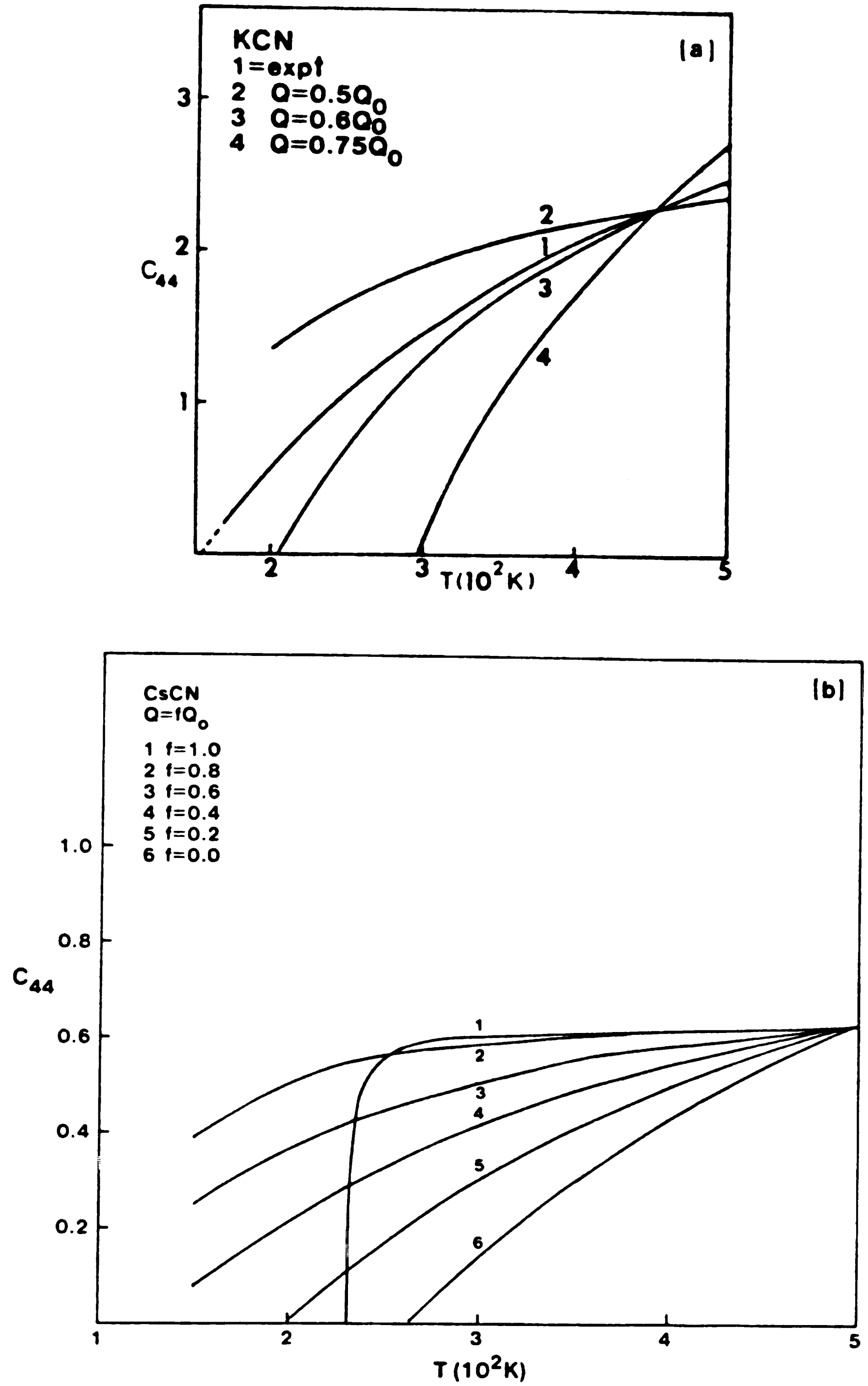

FIGURE 5.6 T- and f-dependence of C_{44} (a)KCN (10^{10}dyn/cm^2) and (b)CsCN (10^{11}dyn/cm^2).

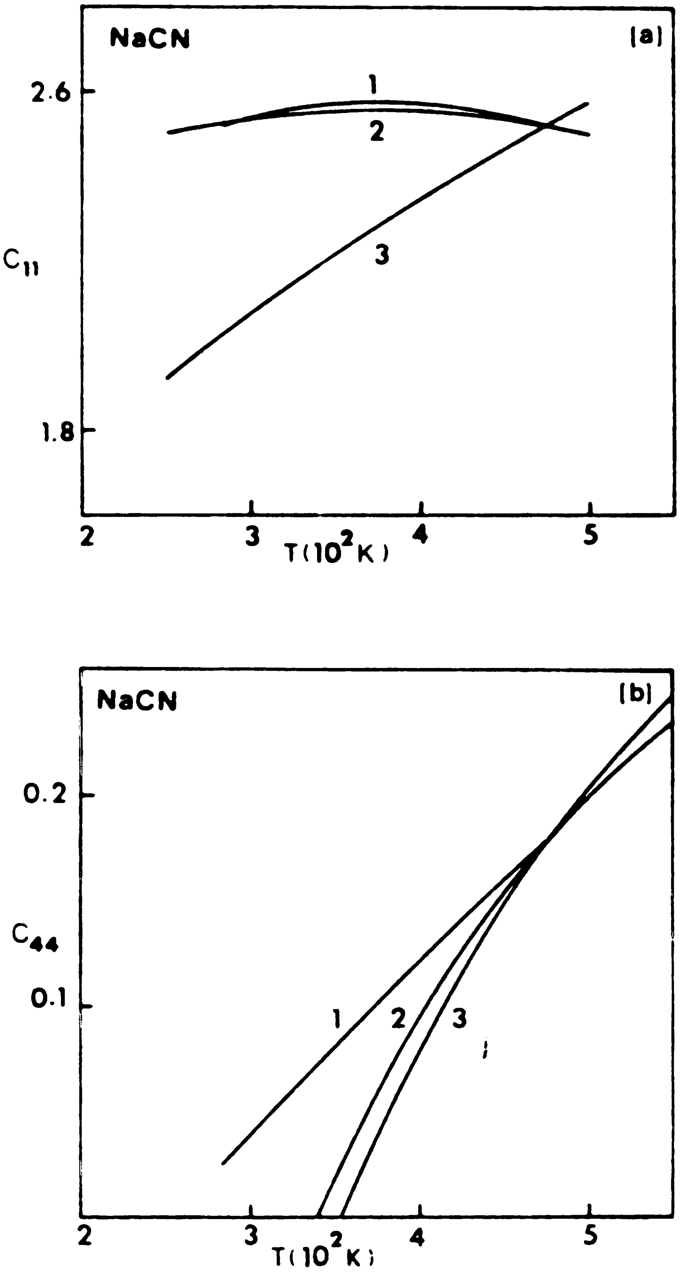

FIGURE 5.7 T-dependence of C_{11} and C_{44} (in units of 10^{11}dyn/cm^2) for NaCN; with f=0.6; 1:expt, 2: theory with anharmonicity 3:theory without anharmonicity

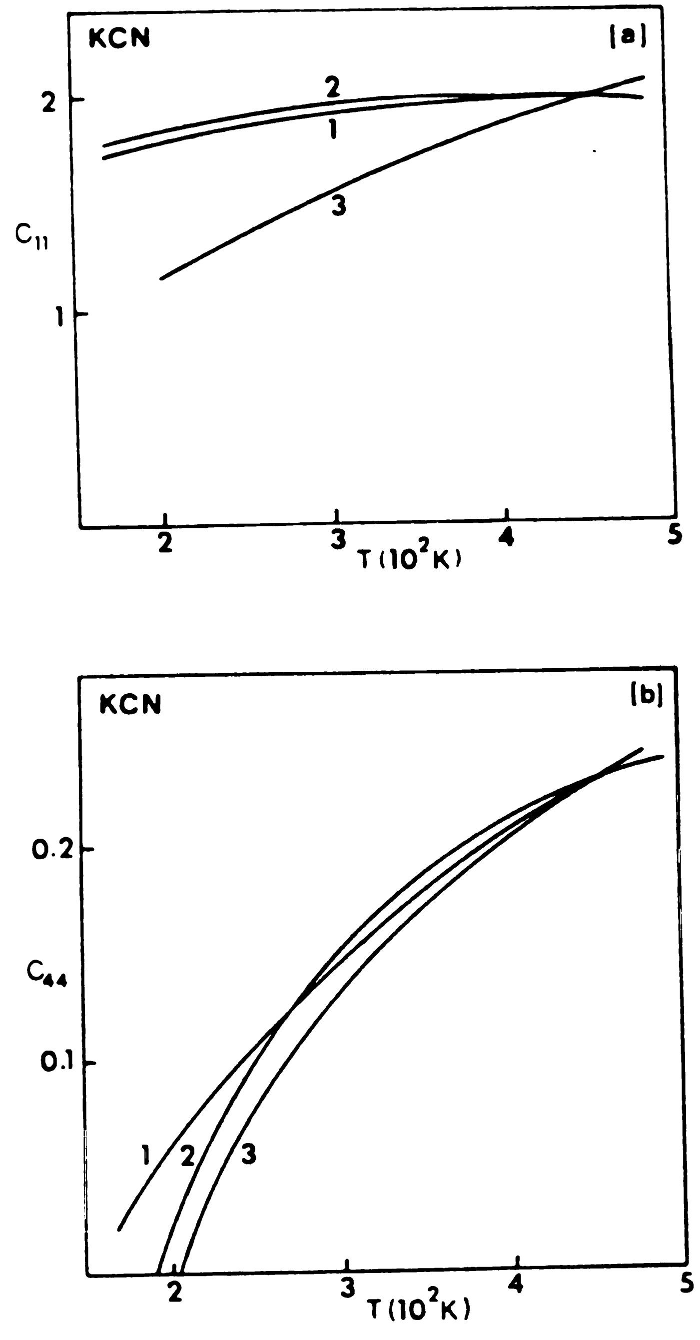

FIGURE 5.8 T-dependence of C_{11} and C_{44} (in units of 10^{11}dyn/cm^2) for KCN, with f=0.6; 1:expt, 2: theory with anharmonicity 3:theory without anharmonicity

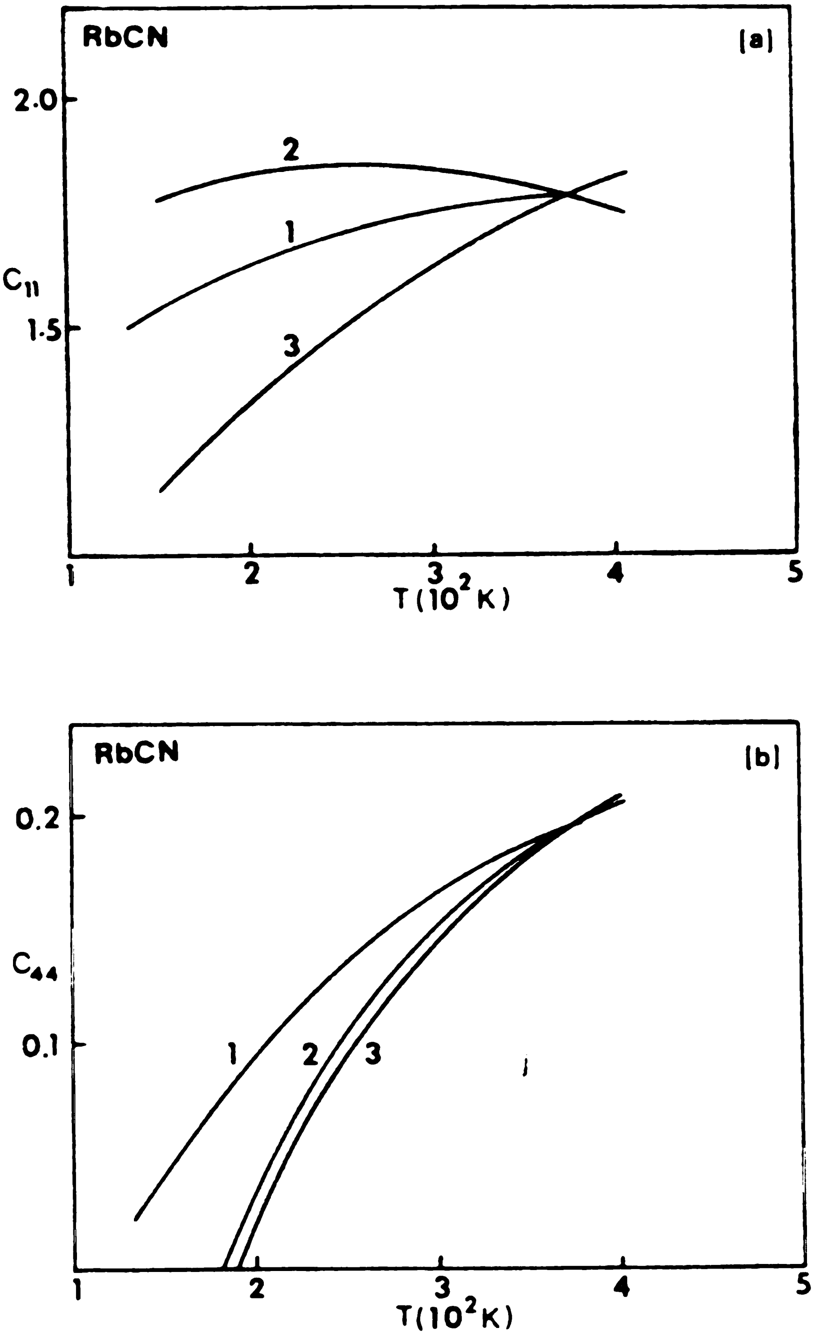

FIGURE 5.9 T-dependence of C_{11} and C_{44} (in units of 10^{11}dyn/cm^2) for RbCN with f=0.6; 1:expt, 2: theory with anharmonicity 3:theory without anharmonicity

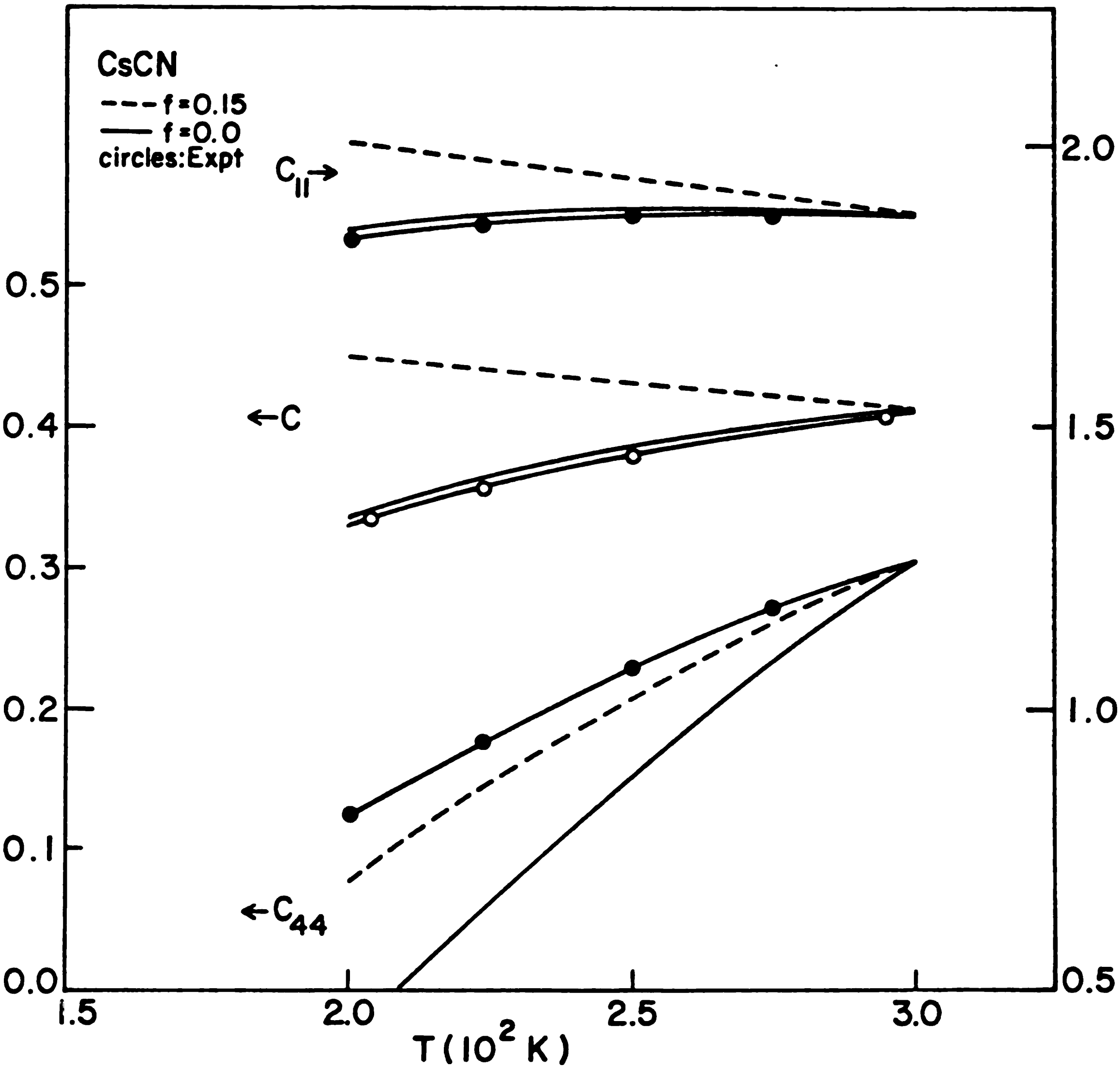

FIGURE 5.10 T-dependence of elastic constants for CsCN (10^{11}dyn/cm^2) including anharmonicity.

city is to reduce T_{44} by about 10K. For CsCN anharmonicity effects are not only important for C_{11}, but also for C_{44} because γ_4/γ_1 is about 0.9 (Table 5.3). We have calculated the elastic softening in CsCN using equation (5.1) for f=0 and f=0.15 which are plotted in Figure 5.10. For f=0, the agreement between our theory and experiment is excellent for C_{11} and $C=(C_{11}-C_{12})/2$, whereas the agreement is reasonable for C_{44} if we note that ours is a mean field theory. Choosing f=0.15 tends to improve the agreement of our theory with experiment for C_{44} but the agreement for C_{11} and C is not as good. This suggests that for CsCN the bare quadrupole moment of the anion has to be reduced by more than 85% to obtain fits to the elastic constant data. The T-dependence of the elastic constants are plotted in Figures 5.6 to 5.10

We conclude this Chapter by giving a brief discussion of the softening of phonons over the entire Brillouin Zone (BZ). For brevity we choose KCN, although the arguments are general.

(d) Phonon Softening in KCN

In chapter 3 we mentioned the two theories of phonon softening (Ehr 80, Str 79) in alkali cyanides which incorporated the TR coupling model. Our phonon calculations are improvements over both the above works since we have incorporated the effects of ionic quadrupole moment on both the TR coupling and the rotational susceptibility. We compare our calculated changes in phonon frequencies due to TR coupling in KCN with the work of (Str 79) who in turn obtained good fit with experiment (Sah 82).

TABLE 5.5 First order FE transition temperature T^*(expt), extrapolated and theoretical C_{44} softening temperatures T_c and T_{44}

system	T^*(K)	T_c(K)	T_{44}(K)
NaCN	288	255.4	337.5
KCN	168	156	190
RbCN	132	130	179
CsCN	193	150	179

It should be pointed out that Strauch et al. considered only nn contribution to $v_{i\alpha}(\kappa,\mathbf{k})$. Our calculation provides a microscopic justification for the validity of this assumption because we showed that the second and third nn contributions to the coupling matrix very nearly cancel each other out for the NaCl structure. However Strauch et al. considered only SR repulsion contribution whereas our analysis also brings out the importance of quadrupolar effects.

We define $\Gamma_{j\mathbf{k}}=(\omega_{j\mathbf{k}}^{02}-\omega_{j\mathbf{k}}^{2})^{1/2}/10^{13}$ as a measure of phonon renormalization. We have calculated $\Gamma_{j\mathbf{k}}$ for the acoustic phonons propagating along the (001) direction. Our results for phonon renormalization and those of Strauch et al. are given in Table VI of (Sah 82). It should be pointed out that the calculation of $\Gamma_{j\mathbf{k}}$ involves the calculation of polarization vectors of phonons. In the limit $\mathbf{k}=0$ one can analytically calculate these polarization vectors. But for arbitrary $\mathbf{k}$ the calculation of polarization vectors is nontrivial. We have calculated these polarization vectors numerically by taking a rigid ion model for an fcc crystal. While it is well known that rigid ion model is inadequate for describing the lattice dynamics of an ionic solid, we have nevertheless used this model to calculate the eigenvectors, mainly for simplicity. We find that at T=300K inclusion of direct interaction affects LA softening by about 7% whereas the TA phonons are affected to a maximum of 25%. It is clear from Figure (5.3) that $D_{11}(00k)$ shows a wider variation in its range of values than $D_{44}(00k)$. In spite of this, the TA phonons are influenced more strongly by direct interaction. This is due to the fact that S_4/S_1 is about 10 in the temperature range 100-500K. As can be seen from Table VI of the attached reprint (Appendix B), for LA phonons our calculated values are about 15-30% higher than experiment while for TA phonons our calculated values are about 7-32% smaller than experiment. These differences most likely arise due to the fact that we have used a static susceptibility in our calculation of the renormalization of phonon frequencies. For a proper phonon calculation one should use the dynamical susceptibility $\chi_{\alpha\beta}(\mathbf{k},\omega)$. As discussed in (Sah 82) the inclusion of proper dynamical susceptibility should improve the agreement with experiment.

CHAPTER 6

LANDAU THEORY OF ORIENTATIONAL ORDER

To study the orientational order in the FE phase of the alkali cyanides we start from a variational form of the free energy due to Bogolyubov. Then we make a Landau expansion of that free energy in terms of the tensor order parameters n_i $(i=1,5)$. The coefficients of the free energy expansion are obtained in terms of the parameters of the microscopic Hamiltonian introduced in Chapter 4. The free energy is then minimized with respect to the orientational order parameters to obtain the ordering. Thus we would like to understand not only the high-T elastic properties of these molecular solids, but also the nature of low-T orientational order with the help of the model that we have introduced. As a concrete example we examine the orientational order in CsCN which undergoes a first order FE phase transition from a pseudo-cubic to a trigonal structure at $T_c=193K$.

(a) Earlier Theory

There has been only one serious attempt (deR 81) to explain the orientational order in the cyanides of Na, K and Rb. We will refer to this as the work by dBM. They eliminate the TR coupling by means of a canonical transformation and write down an effective orientational Hamiltonian which is then approximated by its mean field value H_{mf}. The free energy is then calculated from

$$F_{dBM}=-kT\ln Tr[\exp(-\beta H_{mf})].$$

One should then self-consistently solve the MF equations $n_\alpha=\langle Y_\alpha\rangle_{mf}$ and obtain the free energy. However dBM donot perform such a self-consistent calculation. Instead, they expand F_{dBM} in powers of n_i and minimize the free energy with respect to n_i. Since the above procedure does not necessarily give the true minimum (Sah 83b), we have followed a different procedure and obtained the free energy from Bogolyubov's variational theorem.

In the work of dBM the interaction terms $T_{\alpha\beta}=D_{\alpha\beta}+I_{\alpha\beta}$ appear in all orders in the expansion (see section (c) of Chapter 4 for discussion on direct interaction and equation (4.21) for an expression for indirect interaction). In contrast, in our treatment $T_{\alpha\beta}$ appears only in the second order terms. This is particularly useful since the non-analytic terms involving the indirect interactions as k→0 (the indirect interaction depends on the direction in which k→0; see Geh 75) appear only once in our expression. The Landau coefficients in our theory depend on the single site susceptibilities and hence on the nature of the short range

CF potential. It should be pointed out that for simplicity dBM take the CF potential to be a constant, which is rather unrealistic (Figures 2.4 and 2.5). Our calculation is free from this unrealistic assumption.

Furthermore dBM assume that the ordering fields have T_{2g} symmetry. Before making such an assumption one should examine whether the ordering energies associated with E_g-type symmetry are indeed high enough to be ignored from the minimization process. For NaCN, KCN and RbCN we find that the assumption of dBM about the ordering fields is not quite correct whereas for CsCN ordering energies associated with E_g-type symmetry are considerably higher up in energy than those of T_{2g}-type symmetry.

(b) Effective Hamiltonian

We start by defining normalized symmetry adapted spherical harmonics $\tilde{Y}_\alpha = c_\alpha Y_\alpha$, $c_\alpha^{(-2)} = \int Y_\alpha^2 d\Omega$, where the unnormalized spherical harmonics have been defined through equation (3.3). Then the effective rotational Hamiltonian is

$$H_{eff} = \sum_i [V_0(i) + V_s(i)$$

$$+ (1/2) \sum_j{}' \tilde{T}_{\alpha\beta}(ij) \tilde{Y}_\alpha(i) \tilde{Y}_\beta(j)] \qquad (6.1)$$

For the sake of convenience we will drop the tilde (~) in the following. In equation (6.1) the total interaction matrix T is the sum of the direct quadrupolar interaction matrix D and the indirect interaction matrix I. Matrices D and I can be obtained from equations (4.9) and (4.21) by multiplying these equations by proper normalization constants. In equation (6.1), $V_s(i)$ is the self-interaction part of the indirect interaction which contributes to the single site potential, defined through equation (4.20), and the prime in the second summation indicates that the term i=j should be excluded .

(c) Variational Free Energy

Let us consider the Hamiltonian $H=H_{eff}$ given by equation (6.1). Let F_{ex} be the exact free energy for this Hamiltonian. Then the Bogolyubov variational free energy theorem (Hub 68) states that $F_{ex}<F_{var}$ with

$$F_{var}=\langle H-H_t\rangle_t-kT\ln Tr[\exp(-\beta H_t)] \qquad (6.2)$$

where the subscript t indicates that the trace has to be performed with respect to a trial density matrix

$$\rho_t=\prod_i \rho_{it} \qquad (6.3a)$$

with
$$\rho_{it}=\exp(-\beta H_{it})/Tr\exp(-\beta H_{it}) \qquad (6.3b)$$

and
$$H_{it}=V_0(i)+\sum_{\alpha} h_\alpha(i)Y_\alpha(i) \qquad (6.4)$$

Here $h_\alpha(i)$ is a variational parameter at site i with reference to the trial density matrix. Note that we have neglected the term $V_S(i)$ in equation (6.4) for the sake of simplicity. We define the tensor order parameters by

$$n_\alpha{}^i=tr[Y_\alpha(i)\exp(-\beta H_{it}]/tr[\exp(-\beta H_{it})] \qquad (6.5)$$

Since we are dealing with FE ordering we choose $n_\alpha{}^i=n_\alpha$ for all i. In addition we define the following susceptibilities with respect to the single site SR CF potential (for simplicity of notation we will drop the superscript 0 in the susceptibilities):

$$\chi_{\alpha\beta}=(1/kT)<Y_\alpha Y_\beta>$$

$$\chi_{\alpha\beta\gamma}=(1/kT)^2<Y_\alpha Y_\beta Y_\gamma> \qquad (6.6)$$

$$\chi_{\alpha\beta\gamma\delta}=(1/kT)^3<Y_\alpha Y_\beta Y_\gamma Y_\delta>$$

The order parameters can be expressed as a function of the ordering fields , i.e. $n_\alpha=<Y_\alpha>_t=f(h_\alpha)$ which can be formally inverted to give:

$$h_\alpha=\phi_{\alpha\delta}n_\delta+\phi_{\alpha\delta\delta'}n_\delta n_{\delta'}+\ldots\ldots \qquad (6.7)$$

Consistency then demands that

$$\phi_{\alpha\delta}=-(\chi^{-1})_{\alpha\delta}$$

$$\phi_{\alpha\delta\delta'}=-(1/2)\phi_{\alpha\mu}\phi_{\delta\upsilon}\phi_{\delta'\varepsilon}\chi_{\mu\upsilon\varepsilon} \tag{6.8}$$

We can now expand the free energy in powers of h_α and eliminate the ordering fields in favor of the order parameters through equation (6.7) to obtain

$$f_{var}=(F_{var}-F_0)/N=f_2+f_3+f_4 \tag{6.9}$$

$$f_2=(1/2)[T_{\alpha\beta}(\mathbf{k}\to 0)+(1/p_\alpha)\delta_{\alpha\beta}]n_\alpha n_\beta \tag{6.10a}$$

$$f_3=(-1/6)(1/p_\alpha p_\beta p_\gamma)\chi_{\alpha\beta\gamma}n_\alpha n_\beta n_\gamma \tag{6.10b}$$

$$f_4=1/24(1/p_\alpha p_\beta p_\gamma p_\delta)$$

$$\times[-\chi_{\alpha\beta\gamma\delta}+3\beta p_\alpha p_\gamma\delta_{\alpha\beta}\delta_{\gamma\delta}$$

$$+(3/p_\rho)\delta_{\rho\sigma}\chi_{\alpha\beta\rho}\chi_{\gamma\delta\sigma}]n_\alpha n_\beta n_\gamma n_\delta \tag{6.10c}$$

and $$p_\alpha=\beta\langle Y_\alpha{}^2\rangle$$

Define $$g=p_1$$

$$r=p_3$$

Imposition of cubic symmetry on the susceptibilities further simplifies the third and fouth order terms in the free energy. The nonvanishing susceptibilities in the third order are

$$CA=\chi_{111}=-\chi_{122}=\beta^2e^3(1/2)(54A_6+9A_4-5)$$

$$CB=\chi_{345}=\beta^2 t^3 A_6$$

$$CC=\chi_{331}=\beta^2 (e.t)(1/6)(18A_6+A_4-1)$$

$$CD=\chi_{441}=\chi_{551}=(-1/2)\chi_{331}$$

$$CE=\chi_{442}=-\chi_{552}=-[(\sqrt{3})/2]\chi_{331}$$

where

$$e=\sqrt{(5/16\pi)}$$

$$t=\sqrt{(15/4\pi)}$$

$$A_4=\langle x^4+y^4+z^4\rangle$$

$$A_6=\langle x^2 y^2 z^2\rangle$$

and $$A_{4s}=\langle (x^4+y^4+z^4)^2\rangle$$

Here (x,y,z) specify the orientation of the molecule. Similarly the non-vanishing suceptibilities in the fourth order are

$$CF=\chi_{1111}=\chi_{2222}=3\chi_{1122}=\beta^3 e^4 (3/2)(9A_{4s}-6A_4+1)$$

$$CG=\chi_{3333}=\chi_{4444}=\chi_{5555}=\beta^3 t^4 (1/12)(A_{4s}-2A_4-8A_6+1)$$

$$CH=\chi_{3344}=\chi_{4455}=\chi_{5533}=\beta^3 t^4 A_6/3$$

$$CI=\chi_{1133}=\beta^3 (et)^2 (1/6)(1-A_4-18A_6)$$

$$CJ=\chi_{1144}=\chi_{1155}=\beta^3 (et)^2 (1/12)(13A_4-9A_{4s}+18A_6-4)$$

$$CK=\chi_{2233}=\beta^3(et)^2(1/6)(3A_4-2A_{4s}+6A_6-1)$$

$$CL=\chi_{2244}=\chi_{2255}=\beta^3 3(et)^2(1/12)(A_4-A_{4s}-6A_6)$$

$$CM=\chi_{1244}=-\chi_{1255}=\beta^3\sqrt{3}(et)^2(1/12)(3A_{4s}-5A_4-18A_6+2)$$

We can now express f_3 and f_4 as:

$$f_3=(-1/6)[(CA/g^3)n_1(n_1^2-3n_2^2)+6(CB/r^3)n_3n_4n_5$$

$$+(1.5CC/gr^2)(\ n_1(2n_3^2-n_4^2-n_5^2)+3^{1/2}n_2^2(n_5^2-n_4^2)))]$$

$$f_4=(1/24)[\ A_{41}(n_1^2+n_2^2)^2+A_{42}(n_3^4+n_4^4+n_5^4)$$

$$+A_{43}(n_3^2n_4^2+n_4^2n_5^2+n_5^2n_3^2)$$

$$+B_{41}n_1^2n_3^2+B_{42}n_1^2(n_4^2+n_5^2)+B_{43}n_2^2n_3^2$$

$$+B_{44}n_2^2(n_4^2+n_5^2)+B_{45}n_1n_2(n_4^2-n_5^2)\ ]$$

where $A_{41}=-CF/g^4+3/(T.g^2)+3CA^2/g^5$

$$A_{42}=-CG/r^4+3/(T.r^2)+3CC^2/(g.r^4)$$

$$A_{43}=-6CH/r^4+6/(T.r^2)+(3/r^4)(4CB^2/r-CC^2/g)$$

$$B_{41}=-6CI/(g.r)^2+6/(T.g.r)+(3/g^2r^2)(2CA.CC/g+4CC^2/r)$$

$$B_{42}=-6CJ/(g.r)^2+6/(T.g.r)+(3/g^2r^2)(CC^2/r-CC.CA/g)$$

$$B_{43}=-6CK/(gr)^2+6/(T.g.r)-(6/g^2r^2)CA.CC/g$$

$$B_{44}=-6CL/(gr)^2+6/(T.g.r)+(3/g^2r^2)(CA.CC/g+3CC^2/r)$$

$$B_{45}=-12CM/(g.r)^2+6[(3)^{1/2}/(g.r)^2](CA.CC/g+CC^2/r)$$

The B-coefficients are not all independent. In fact a symmetry analysis of the fourth order terms using polynomial invariants (syzygies) of rank 2 gives (Sah 83b)

$$B_{41}/B_{43}=(4R-1)/3;\ B_{42}/B_{43}=(R+2)/3$$

$$B_{45}/B_{43}=2(R-1)/(3)^{1/2}$$

$$R=B_{44}/B_{43}$$

These relations provide a check on the B-coefficients in equation (6.10c') that we obtain by using the parameters of equation (6.1). Before presenting our results of orientational order in CsCN, we would like to discuss about the indirect interaction matrix I which appears in equation (6.10a).

(d) Indirect Interaction

It is well known (Geh 75) that the indirect interaction matrix I is non-analytic as $\mathbf{k}\to 0$. As a result, the eigen values of the matrix I depend on the direction in which $\mathbf{k}$ approaches zero. We examine the eigen values of I along the three symmetry directions (001), (110) and (111) in the limit of long wavelengths. For CsCN we find that the lowest eigen values are realized for both (001) and (110) directions. We would like to remind the reader that in order to fit our theory to the elastic softening data, we had to choose a value of the quadrupole moment of the anion in the which was considerably reduced from its free ion value, namely f=0.15. With this choice of f, the non-vanishing elements of the indirect interaction matrix I for the (001) direction in **k**-space are:

$$I_{11}=-2A_{eff}^2/(C_{11}^0a)=-3.6K,$$

$$I_{44}=I_{55}=-B_{eff}^2/(2C_{44}^0a)=-2924K$$

For (110) direction the I matrix is complicated because there is some mixing between E_g and T_{2g} symmetries. However since this mixing is less than 2%, we ignore the mixing and confine ourselves to T_{2g} symmetry for which all elements of I have lower energy compared to those of E_g symmetry. We have

$$I_{33}=-2B_{eff}^2/[a(C_{11}^0+C_{12}^0+2C_{44}^0)]=-1447K$$

and $$I_{44}=I_{55}=I_{45}=-B_{eff}^2/[2aC_{44}^0]=-1462K.$$

Eventhough both the directions give the lowest energy in the $(n_4,\ n_5)$ space, we have preferred the (110) direction over the (001) direction for our analysis because the former gives the possibility of obtaining a lower free energy through a non-vanishing n_3 order.

(e)Results

We discuss our results for CsCN in two limiting cases of the total interaction: (i) in which the direct interaction is dominant and we assume that $I=0$ and, (ii) in which the indirect interaction is dominant (i.e. $Q=.15Q_0$ or $Q=0$). It should be reminded that in the latter case alone we were able to explain the elastic softening in CsCN (Sah 83a).

(i) In the quadrupole dominated direct interaction regime, i.e. when $f=1$, we find that $D_{11}(0)=D_{22}(0)=5916K$ and $D_{33}(0)=D_{44}(0)=D_{55}(0)=-3942K$. Thus the ordering is in a manifold which has T_{2g} symmetry. Hence putting $n_1=n_2=0$ and $n_3=n_4=n_5=n$ in the free energy we obtain

$$f_{var}=(3/2)(D_{33}(0)+1/r)n^2-(1/r^3).CB.n^3+(1/8)(A_{42}+A_{43})n^4$$

Minimizing with respect to n we find that there is a first order phase transition at $T_c=255K$; $n=.3n_0$ at $T=T_c-\varepsilon$ where $n_0=(1/3)\sqrt{(15/4\pi)}$ and $\varepsilon\to0(+)$. When the strength of the single site potential is reduced to zero (free rotator limit), we obtain $T_c=335K$ and $n=.3n_0$. Thus we see that the effect of the single site potential is to lower the transition temperature. Physically this makes sense because the single site potential has minima along (001) directions and hence disfavors ordering with T_{2g} symmetry.

(ii) Eventhough (i) provides an explanation for the first order nature of the transition and gives rise to an (111) ordering as seen in the experiment for CsCN, the direct quadrupole dominated interaction is inconsistent with elastic softening. Hence we take the reduced values of Q (with f=.15 and 0) to investigate nature of the order. For the **k**-vector along the (110) direction we find that the transition is second order with T_c=175.2K and n_3=.0005n_0, n_4=n_5=.02n_0 at $T=T_c-\varepsilon$. For Q=0, the results are not qualitatively different, although the transition temperature is increased to 209K because B_{eff} is increased.

It should be noted that if one arbitrarily increased I_{33} by a factor of 2, one could get a first order phase transition. One has this freedom in a phenomenological theory, but not in a microscopic theory. Hence although in principle we know how to obtain a first order transition in CsCN having a (111) ordering, such a transition is not compatible with values of the parameters used in the theory to explain the experimentally observed elastic softening in the high-T disordered phase.

Thus on the basis of the microscopic Hamiltonian used by us, we can understand the origin of (111) orientational order in CsCN, but the order of the transition obtained by us is different from that of experiment. We obtain a second order I-II phase transition, whereas experimentally the transition is first order. In our work we investigated the effect of quadrupole moment of the anion on TR coupling and the direct interaction between anions and also on the order of the transition. Since the cyanide ion has higher electric multipole moments (LeS 82), it would be interesting to investigate the effect of these moments on the couplings and interactions mentioned above and to the order of the transition.

CHAPTER 7

SUMMARY

In this thesis we have investigated the orientational order-disorder phase transitions in the alkali cyanides with the help of a microscopic Hamiltonian. We have tried to understand both the elastic properties of the disordered phase and the nature of orientational order in the FE phase in terms of a given microscopic Hamiltonian. We have proposed a physical mechanism, e.g. the quadrupole moment of the anion interacting with the fluctuating efg which contributes to TR coupling in the cyanides. We have showed that in the absence of this mechanism previous explanations of acoustic phonon softening become incorrect. Evidence in support of the contribution of Q of the anion to the properties of KCN crystal has come from MD simulations (Bou 81). For CsCN, the MD simulations (Kle 82) do not predict a strong dependence of the properties of phase I on the quadrupole moment of the anion. In contrast, we find that the elastic properties of CsCN depend on the quadrupole moment of the anion. Furthermore diffuse inelastic neutron scattering data for KCN and NaCN (Row 82) has established the fact that sign of the coupling constant B_{eff} is positive. This is in agreement with our theory, but does not agree with the earlier work of MN. It would be intersting to see if our prediction of a positive B_{eff} for CsCN is borne out by diffuse inelastic neutron scattering studies in this system.

This work has focused attention, for the first time, on several important competition effects in the alkali cyanides . These are: (i) competition between SR repulsion and Q-efg contribution to TR coupling, (ii) competition between SR CF potential and ordering via direct quadrupolar interaction and (iii) competition between direct and lattice mediated interactions. We have also found that the nature of this competition depends sensitively on the crystal structure. Exploring these competing mechanisms has been one of the major contributions of this thesis.

We have also studied the orientational order in the alkali cyanides by deriving an expression for the free energy based on Bogolyubov's variational theorem. We found that the third order terms in the free energy involve terms which not only have E_g and T_{2g} symmetries, but also have $E_g x T_{2g}$ mixed symmetry. This finding holds promise for explaining observed (110) order in KCN because such an order can be expressed as a combination of the two types of symmetries involed. As a concrete example of the application of our variational theory, we have investigated the cubic to trigonal distortion in CsCN. Eventhough we understand the circumstances in which our theory can give a first order phase transition, the actual parameters used in the calculation of elastic softening give a second order transition for CsCN. It would be intersting to see how inclusion of other interactions affect our results

Our study has shown that the anomalous thermoelastic properties of the cyanides can be understood by postulating a reduction in the value value of the free ion Q, e.g. 40% for NaCl structure and more than 85% for CsCl structure. One can therefore ask: what is the physical basis for such a reduction? This is a difficult question to answer and perhaps electronic band structure calculations might throw more light on this aspect of the problem. In a recent density functional calculation (LeS 82) it was found that there is no evidence for appreciable reduction of quadrupole and higher order electric multipole moments of the cyanide ions in the 'solid'. Therefore one can ask the following questions: what are the effects of including higher order ($l>2$) electric multipole moments on the TR coupling? Do these higher moments always lead to a softening of elastic constants or do they compete with quadrupolar and SR coupling terms in the TR Hamiltonian? In the former case one has to look for additional mechanisms that suppress the softening. In the latter case, on the other hand, it would be necessary to examine whether the assumption of an effective quadrupole moment is equivalent to full Q plus higher order multipole moments.

For the sake of simplicity we have assumed a very simple model for anharmonicity and obtained the parameters in a phenomenological way. One needs to investigate why anharmonicity effects are important for LA phonons and not so important for TA phonons for NaCl structure. One needs also to understand why anharmonicity effects are important for both LA and TA phonons for CsCl structure.

A source of difficulty in the study of orientational order is the non-analyticity of indirect interaction matrix $I(\mathbf{k})$ as $\mathbf{k}\rightarrow 0$. We have looked at the symmetry directions of $\mathbf{k}$ and took that direction as the ordering direction that gave minimum eigen value. One needs to find out if there is a better way of handling this non-analyticity of the lattice mediated interactions.

Another intersting question is: does the application of an external perturbation to the Hamiltonian (6.1) lead to a cross over from first order to second order behavior? If indeed such a cross over point exists then one should study the nature of elastic softening near the tricritical point. Moreover one can make a renormalization group calculation and extract the critical exponents.

We would like to conclude by saying that our work on the alkali cyanides has focused attention on the importance of some of the physical mechanisms involved in the understanding of structural phase transitions in these systems. Improvements over our work could be the starting point for further future studies.

APPENDICES

APPENDIX A

EQUIVALENCE WITH AN EARLIER THEORY

In this appendix we prove that equations (3.5) along with equation (3.6) [which were derived by MN (Mic 77a)] reduces to equation (4.13) derived by us for arbitrary **k** if we assume that direct intermolecular interactions are zero in equation (4.13). Incidentally, it may be mentioned that our method is less cumbersome because we donot have to invert matrices, whereas this is the case in the work of MN.

From equation (3.5) and (3.6), the dynamical matrix in presence of TR coupling is

$$M=[1+F.R]^{-1}M^0 \tag{A.1}$$

$$F=v\chi v^t \tag{A.2}$$

where χ, the rotational susceptibility in presence of lattice mediated interaction is given from equation (3.6) by

$$\chi^{-1}=\chi_0{}^{-1}-I$$

and

$$I=-v^tRv$$

Hence

$$R=(M^0)^{-1}=-(v^t)^{-1}Iv^{-1}$$

Let

$$F_0=v\chi_0v^t$$

where χ_0 is the bare susceptibility in the absence of any interaction. Then

$$F^{-1}=F_0^{-1}-(M^0)^{-1} \tag{A.3}$$

From equation (A.1) using equation (A.3) we obtain

$$M^0M^{-1}=(F_0^{-1}-R)^{-1}F_0^{-1}$$

which gives $$M=M^0-F_0=M^0-v\chi_0v^t \tag{A.4}$$

Since the eigenvalues of the dynamical matrices M and M^0 are ω^2 and ω_0^2 respectively, it is easy to see that equation (A.4) is the same equation (4.13) derived by us provided we put the direct interaction to be zero in the latter equation. This proves the equivalence of the two approaches.

APPENDIX B

REPRINT FROM Phys. Rev. B (Sah 82)

PHYSICAL REVIEW B VOLUME 26, NUMBER 6 15 SEPTEMBER 1982

Theory of elastic and phonon softening in ionic molecular solids. Application to alkali cyanides

D. Sahu and S. D. Mahanti
Department of Physics and Astronomy, Michigan State University, East Lansing, Michigan 48824

(Received 18 February 1982)

We have carried out a theoretical study of the effect of coupling between rotational and translational degrees of freedom first proposed by Michel and Naudts on the elastic constants and phonon frequencies of ionic molecular solids. We have applied our theory to the high-temperature plastic phase of alkali cyanides NaCN, KCN, and RbCN. We find that the competition between short-range repulsion and the interaction of the electric quadrupole moment of the CN^- ion with the fluctuating electric field gradient strongly influences the elastic softening and ferroelastic instabilities in these systems. The effect of direct intermolecular interaction and anharmonicity is found to be significant in some cases. The ferroelastic transition temperatures for the above three compounds are found to be 337.5, 190, and 179 K which compare favorably with the experimental values 255.4, 156, and 130 K if we note the mean-field nature of our theory. Within our model we can understand the qualitative differences between the cyanides and the superoxides, a similar class of compounds showing drastically different ferroelastic behavior. Our calculations provide a microscopic justification for the use of certain phenomenological parameters by Strauch *et al.* in their calculation of phonon frequencies in NaCN and KCN at 300 K.

I. INTRODUCTION

Ionic molecular solids undergo a series of structural phase transitions and show anomalous thermoelastic properties which are intimately connected with the orientational, spin, and orbital degrees of freedom of the ionic molecular species. Typical examples are alkali cyanides[1–7] (MCN), superoxides[8–10] (MO_2), azides[11] (MN_3), hydroxides[12] (MOH), and nitrites[13] (MNO_2) where M is an alkali ion. In this class cyanides are the simplest, the $(CN)^-$ molecular ion possessing only orientational degrees of freedom whereas the superoxides are perhaps the most complex, the O_2^- ion possessing all three, i.e., orientational, orbital, and spin degrees of freedom.

The structure of the highest-temperature solid phase in almost all these systems is face-centered pseudocubic, the molecules undergoing hindered rotations between several equivalent directions of minimum energy. This high-temperature solid phase (referred to as phase I in the literature) shows anomalous thermoelastic properties and the systems behave like plastic crystals. In the case of cyanides careful measurements[1–3,6] of elastic constants have been made and it is found that C_{11} and C_{44} decrease with temperature and C_{44} approaches zero at a temperature T^* where one expects a ferroelastic instability of the pseudocubic phase. However, the transition to the ferroelastic phase is usually[1–3,8,14] first order, the transition temperature T_c being higher than T^* (see Table I for values of T_c and T^* in cyanides).

The symmetry of the low-temperature phase (phase II) is different for different classes of these systems. For example, in cyanides, the orientation of the $(CN)^-$ molecular axis is along the original [110] direction[15] of the phase I; the structure of phase II is body-centered orthorhombic. In contrast, the average orientation of the superoxide molecule is parallel to the z axis, and the structure of phase II is body-centered tetragonal (CaC_2 structure). There are, however, significant fluctuations in the molecular orientations about the c axis due to the Jahn-Teller (JT) splitting of the O_2^- orbital degeneracy.[8] In this work we are primarily concerned with the cyanides and superoxides al-

TABLE I. First-order ferroelastic transition temperature T_c (experimental), extrapolated and theoretical C_{44} softening temperatures T^*, and T_{44}.

System	T_c (K)	T^* (K)	T_{44} (K)
NaCN	283.5	255.4	337.5
KCN	168	156	190
RbCN	133	130	179

though our results should be applicable to other ionic molecular solids as well.

In this paper we develop a microscopic theory of elastic softening and phonon renormalization in these systems. We analyze the effect of the orientational degrees of freedom on the elastic properties and phonons by extending the earlier work of Michel and Naudts[16] (MN). In the evaluation of the coupling between the translational and rotational degrees of freedom, we include[17] the effects of (i) short-range steric (repulsion) forces, (ii) anisotropic electrostatic forces,[18] and (iii) the effects associated with the splitting of the orbital degeneracy of the molecular ions. In addition we include the direct interaction between the molecules. We do not consider here the coupling between the spin and either the translational or the rotational degrees of freedom. Alkali superoxides show low-T structural phase transitions involving large-scale molecular reorientations (referred to as magnetogyric phase transitions) which can be understood in terms of spin-rotational coupling (see Ref. 19). This interaction does not appreciably affect the high-T ferroelastic phase transitions. One possible exception is the ordered pyrite to marcasite transition in NaO_2 (see Ref. 20) which occurs at about 200 K.

For cyanides, (iii) is not present and only (i) was considered in the earlier work[16] on elastic softening. The importance of (ii) for the cubic phase of cyanides was recently discussed by Bound *et al.*,[21] although for the noncubic phase of superoxides it has been pointed out by Mahanti and Kemeny.[20] Bound *et al.*, in their molecular dynamics calculation of the rotational-translational dynamics of KCN, NaCN, and RbCN, have found that the inclusion of the electric quadrupole moment Q of the $(CN)^-$ ion was essential to understand the experimental orientational probability distribution functions (OPDF) and other low-frequency local dynamic properties. A careful study of the interplay of (i) and (ii) in the observed[1-3] anomalous elastic softening, ferroelastic phase transitions, and phonon softening in cyanides is the main subject of this paper. In a separate paper we will report the combined effects of (i), (ii), and (iii) on the ferroelastic instabilities and apply our theory to the case of superoxides.

Our main results can be summarized as follows. Because of the large electric quadrupole moment (Q) of the $(CN)^-$ molecular ion, there is an appreciable contribution to the rotational-translational coupling (Γ_Q) arising from the interaction between Q and the fluctuating electric field gradient (EFG) present in the high-T orientationally disordered pseudocubic phase. Because of the negative sign of Q, this coupling has opposite sign to that obtained from considering short-range repulsive forces alone (to be denoted as Γ_R). We find that when $\Gamma_R \neq 0$ and $\Gamma_Q = 0$, $C_{11} \rightarrow 0$ at a temperature T_{11} which is higher than T_{44} where $C_{44} \rightarrow 0$. On the other hand, when $\Gamma_R = 0$ and $\Gamma_Q \neq 0$, $T_{44} > T_{11}$, i.e., C_{44} softens at a higher temperature than C_{11} which is observed experimentally in NaCN, KCN, and RbCN. Actually Γ_Q and Γ_R are nonzero and appreciable, with Γ_Q dominating the ferroelastic instabilities in cyanides. In contrast, Γ_R is more important in superoxides because of smaller value of Q of the O_2^- ions. As a result $C_{11} \rightarrow 0$ at higher temperature than C_{44} and since C_{11} couples to the order parameter $\langle Y_{20} \rangle$, one expects the molecules to orient parallel to the c axis, giving rise to a CaC_2 structure. This structure is seen experimentally.[8] However, for a quantitative understanding of the ferroelastic transition temperature in the superoxides one must incorporate the orbital degeneracy of the superoxide ion and go beyond simple molecular field theory.[22] Within a molecular field treatment of translational-rotational coupling and the intermolecular interaction, our theoretical transition temperature T_{44} compares favorably with the experimental values for the three cyanides (see Table I).

For a better agreement between theoretical and experimental C_{11} and C_{44} values, we find that anharmonicity effects,[23] particularly for C_{11} are very important. As a measure of the anharmonicity we take the values of dC_{11}/dT (for $T \approx 300$ K) appropriate for alkali-halide crystals and find that the observed peak in $C_{11}(T)$ for the cyanides can be understood in terms of two canceling contributions to dC_{11}/dT; one coming from anharmonicity effects and the other from the rotational-translational coupling. The results for NaCN and KCN are extremely good but for RbCN there are discrepancies.

The outline of the paper is as follows. In Sec. II we discuss the model and the Hamiltonian that we have used to study the elastic properties and phonons of ionic molecular solids. In Sec. III, a Green's-function method is used to calculate phonon frequencies and elastic constants which are renormalized by the coupling between the translational and rotational degrees of freedom. Section IV contains a brief discussion on the isothermal rotational susceptibility which plays an important role in the T dependence of elastic softening. In Sec. V, we discuss the different contributions to the translational-rotational coupling. Finally in Sec. VI we discuss our results and make comparison with earlier theories and available experiments.

II. HAMILTONIAN

A. Model

We treat the CN^- ion as a rigid dumbbell consisting of two identical centers separated by a distance $2d$. Each molecule sits in an octahedral cage (in the high-T phase) of six nearest-neighbor (NN) M^+ ions, the NN distance being a. The M^+ ions are represented by spherically symmetric charge distributions.

In addition to the electrostatic forces, there are short-range (SR) repulsive forces between the ions. This repulsion can be expressed in a Born-Mayer form,

$$V^{SR}_{\alpha\beta}(\vec r)=(C_1)_{\alpha\beta}e^{-(C_2)_{\alpha\beta}|\vec r|}\,, \tag{2.1}$$

where α (or β) stands for any one of the two atoms of the anion or cation. The constants $(C_1)_{\alpha\beta}$ and $(C_2)_{\alpha\beta}$ represent the strength and the inverse of the range of the repulsion potential, respectively. The quantities $(C_1)_{\alpha\alpha}$ and $(C_2)_{\alpha\alpha}$ are available in the literature,[24,25] and one can use the equations

$$(C_1)_{\alpha\beta}=\sqrt{(C_1)_{\alpha\alpha}(C_1)_{\beta\beta}}$$

and (2.2)

$$(C_2)_{\alpha\beta}=\tfrac{1}{2}[(C_2)_{\alpha\alpha}+(C_2)_{\beta\beta}]$$

to obtain the values of C_1 and C_2 for appropriate systems.

The short-range repulsive interaction between a $(CN)^-$ ion whose center of mass (c.m.) is at $\vec R_i$ and a M^+ ion at $\vec R_j$ is given by a sum of atom-atom potential,

$$V^{SR}_{M^+(CN)^-}(ij)=C_1\sum_{s=\pm1}e^{-C_2|\vec R_{ij}+sd\hat n_i|}\,, \tag{2.3}$$

where $\hat n_i$ is a unit vector specifying the orientation of the $(CN)^-$ ion with respect to the crystal axes. We have also assumed that both C and N atoms can be replaced by an average atom whose repulsion with M^+ is characterized by the parameters C_1 and C_2. Following MN we discuss the elastic properties of these systems using a Hamiltonian H that consists of three parts, i.e.,

$$H=H_{tr}+H_{rot}+H_{tr\text{-}rot}\,, \tag{2.4}$$

where

$$H_{tr}=\sum_{\vec k,\kappa,\mu}\frac{1}{2m_\kappa}p^\dagger_\mu(\kappa\,|\,\vec k)p_\mu(\kappa\,|\,\vec k)+\frac{1}{2}\sum_{\vec k,\kappa\kappa',\mu\mu'}C_{\mu\mu'}(\kappa\kappa'\,|\,\vec k)u^\dagger_\mu(\kappa\,|\,\vec k)u_{\mu'}(\kappa'\,|\,\vec k) \tag{2.5}$$

represents the translational part of the Hamiltonian in the harmonic approximation and is obtained by treating the ions as spherical charge distributions. For example, this part would be analogous to that of a KBr crystal.[26] Here m_κ is the mass of the κth ion (+ or −) in a unit cell, $\vec k$ is the wave vector, μ is the Cartesian component x,y,z; $C_{\mu\mu'}(\kappa\kappa'\,|\,\vec k)$ is the dynamical matrix and $\vec u,\vec p$ are the Fourier transforms of the displacements (from the fcc structure) and momentum, respectively. Here and in the following we define Fourier transforms by the equation

$$f(\vec r)=\frac{1}{\sqrt N}\sum_{\vec k}f(\vec k)e^{i\vec k\cdot\vec r}\,, \tag{2.6}$$

where N is the total number of unit cells. We will use $1/\sqrt N$ in the definition unless otherwise specified. The rotational part of H is obtained by fixing the c.m. of all the ions at fcc sites $(\vec R^0_i)$ and is given by

$$H_{rot}=\sum_{\vec k}\sum_{\lambda=1}^{2}\frac{1}{2I}L^\dagger_\lambda(\vec k)L_\lambda(\vec k)+\sum_{i=1}^{N}V_0(\hat n_i)+\sum_{\langle ij\rangle}V_d(ij)\,. \tag{2.7}$$

Here I is the moment of inertia of the dumbell about each of the two principal axes and $\vec L$ is the angular momentum. $V_0(\hat n_i)$ is the orientation-dependent single-site potential which is given by

$$V_0(\hat n_i)=C_1\sum_{j=1}^{6}\sum_{s=\pm1}e^{-C_2|\vec R^0_{ij}+sd\hat n_i|}\,. \tag{2.8}$$

Only the repulsion contributes to $V_0(\hat n_i)$ because the electric field and electric field gradient at the lattice sites vanish because of cubic symmetry. In Eq. (2.8) only NN contributions are retained because of the short-range nature of the repulsive potential. The other contribution to the cubic single-site potential will come from the anisotropic dispersion interaction between $(CN)^-$ molecules. This contribution was evaluated[20] for sodium superoxide (NaO_2) and was found to be about 6% of the short-range repulsion contribution. We expect a similar behavior for the cyanides.

We have included the term $V_d(ij)$ in Eq. (2.7) which represents the direct interaction between two $(CN)^-$ ions at sites $\vec R^0_i$ and $\vec R^0_j$. We write

$$V_d(ij)=\sum_{m=-2}^{2} A_m Y_2^m(\hat{\omega}_i)Y_2^{-m}(\hat{\omega}_j)\,, \qquad (2.9)$$

$$A_m=A_m^{QQ}+A_m^{\text{rep}}+A_m^{\text{AD}}\,. \qquad (2.10)$$

Here A_m is a measure of the strength of the direct interaction which has three main sources[27]: quadrupole-quadrupole interaction, short-range repulsion, and anisotropic dispersion, the last one arising from the fluctuating dipole moments of the $(\text{CN})^-$ ion. In addition, for cyanides there is a direct electric dipole-dipole contribution to $V_d(ij)$ and its effect will be discussed later. The unit vectors $\hat{\omega}_i$ and $\hat{\omega}_j$ are the orientations of the molecules i and j with respect to the intermolecular axis taken as polar axis. The coefficients A_m^{QQ} are explicitly given as follows:

$$\begin{aligned} A_0^{QQ}&=(24\pi/5)Q^2/(\sqrt{2}a)^5\,,\\ A_1^{QQ}&=A_{-1}^{QQ}=\tfrac{2}{3}A_0^{QQ}\,,\\ A_2^{QQ}&=A_{-2}^{QQ}=\tfrac{1}{6}A_0^{QQ}\,, \end{aligned} \qquad (2.11)$$

where Q is the quadrupole moment of the molecule. For the rest of the coefficients we refer the reader to the literature.[28]

In order to go from a system of reference where the intermolecular axis is the z axis to the crystal axis system one makes a transformation involving the Euler angles[29] $(\alpha_{ij},\beta_{ij},\gamma_{ij})$ associated with the vector $\vec{R}_{ij}^{0}$ to obtain

$$V_d(ij)=\sum_{l=0}^{4}\sqrt{4\pi(2l+1)}\sum_{m=-2}^{2}A_m\begin{bmatrix}2 & 2 & l\\ m & \bar{m} & 0\end{bmatrix}\sum_{m_1,m_2}\begin{bmatrix}2 & 2 & l\\ m_1 & m_2 & -(m_1+m_2)\end{bmatrix}$$
$$\times Y_{l,m_1+m_2}(\beta_{ij},\gamma_{ij})Y_{2m_1}(\hat{n}_i)Y_{2m_2}(\hat{n}_j)\,, \qquad (2.12)$$

where the quantities in the square brackets are the Clebsch-Gordan (CG) coefficients. Using the properties of CG coefficients one finds that only even l terms contribute in Eq. (2.12). Further if one considers only the quadrupole contribution to A_m then only the $l=4$ term survives.

Next we introduce the five symmetry-adapted spherical harmonics Y_α (see Ref. 16) through

$$Y_{2m}(\hat{n}_i)=\sum_{\alpha=1}^{5}c_{m\alpha}Y_\alpha(\hat{n}_i)\,, \qquad (2.13)$$

where the 5×5 matrix $\{c_{m\alpha}\}$ is given in Table II, and obtain

$$\sum_{\langle ij\rangle}V_d(ij)=\tfrac{1}{2}\sum_{\vec{k}}\sum_{\alpha,\beta=1}^{5}D_{\alpha\beta}(\vec{k})Y_\alpha^\dagger(\vec{k})Y_\beta(\vec{k})\,, \qquad (2.14)$$

where

$$D_{\alpha\beta}(\vec{k})=\sum_{\vec{R}\neq0}e^{i\vec{k}\cdot\vec{R}}\sum_{m_1,m_2}\sqrt{36\pi}\begin{bmatrix}2 & 2 & 4\\ m_1 & m_2 & -(m_1+m_2)\end{bmatrix}\sum_{m}A_m\begin{bmatrix}2 & 2 & 4\\ m & -m & 0\end{bmatrix}$$
$$\times Y_{4m_1+m_2}(\beta_{\vec{R}},\gamma_{\vec{R}})c_{m_1\alpha}c_{m_2\beta}\,. \qquad (2.15)$$

Here the sum $\vec{R}$ is over $(\text{CN})^-$ ions surrounding the central $(\text{CN})^-$ ion at $\vec{R}=0$.

Finally the last term in Eq. (2.4) represents a coupling between the orientational degrees of freedom Y_α of the molecular ion and the translational degrees of freedom of the anions and cations. We write

$$H_{\text{tr-rot}}=i\sum_{\vec{k},\alpha,\mu}\sum_{\kappa=\pm}Y_\alpha^\dagger(\vec{k})v_{\alpha\mu}(\kappa\,|\,\vec{k})u_\mu(\kappa\,|\,\vec{k})\,. \qquad (2.16)$$

This is obtained by displacing the center of mass from the equilibrium position, i.e., $\vec{R}_l=\vec{R}_l^0+\vec{u}_l$ and calculating terms in the Hamiltonian which are linear in the displacements $\vec{u}_l$. The elements of the coupling constant matrix $v_{\alpha\mu}$ form a 3×5 matrix. An explicit form of $v_{\alpha\mu}$ including different contributions will be given in Sec. V.

B. Phonon description

If we describe the translational degrees of freedom in terms of phonons, then H_{tr} and $H_{\text{tr-rot}}$ can be rewritten in terms of creation $(b_{j\vec{k}}^\dagger)$ and destruc-

TABLE II. Coefficients of expansion of unnormalized real order parameters Y_α in terms of Y_{2m}'s.

$m \backslash \alpha$	1	2	3	4	5
-2	0	$\sqrt{1/6}$	$i/2$	0	0
-1	0	0	0	$-\frac{1}{2}$	$i/2$
0	1	0	0	0	0
1	0	0	0	$\frac{1}{2}$	$i/2$
2	0	$\sqrt{1/6}$	$-i/2$	0	0

tion ($b_{j\vec{k}}$) operators of phonons of wave vector $\vec{k}$ and polarization index j. We have

$$H_{\mathrm{tr}}=\sum_{j,\vec{k}}\hbar\omega^0_{j\vec{k}}(b^\dagger_{j\vec{k}}b_{j\vec{k}}+\tfrac{1}{2})\ . \tag{2.17}$$

The bare phonon frequencies $\omega^0_{j\vec{k}}$ are obtained by solving the secular equation

$$|\,C_{\mu\mu'}(\kappa\kappa'\,|\,\vec{k})-\omega^{0^2}_{\vec{k}}\delta_{\mu\mu'}\delta_{\kappa\kappa'}\,|=0\ . \tag{2.18}$$

In terms of phonon creation and destruction operators, we have

$$H_{\mathrm{tr\text{-}rot}}=i\sum_{\vec{k},j,\alpha}Y^\dagger_\alpha(\vec{k})V_{\alpha j}(\vec{k})(b_{j\vec{k}}+b^\dagger_{j-\vec{k}})\ , \tag{2.19}$$

$$V_{\alpha j}(\vec{k})=(1/2\omega^0_{j\vec{k}})^{1/2}\sum_{\mu,\kappa}\frac{1}{\sqrt{m_\kappa}}e_\mu(\kappa\,|\,\vec{k}j)v_{\alpha\mu}(\kappa\,|\,\vec{k})\ . \tag{2.20}$$

In Eq. (2.20), $e_\mu(\kappa\,|\,\vec{k}j)$ gives the μth component of polarization vector for κ-type ion for the mode $j\vec{k}$. $V_{\alpha j}(\vec{k})$ is determined from a knowledge of bare phonon frequencies, the masses, polarization vectors, and the coefficients $v_{\alpha\mu}$.

III. RENORMALIZATION OF PHONON FREQUENCIES AND ELASTIC CONSTANTS

The rotation-phonon coupling [Eq. (2.19)] renormalizes the phonon frequencies from their bare value $\omega^0_{j\vec{k}}$. We use the Zubarev's Green's-function method[30] to obtain the renormalized phonon frequencies $\omega_{j\vec{k}}$. We define the time- and temperature-dependent retarded Green's function G by

$$G_{j\vec{k}}(t-t')=\frac{1}{i}\langle[\phi_{j\vec{k}}(t),\phi^\dagger_{j\vec{k}}(t')]\rangle\Theta(t-t')\ , \tag{3.1}$$

where $\phi_{j\vec{k}}(t)=b_{j\vec{k}}(t)+b^\dagger_{j-\vec{k}}(t)$ is the phonon field operator in the Heisenberg representation. The square bracket is the commutator, $\langle\ \rangle$ stands for the average over a grand canonical ensemble, and $\Theta(t-t')$ is the step function. The equation of motion for G is

$$\begin{aligned}i\frac{d}{dt}G_{j\vec{k}}(t-t')&=\delta(t-t')\langle[\phi_{j\vec{k}}(t),\phi^\dagger_{j\vec{k}}(t')]\rangle\\&\quad+\frac{1}{i}\Theta(t-t')\langle[[\phi_{j\vec{k}}(t),H],\phi^\dagger_{j\vec{k}}(t')]\rangle\ .\end{aligned} \tag{3.2}$$

For simplicity of notation let $\omega_0=\omega^0_{j\vec{k}}$ and $\phi_{j\vec{k}}=\phi_{j\vec{k}}$ ($t=0$). The Fourier transform of $G_{j\vec{k}}(t-t')$ is given by the equation

$$\begin{aligned}\omega\langle\langle\phi_{j\vec{k}};\phi^\dagger_{j\vec{k}}\rangle\rangle_\omega&=\langle[\phi_{j\vec{k}},\phi^\dagger_{j\vec{k}}]\rangle\\&\quad+\langle\langle[\phi_{j\vec{k}},H];\phi^\dagger_{j\vec{k}}\rangle\rangle_\omega\ ,\end{aligned} \tag{3.3}$$

where

$$\langle\langle\phi_{j\vec{k}};\phi^\dagger_{j\vec{k}}\rangle\rangle_\omega\equiv G_{j\vec{k}}(\omega)=\int_{-\infty}^{\infty}G_{j\vec{k}}(t)e^{i\omega t}dt\ . \tag{3.4}$$

Since $b_{j\vec{k}}$ and $b^\dagger_{j\vec{k}}$ satisfy the usual boson commutation relations, we obtain

$$\begin{aligned}&[\phi_{j\vec{k}},H_{\mathrm{tr}}]=\omega_0\psi_{j\vec{k}}\ ,\\&[\phi_{j\vec{k}},H_{\mathrm{rot}}]=[\phi_{j\vec{k}},H_{\mathrm{tr\text{-}rot}}]=0\ ,\\&[\psi_{j\vec{k}},H_{\mathrm{tr}}]=\omega_0\phi_{j\vec{k}}\ ,\end{aligned} \tag{3.5}$$

where

$$\psi_{j\vec{k}}=b_{j\vec{k}}-b^\dagger_{j\vec{k}}\ . \tag{3.6}$$

Using the above equalities it follows that

$$\begin{aligned}(\omega^2-\omega_0^2)\langle\langle\phi_{j\vec{k}};\phi^\dagger_{j\vec{k}}\rangle\rangle_\omega&\\=2\omega_0\left[1+\sum_\alpha V^*_{\alpha j}\langle\langle Y_\alpha;\phi^\dagger_{j\vec{k}}\rangle\rangle_\omega\right]&,\end{aligned} \tag{3.7}$$

and

$$\omega\langle\langle Y_\alpha;\phi^\dagger_{j\vec{k}}\rangle\rangle_\omega=\langle\langle Y_{1,\alpha};\phi^\dagger_{j\vec{k}}\rangle\rangle_\omega\ , \tag{3.8}$$

where

$$Y_{1,\alpha}(\vec{k})\equiv[Y_\alpha(\vec{k}),H_{\mathrm{rot}}]\ . \tag{3.9}$$

It is clear that to obtain the Green's functions on the right-hand side (RHS) of Eq. (3.7) one needs the Green's function on the RHS of Eq. (3.8) and the hierarchy of equations extends to infinity. We further write

$$Y_{r,\alpha}(\vec{k})=[Y_{r-1,\alpha}(\vec{k}),H_{\mathrm{rot}}]\quad(r=2,3,\ldots,\infty)\ . \tag{3.10}$$

Note that the operators $Y_{1,\alpha}, Y_{2,\alpha}, \ldots$ do not contain the operators b and $b^{\dagger}$ and hence commute with ϕ and H_{tr}. Hence one can write, using Eq. (2.19),

$$\omega \langle\langle Y_{1,\alpha};\phi^{\dagger}_{j\vec{k}}\rangle\rangle_{\omega} \approx \langle\langle Y_{2,\alpha};\phi^{\dagger}_{j\vec{k}}\rangle\rangle_{\omega} + \sum_{\beta\vec{k}} V_{\beta j}(\vec{k}) \langle [Y_{1,\alpha}(\vec{k}), Y_{\beta}(\vec{k})]\rangle \langle\langle \phi_{j\vec{k}};\phi^{\dagger}_{j\vec{k}}\rangle\rangle_{\omega} \,. \tag{3.11}$$

In obtaining Eq. (3.11) we have replaced the commutator $[Y_{1,\alpha}, Y^{\dagger}_{\beta}]$ by its average value. This is equivalent to a random-phase approximation. We can now generalize Eq. (3.11) to higher-order Green's functions and obtain

$$[\omega^2-\omega_0^2-\Sigma_{j\vec{k}}(\omega)]\langle\langle \phi_{j\vec{k}};\phi^{\dagger}_{j\vec{k}}\rangle\rangle_{\omega} = 2\omega_0 \,, \tag{3.12}$$

where the phonon self-energy $\Sigma_{jk}(\omega)$ is given by

$$\Sigma_{j\vec{k}}(\omega) = 2\omega_0 \sum_{\alpha\beta} V^{*}_{\alpha j}(k) V_{\beta j}(\vec{k}) \sum_{r=1}^{\infty} \frac{1}{\omega^{r+1}} \langle [Y_{r,\alpha}(\vec{k}), Y^{\dagger}_{\beta}(\vec{k})]\rangle \,. \tag{3.13}$$

We will now relate the phonon self-energy to the frequency and wave-vector-dependent rotational susceptibility $\chi_{\alpha\beta}(\vec{k},\omega)$.

The rotational susceptibility is defined by a related orientational Green's function,

$$\chi_{\alpha\beta}(\vec{k},t-t') = -\frac{1}{i}\langle [Y_{\alpha}(\vec{k},t), Y^{\dagger}_{\beta}(\vec{k},t')]\rangle \Theta(t-t') \,. \tag{3.14}$$

The time Fourier transform of $\chi_{\alpha\beta}(\vec{k},t-t')$ is given by the equation

$$\chi_{\alpha\beta}(\vec{k},\omega) = -\langle\langle Y_{\alpha}(\vec{k});Y_{\beta}(\vec{k})\rangle\rangle_{\omega} = -\frac{1}{i}\int_{-\infty}^{\infty} dt\, e^{i\omega t}\Theta(t-t')\langle [Y_{\alpha}(\vec{k},t), Y^{\dagger}_{\beta}(\vec{k},t')]\rangle \,, \tag{3.15}$$

$$\omega\langle\langle Y_{\alpha}(\vec{k});Y_{\beta}(\vec{k})\rangle\rangle_{\omega} = \langle\langle Y_{1,\beta}(\vec{k}), Y^{\dagger}_{\beta}(\vec{k})\rangle\rangle_{\omega} \,. \tag{3.16}$$

Let us assume that the rotational response is determined by H_{rot} alone. With this approximation, which is equivalent to the assumption that rotational dynamics has a faster time scale compared to translation,[31] we obtain

$$\omega\langle\langle Y_{1,\alpha};Y^{\dagger}_{\beta}\rangle\rangle_{\omega} = \langle [Y_{1,\alpha}, Y^{\dagger}_{\beta}]\rangle + \langle\langle Y_{2,\alpha};Y^{\dagger}_{\beta}\rangle\rangle_{\omega} \,. \tag{3.17}$$

Generalizing this procedure to higher-order Green's functions, we obtain

$$\langle\langle Y_{\alpha};Y^{\dagger}_{\beta}\rangle\rangle_{\omega} = \sum_{r=1}^{\infty} \langle [Y_{r,\alpha}(\vec{k}), Y^{\dagger}_{\beta}(\vec{k})]\rangle \frac{1}{\omega^{r+1}} \,. \tag{3.18}$$

Using Eqs. (3.18) and (3.15) in Eq. (3.13) we get

$$\Sigma_{j\vec{k}}(\omega) = -2\omega_0 \sum_{\alpha,\beta} V^{*}_{\alpha j}(\vec{k}) V_{\beta j}(\vec{k}) \chi_{\alpha\beta}(\vec{k},\omega) \,. \tag{3.19}$$

Thus from (3.11) and (3.18) and noting that the renormalized phonon frequencies $\omega_{j\vec{k}}$ are obtained from the poles of the Green's function $\langle\langle \phi_{j\vec{k}};\phi^{\dagger}_{j\vec{k}}\rangle\rangle_{\omega}$, we get

$$\omega^2_{j\vec{k}} = \omega^{0^2}_{j\vec{k}} - 2\omega^0_{j\vec{k}} \sum_{\alpha,\beta} V^{*}_{\alpha j}(\vec{k}) \chi_{\alpha\beta}(\vec{k},\omega) V_{\beta j}(\vec{k}) \,. \tag{3.20}$$

The above equation ignores vertex corrections and is not adequate when the time scales of rotational and translational dynamics are comparable. However, we are primarily interested in the elastic softening ($\omega_{j\vec{k}} \to 0$) at relatively high temperatures where the rotational motion is rapid and the above approximation is quite reasonable. For the calculation of phonon frequencies at finite $\vec{k}$ particularly when $\omega_{jk} \sim \omega_{\text{rot}}$, where ω_{rot} is a characteristic rotational frequency, one has to consider the frequency dependence[31] of $\chi_{\alpha\beta}(\vec{k},\omega)$ and also include vertex corrections.

From Eq. (3.20) one can easily obtain the effect of rotational-translational coupling on the elastic constants by choosing $\vec{k}$ along several symmetry directions and studying the frequencies of longitudinal and transverse phonons in the limit $\vec{k},\omega \to 0$. The details of the calculation of $\chi_{\alpha\beta}(\vec{k},0)$ are discussed in Sec. IV and in Sec. V, we will give explicit expressions for the renormalized elastic constants.

IV. ROTATIONAL SUSCEPTIBILITY $\chi_{\alpha\beta}(\vec{k},\omega=0)$

For the calculation of elastic constants and phonon frequencies we replace $\chi_{\alpha\beta}(\vec{k},\omega)$ by its static values $\chi_{\alpha\beta}(\vec{k})\equiv\chi_{\alpha\beta}(\vec{k},\omega=0)$. This is adequate for the elastic constants and the limitations for phonon frequency calculation will be discussed in Sec. VI E. $\chi_{\alpha\beta}(\vec{k})$ is the static susceptibility of an isolated system subjected to an adiabatic perturbation. Following the commonly made approximation for large systems we replace $\chi_{\alpha\beta}(\vec{k})$ by the isothermal susceptibility $\chi^{T}_{\alpha\beta}(\vec{k})$, i.e., we assume that $\chi_{\alpha\beta}(\vec{k})\approx\chi^{T}_{\alpha\beta}(\vec{k})$ even though the differences between the two need not be zero in general.[32] Next we calculate $\chi^{T}_{\alpha\beta}(\vec{k})$ in the presence of only the direct intermolecular interaction $D_{\alpha\beta}(\vec{k})$ using a molecular field approximation.

The rotational response is determined by H_{rot}, which is replaced by its mean-field value H_{MF}:

$$H_{\text{MF}}=\sum_{\alpha,\beta,\vec{k}} D_{\alpha\beta}(\vec{k})Y_{\alpha}(\vec{k})m_{\beta}(\vec{k})+\sum_{i} V_0(\hat{n}_i)\,, \tag{4.1}$$

where

$$m_{\beta}(\vec{k})=\langle Y_{\beta}(\vec{k})\rangle\,. \tag{4.2}$$

We apply a staggered external field $h_{\beta}(\vec{k})$ which adds a term H_{ext} to the Hamiltonian H_{MF},

$$H_{\text{ext}}=-\sum_{\beta} h_{\beta}(\vec{k})Y_{\beta}(\vec{k})\,, \tag{4.3}$$

and calculate the susceptibility χ in the limit when the external field vanishes. In the presence of $h_{\beta}(\vec{k})$

$$m_{\alpha}(\vec{k}')=\frac{\text{Tr}e^{-(1/k_BT)(H_{\text{MF}}+H_{\text{ext}})}Y^{\dagger}_{\alpha}(\vec{k}')}{\text{Tr}e^{-(1/k_BT)(H_{\text{MF}}+H_{\text{ext}})}}\,. \tag{4.4}$$

The generalized susceptibility matrix $\chi_{\alpha\beta}(\vec{k},\vec{k}')$, defined by the equation

$$\chi_{\alpha\beta}(\vec{k}',\vec{k})\equiv\lim_{h_{\beta}\to 0}\frac{\partial}{\partial h_{\beta}(\vec{k})}m_{\alpha}(\vec{k}')\,, \tag{4.5}$$

is found to satisfy the matrix integral equation,

$$\chi_{\alpha\beta}(\vec{k}',\vec{k})=\chi^{0}_{\alpha\beta}(\vec{k}',\vec{k})-\sum_{\alpha'\beta'\vec{k}''}\chi^{0}_{\alpha\alpha'}(\vec{k}',\vec{k}'')\times D_{\alpha'\beta'}(\vec{k}'')\chi_{\beta'\beta}(\vec{k}'',\vec{k})\,, \tag{4.6}$$

where

$$\chi^{0}_{\alpha\beta}(\vec{k},\vec{k}')=\frac{1}{k_BT}[\langle Y^{+}_{\alpha}(\vec{k}')Y_{\beta}(\vec{k})\rangle-\langle Y^{+}_{\alpha}(\vec{k}')\rangle\langle Y_{\beta}(\vec{k})\rangle]\,, \tag{4.7}$$

the thermal averages being taken in the absence of H_{ext}. For the disordered phase $\langle Y^{+}_{\alpha}(\vec{k})\rangle=0$ and $H_{\text{MF}}=\sum_i V_0(\hat{n}_i)$ and we have

$$\chi^{0}_{\alpha\beta}(\vec{k}',\vec{k})=\chi^{0}_{\alpha\beta}\,\delta_{\vec{k},\vec{k}'}\,, \tag{4.8}$$

where $\chi^{0}_{\alpha\beta}$ is the $\vec{k}$-independent single-site susceptibility.[16] In this case $\chi_{\alpha\beta}(\vec{k},\vec{k}')$ is diagonal in the $\vec{k}$ index and defining $\chi_{\alpha\beta}(\vec{k})\equiv\chi_{\alpha\beta}(\vec{k},\vec{k})$, we obtain

$$\chi_{\alpha\beta}(\vec{k})=\chi^{0}_{\alpha\beta}-\sum_{\alpha'\beta'}\chi^{0}_{\alpha\alpha'}D_{\alpha'\beta'}(\vec{k})\chi_{\beta'\beta}(\vec{k})\,. \tag{4.9}$$

From Eq. (4.9) one obtains, symbolically, the formal solution

$$\chi=(1+\chi^{0}D)^{-1}\chi^{0}\,. \tag{4.10}$$

As shown in Ref. 16 because of cubic symmetry χ^{0} is a diagonal matrix with

$$\chi^{0}_{\alpha\alpha}=(\chi^{0}_{11},3\chi^{0}_{11},\chi^{0}_{33},\chi^{0}_{33},\chi^{0}_{33})\,, \tag{4.11}$$

where the first two quantities have e_g symmetry and the last three have t_{2g} symmetry. Similarly in the $\vec{k}\to 0$ limit $D(\vec{k})$ is diagonal with

$$D_{\alpha\alpha}(\vec{k}\to 0)=(D^{0}_{11},\tfrac{1}{3}D^{0}_{11},D^{0}_{33},D^{0}_{33},D^{0}_{33})\,. \tag{4.12}$$

From (4.8)–(4.10) it follows that in the $\vec{k}\to 0$ limit χ is diagonal with

$$\chi_{\alpha\alpha}=(\chi_{11},3\chi_{11},\chi_{33},\chi_{33},\chi_{33})\,.$$

The $\vec{k}$-independent susceptibility $\chi^{0}_{\alpha\beta}(T)$ is calculated from

$$\chi^{0}_{\alpha\beta}(T)=\frac{1}{k_BT}\frac{\int e^{-V_0(\theta,\phi)/k_BT}Y^{*}_{\alpha}(\theta,\phi)Y_{\beta}(\theta,\phi)\sin\theta\,d\theta\,d\phi}{\int e^{-V_0(\theta,\phi)/k_BT}\sin\theta\,d\theta\,d\phi}\,. \tag{4.13}$$

V. ROTATIONAL-TRANSLATIONAL COUPLING COEFFICIENTS

As discussed in the Introduction, there are two main physical sources that contribute to the rotational-translational coupling matrix $v_{\alpha\mu}(\kappa\mid\vec{k})$ and we write down this as a sum of two parts,

$$v_{\alpha\mu}(\kappa\,|\,\vec{k})=v^{R}_{\alpha\mu}(\kappa\,|\,\vec{k})+v^{\text{EFG}}_{\alpha\mu}(\kappa\,|\,\vec{k})\quad(\kappa=\pm)\,, \tag{5.1}$$

where $v^{R}_{\alpha\mu}(\kappa\,|\,\vec{k})$ denotes the short-range repulsion contribution and $v^{\text{EFG}}_{\alpha\mu}(\kappa\,|\,\vec{k})$ denotes the contribution coming from the interaction between electric quadrupole moment of the $(\text{CN})^-$ ion and the fluctuating EFG produced at its site by all the other ions (taken to be point charges). We denote by 1,2,3,... the contributions from first, second, third, etc., ... neighbors, respectively, which have charges +, −, +, and so on. Then

$$v^{i}_{\alpha\mu}(+\,|\,\vec{k})=v^{i}_{\alpha\mu}(+\,|\,\vec{k})_1+v^{i}_{\alpha\mu}(+\,|\,\vec{k})_3+\cdots\quad(i=R,\ \text{EFG})\,, \tag{5.2a}$$

$$v^{i}_{\alpha\mu}(-\,|\,\vec{k})=v^{i}_{\alpha\mu}(-\,|\,\vec{k})_2+v^{i}_{\alpha\mu}(-\,|\,\vec{k})_4+\cdots\quad(i=R,\ \text{EFG})\,. \tag{5.2b}$$

Following Michel and Naudts[16] we will take $v^{R}_{\alpha\mu}(\kappa\,|\,\vec{k})=v^{R}_{\alpha\mu}(+\,|\,\vec{k})_1$ because the short-range repulsion falls off rapidly with distance. In calculating $v^{\text{EFG}}_{\alpha\mu}(\kappa\,|\,\vec{k})$ we include contributions up to fourth neighbors only, further neighbors making insignificant contributions since the interaction falls off as $1/r^4$.

A. Short-range repulsion contribution $v^{R}_{\alpha\mu}(+\,|\,\vec{k})_1$

The coefficients v^R in $\vec{k}$ space can be obtained from their $\vec{r}$-space values through the relation

$$v^{R}_{\alpha\mu}(+\,|\,\vec{k})_1=\sum_{nn}v^{R}_{\alpha\mu}(+\,|\,\vec{R}^{0}_{ij})e^{i\vec{k}\cdot\vec{R}^{0}_{ij}}\,, \tag{5.3}$$

where the sum is to be carried over all the NN positions $\vec{R}^{0}_{ij}$ given by $(\pm a\hat{x},0,0)$, $(0,\pm a\hat{y},0)$, $(0,0,\pm a\hat{z})$. From Ref. 16 we have

$$v^{R}_{\alpha\mu}(+\,|\,a\hat{x})_1=\begin{bmatrix}A_R & -A_R & 0 & 0 & 0\\ 0 & 0 & B_R & 0 & 0\\ 0 & 0 & 0 & B_R & 0\end{bmatrix},$$

$$v^{R}_{\alpha\mu}(+\,|\,a\hat{y})_1=\begin{bmatrix}0 & 0 & B_R & 0 & 0\\ A_R & A_R & 0 & 0 & 0\\ 0 & 0 & 0 & 0 & B_R\end{bmatrix}, \tag{5.4}$$

$$v^{R}_{\alpha\mu}(+\,|\,a\hat{z})_1=\begin{bmatrix}0 & 0 & 0 & B_R & 0\\ 0 & 0 & 0 & 0 & B_R\\ -2A_R & 0 & 0 & 0 & 0\end{bmatrix}.$$

The quantities A_R and B_R depend on C_1, C_2, d, and a. They are explicitly given in Eqs. (A13) and (A15) of Ref. 16. The values of C_1, C_2, d, and a for the cyanides are given in Table III and the values of A_R and B_R are given in Table IV. The Fourier-transformed quantities $v^{R}_{\alpha\mu}(+\,|\,\vec{k})_1$ are then

$$v^{R}_{\alpha\mu}(+\,|\,\vec{k})_1=2\begin{bmatrix}A_RS_x & -A_RS_x & B_RS_y & B_RS_z & 0\\ A_RS_y & A_RS_y & B_RS_x & 0 & B_RS_z\\ -2A_RS_z & 0 & 0 & B_RS_x & B_RS_y\end{bmatrix}, \tag{5.5}$$

where

$$S_i=\sin k_ia,\quad C_i=\cos k_ia\quad(i=x,y,z)\,. \tag{5.6}$$

B. Calculation of $v^{\text{EFG}}_{\alpha\mu}(\kappa\,|\,\vec{k})$

As the lattice vibrates there is deviation from the local cubic symmetry at the positions of the molecules and the resulting EFG couples to Q. To the lowest order in displacement this leads to an additional coupling between rotation and translation with strength given by $v^{\text{EFG}}_{\alpha\mu}(\kappa\,|\,\vec{k})$. Depending on the sign of the quadrupole moment Q the net rotation translation coupling is either enhanced or suppressed.

TABLE III. Repulsion parameters (C_1,C_2), lattice constant (a), molecular size $(2d)$, and free-ion quadrupole moment value (Q_0). See Eq. (2.11) for A_0^{QQ}.

	NaCN	KCN	RbCN
C_1 (10^7 K)	1.013	2.347	3.421
C_2 (Å^{-1})	3.3382	3.3382	3.3382
a (Å)	2.944	3.250	3.415
d (Å)	0.615	0.600	0.575
Q_0 (10^{-10} esu Å^2)	−4.64	−4.64	−4.64
A_0^{QQ} (K)	1870	1143	892

TABLE IV. Repulsion (A_R, B_R) and quadrupolar (A_Q, B_Q) contributions to the translation-rotation coupling.

	NaCN	KCN	RbCN
$Q=$	$0.6Q_0$	$0.6Q_0$	$0.6Q_0$
A_R (K/Å)	5578	4379	3323
B_R (K/Å)	−1390	−988	−713
A_Q (K/Å)	−3065	−2064	−1693
B_Q (K/Å)	2503	1685	1382
B_R/A_R	−0.249	−0.226	−0.215
B_Q/A_Q	−0.816	−0.816	−0.816

The quadrupole EFG interaction can be written as[33]

$$H'=\frac{1}{6}\sum_{i}\sum_{\mu,\nu}Q^{i}_{\mu\nu}U^{i}_{\mu\nu}\,, \tag{5.7}$$

where the Cartesian components of the quadrupole moment and the field gradient tensor at site i are

$$\begin{aligned} Q^{i}_{\mu\nu}&=\int(3x_{i\mu}x_{i\nu}-\delta_{\mu\nu}r_i^2)\rho(\vec{r}_i)\,d\vec{r} \\ &\qquad(\mu,\nu=x,y,z;\vec{r}_i=\vec{r}-\vec{R}_i)\,, \end{aligned} \tag{5.8}$$

$$\begin{aligned} U^{i}_{\mu\nu}&=\frac{\partial}{\partial X_\mu}\frac{\partial}{\partial X_\nu}U(\vec{X}) \\ &=\frac{\partial}{\partial X_\mu}\frac{\partial}{\partial X_\nu}\sum_j{}'\frac{q_j}{|\vec{R}_i-\vec{R}_j|}\quad(\vec{X}\in\vec{R}_i)\,. \end{aligned} \tag{5.9}$$

Here $\rho(\vec{r}_i)$ is the charge density at the site i and $U(\vec{R}_i)$ is the electrostatic potential at the ith site due to all other charges q_j at the $\vec{R}_j$. We can express $Q^{i}_{\mu\nu}$ as a linear combination of spherical quadrupole moment tensors of rank 2 defined by

$$Q^{i}_{2m}=\int r_i^2Y_{2m}(\hat{r}_i)\rho(\vec{r}_i)\,d\vec{r} \tag{5.10}$$

so that Eq. (5.7) can be rewritten as

$$H'=\sum_i\sum_{m=-2}^{2}Q^{i}_{2m}U_2^{-m}(i)\,, \tag{5.11}$$

where U_2^{-m}'s are appropriate linear combinations of $U^{i}_{\mu\nu}$'s. Since Q is measured with respect to molecular axes (MA) one should transform from the lab axes to the molecular axes, i.e.,

$$Q^{i}_{2m}=Y_{2m}(\hat{n}_i)Q\,, \tag{5.12}$$

$$Q=\int\left[\left(\frac{3z^2-r^2}{2}\right)\rho(\vec{r})\,d\vec{r}\right]_{\mathrm{MA}}\,. \tag{5.13}$$

Using (5.11) and (5.12) we can write

$$H'=Q\sum_i\sum_{\alpha=1}^{5}Y_\alpha(\hat{n}_i)U^{i}_{\alpha}\,, \tag{5.14}$$

where (dropping the superscript i in U^{i}_{α})

$$\begin{aligned} U_1&=\sqrt{\pi/5}\,U_{zz}\,, \\ U_2&=\sqrt{\pi/45}\,(U_{xx}-U_{yy})\,, \\ U_3&=-\sqrt{2\pi/15}\,U_{xy}\,, \\ U_4&=-\sqrt{2\pi/15}\,U_{xz}\,, \\ U_5&=-\sqrt{2\pi/15}\,U_{yz}\,. \end{aligned} \tag{5.15}$$

The components $U_{\mu\nu}$ are obtained from Eq. (5.9), i.e.,

$$\begin{aligned} U^{i}_{\mu\nu}=\sum_j\frac{3q_j}{X_{ij}^4}&[(\hat{X}_{ij\nu}u_{j\mu}+\hat{X}_{ij\mu}u_{j\nu}) \\ &-(5\hat{X}_{ij\mu}\hat{X}_{ij\nu}-\delta_{\mu\nu})\vec{X}_{ij}\cdot\vec{U}_j]\,, \end{aligned} \tag{5.16}$$

where $\vec{X}_{ij}=\vec{R}^0_j-\vec{R}^0_i$, $\hat{X}_{ij}=\vec{X}_{ij}/X_{ij}$, and $X_{ij\nu}$ is the νth component of $\hat{X}_{ij}$. In obtaining Eq. (5.16), because of inversion symmetry the $\vec{u}_i$ terms drop out when the sum over j is carried out. Finally one obtains the coefficients $v^{\mathrm{EFG}}_{\alpha\mu}(\kappa\,|\,\vec{X}_{ij})$ and its Fourier components from the identity

$$\begin{aligned} H'&=\sum_i Y_\alpha(\hat{r}_i)U^{i}_{\alpha} \\ &\equiv\sum_{i,j,\alpha,\mu}Y_\alpha(\hat{n}_i)v^{\mathrm{EFG}}_{\alpha\mu}(\vec{X}_{ij})u_{j\mu} \\ &\equiv i\sum_{\vec{k},\mu,\kappa}Y^{\dagger}_{\alpha}(\vec{k})v^{\mathrm{EFG}}_{\alpha\mu}(\kappa\,|\,\vec{k})u_\mu(\kappa\,|\,\vec{k})\,. \end{aligned} \tag{5.17}$$

The quantities $v^{\mathrm{EFG}}_{\alpha\mu}(\kappa\,|\,\vec{k})$ have been explicitly calculated in Appendix A.

C. Elastic limit

To extract information regarding the elastic constants C_{ij}, we take the long-wavelength limit $(\vec{k}\rightarrow0)$ and retain the leading terms in sines and cosines and obtain

$$v_{\alpha\mu}(+\,|\,\vec{k})+v_{\alpha\mu}(-\,|\,\vec{k})=2a\begin{vmatrix} A_{\mathrm{eff}}k_x & -A_{\mathrm{eff}}k_x & B_{\mathrm{eff}}k_y & B_{\mathrm{eff}}k_z & 0 \\ A_{\mathrm{eff}}k_y & A_{\mathrm{eff}}k_y & B_{\mathrm{eff}}k_x & 0 & B_{\mathrm{eff}}k_z \\ -2A_{\mathrm{eff}}k_z & 0 & 0 & B_{\mathrm{eff}}k_x & B_{\mathrm{eff}}k_y \end{vmatrix}\,, \tag{5.18}$$

where

$$A_{\text{eff}}=A_R+\alpha A_Q\ , \tag{5.19a}$$

$$B_{\text{eff}}=B_R+\alpha B_Q\ , \tag{5.19b}$$

and

$$A_Q=\sqrt{9\pi/5}\,\frac{Q\,|e\,|}{a^4}=-\sqrt{3/2}B_Q\ ,$$

$$\alpha=1+1/(4\sqrt{2})-8/(27\sqrt{3})-\tfrac{1}{16}+\cdots\ . \tag{5.20}$$

1. *Case 1*

For a wave along [001] direction we take $k_x=k_y=0$ and $k_z=k$ and consider the frequencies of LA and TA branches.[34] The longitudinal acoustic (LA) frequency in the limit $\vec{k}\to 0$ is given by

$$\omega_{\text{LA}}^2=(C_{11}/\rho)k^2 \tag{5.21a}$$

and the polarization of the vibration is

$$e_\mu(\kappa\,|\,\vec{k})=\sqrt{m_\kappa/m}\begin{bmatrix}0\\0\\1\end{bmatrix}, \tag{5.21b}$$

where m_κ is the mass of the κ-type ion, $m=m_+ + m_-$, and ρ is the mass density $(m/2a^3)$. Substituting (5.18) and (5.21) in (2.20) and using (3.20) we obtain

$$C_{11}=C_{11}^0-\frac{8}{a}A_{\text{eff}}^2\chi_{11}(T)\ . \tag{5.22}$$

Similarly for the transverse acoustic branch (TA), using

$$\omega_{\text{TA}}^2=(C_{44}/\rho)k^2$$

and

$$e_\mu(\kappa\,|\,\vec{k})=\sqrt{m_\kappa/m}\begin{bmatrix}1\\0\\0\end{bmatrix},$$

we obtain

$$C_{44}=C_{44}^0-\frac{2}{a}B_{\text{eff}}^2\chi_{44}(T)\ . \tag{5.23}$$

2. *Case 2*

For a wave propagating along the [110] direction, we take $k_x=k_y=k/\sqrt{2}$, $k_z=0$. For a TA wave in the xy plane, using

$$\omega_{\text{TA}}^2=k^2(C_{11}-C_{12})/(2\rho)$$

and

$$e_\mu(\kappa\,|\,\vec{k})=\sqrt{m_k/m}\;1/\sqrt{2}\begin{bmatrix}1\\-1\\0\end{bmatrix},$$

we obtain

$$C_{12}=C_{12}^0+\frac{4}{a}A_{\text{eff}}^2\chi_{11}(T)\ . \tag{5.24}$$

Equations (5.22)–(5.24) are in agreement with the results of Ref. 16 when $Q=0$, although they have been derived in a completely different way. These equations will be used in the next section to study the T dependence of the elastic constants for the cyanides.

VI. RESULTS AND DISCUSSION

The temperature dependence of elastic constants C_{11}, C_{44}, and C_{12} given in Eqs. (5.22)–(5.24) depend upon (i) the short-range repulsion (A_R,B_R) and quadrupole contributions (A_Q,B_Q) to the translational rotational coupling, and (ii) the rotational susceptibility $\chi_{\alpha\beta}(\vec{k})$ obtained in the presence of direct interaction $D_{\alpha\beta}(\vec{k})$. The T dependence of $\chi_{\alpha\beta}(\vec{k})$ comes from that of $\chi_{\alpha\beta}^0$, the single-site susceptibility. From Eq. (4.13) we see that apart from the $1/k_BT$ factor, the T dependence of $\chi_{\alpha\beta}^0(\vec{k})$ is determined by the single-site potential $V_0(\hat{n}_i)$. In the cubic phase, the electric field and the electric field gradient vanish at the lattice sites and therefore the only contribution to $V_0(\hat{n}_i)$ comes from the repulsive (steric) forces and because of the short-range nature of the latter only the neighboring cations contribute to $V_0(\hat{n}_i)$. In Fig. 1 we give the (θ,ϕ) dependence of $V_0(\hat{n}_i)$ for KCN which shows the four minima along the [111] and equivalent body-diagonal directions. The maxima are along the [±100], [0±10], [00±1], and the saddle points are along the [110] and its equivalent directions. The values and the T dependence of the different components of the single-site susceptibility χ_{ii}^0 are determined by the strength of the repulsion and will be discussed in detail later. For the superoxides, there is an additional contribution to $V_0(\hat{n}_i)$ which comes from the splitting of the orbital degeneracy of the O_2^- ion as the molecule orients away from the symmetry directions.[20]

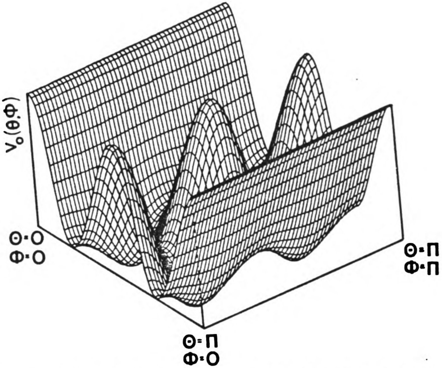

FIG. 1. Single-site potential $V_0(\theta,\phi)$ for KCN. $V_0(0,0)=9914$ K (max); $V_0(\theta_0,\pi/4)=8350$ K (min), where $\theta_0=54°$; $V_0(\pi/2,\pi/4)=8387$ K (saddle point). θ is measured from the [001] and ϕ from the [100] axis.

A. Repulsion parameters and quadrupole moment

In the present and all earlier[16,21] calculations, C and N atoms of the $(CN)^-$ molecule have been assumed to be equivalent so far as the strength of atom-atom repulsion is concerned. In other words, the repulsion parameter between a positive ion M and any one atom of the CN molecule is given by

$$\begin{aligned} C_1 &= \sqrt{(C_1)_{M\text{-}C}(C_1)_{M\text{-}N}}\ , \\ C_2 &= \tfrac{1}{2}[(C_2)_{M\text{-}C}+(C_2)_{M\text{-}N}]\ . \end{aligned} \tag{6.1}$$

Using Tosi-Fumi[24] parameters for metal ions and the parameters of Mirsky *et al.*[25] for CC and NN, we have calculated C_1 and C_2 and the values are given in Table III. Bound *et al.*[21] have used the same values (excepting for a few minor differences) in their molecular dynamic (MD) study. Actually there are two sets of parameters given in the paper by Tosi and Fumi; our final results are not very sensitive to the choice of these two different sets. The value[21] of the quadrupole moment (Q_0) of the free $(CN)^-$ ion is given in Table III. In their MD study involving KCN molecules confined to a finite cube, Bound *et al.*[21] found that in order to explain the orientational probability distribution function (OPDF) they had to reduce the value of Q by a factor $f=0.5$, i.e., $Q=fQ_0$. They argued that such a reduction could arise from the charge redistribution of $(CN)^-$ ion when it is placed in a solid environment. While this is an important physical effect, the precise value of f depends on the nature of the approximations made in obtaining the OPDF. In particular, Bound *et al.* considered a small system and did not allow for volume fluctuations. Instead of using their value of f, we have used a slightly different value, i.e., $f=0.6$ to fit the long-wavelength elastic constant data for the three compounds NaCN, KCN, and RbCN.

For the superoxides we find that the repulsive forces are slightly stronger compared to cyanides whereas the free-ion quadrupole moment[20] is about a factor of 2 smaller. These differences along with the orbital degeneracy of the O_2^- ion are primarily responsible for the experimentally observed[8,5] qualitative differences between the cyanides and superoxides as regards the nature of structural phase transition in these systems is concerned. In Table III we also give the values of a quantity $A_0^{QQ}=(24\pi/5)Q_0^2(\sqrt{2a})^5$ which measures the strength of the direct intermolecular quadrupole interaction. The repulsion and anisotropic dispersion contribution to the direct interaction which was found[20] to be important for NaO_2 are not so important for the cyanides because of large Q and for the other superoxides because of a large value of a. In the present calculation, repulsion and anisotropic dispersion contributions to the direct intermolecular interaction are ignored.

We would like to make a few comments about the effect of the nonzero electric dipole moment ($\vec{\mathscr{D}}$) of the $(CN)^-$ ion on the elastic softening at high temperatures. Taking the calculated value[21] of $|\vec{\mathscr{D}}| = 0.3D$, we find that the strength of the dipole-dipole interaction measured by the quantity $\epsilon_d = \mathscr{D}^2/(a\sqrt{2})^3 \approx 10$ K which is a factor of 10 smaller than the quadrupole-quadrupole interaction energy measured by $\epsilon_Q = Q_0^2/(a\sqrt{2})^5 \cong 100$ K. Therefore the dipole-dipole interaction can be neglected while calculating $\chi_{\alpha\beta}$. The coupling between $\vec{\mathscr{D}}$ and the fluctuating electric field $\vec{E}$ can soften the phonons just like the coupling between Q and the fluctuating EFG. But we have found that for symmetry reasons the former does not contribute to the softening of the elastic constants because in the presence of this coupling only $\omega^2 - \omega_0^2 \propto k^4$ for $k \to 0$.

B. Rotational-translational coupling A_R, B_R, A_Q, B_Q

Knowing C_1 and C_2 for the various compounds we have calculated A_R and B_R using the expressions of Michel and Naudts (MN).[16] For the sake of completeness we have reproduced their expressions for A_R and B_R in Appendix B. Our values of A_R and B_R (see Table IV) for KCN are about a factor of 2 larger than that given by MN and this difference is due to the large value of C_1 given by Tosi-Fumi parameters. An important quantity that determines the nature of the ferroelastic instability, i.e., which of the two elastic constants C_{11} or C_{44} softens first, is the ratio B_R/A_R. This ratio (see Appendix B) is given by

$$\delta_R = \frac{B_R}{A_R} = -\sqrt{6}\left[\frac{d}{a}\right]\left[(f_1 - f_3)\Big/\left[3f_2 - f_0 + \frac{d}{a}(f_1 - 3f_3)\right]\right] \tag{6.2}$$

and depends upon the parameters (d/a) and $(C_2 a)$. For the cyanides $\delta_R \simeq -0.25$ (see Table IV) and it turns out that if one considers repulsion alone, C_{11} goes to zero at a higher temperature than C_{44}.

The parameters A_Q and B_Q depend on the values of the quadrupole moment of the $(CN)^-$ ion in the solid. As has been pointed out before, there is some evidence from the molecular dynamic studies[21] of rotational autocorrelation functions in the cubic phase of KCN that $Q_{\text{solid}} < Q_0$, the free-ion value. For the entries in the Table IV, we have used the value $Q = 0.6Q_0$; this value was obtained by making a reasonable fit to the experimental values of elastic constants C_{11} and C_{44} over a large temperature range. With $Q = 0.5Q_0$ (a value suggested by Bound *et al.*) we were unable to obtain a decent fit over the entire experimental temperature range. Of course it is possible to change the value of repulsion parameters slightly and obtain a different value for Q which gives an equally good fit. However, our main purpose is to point out the important role of the quadrupole-fluctuating EFG interaction on the elastic softening rather than to obtain a very good fit to the experiment. It will be pointed out later that anharmonicity and non-mean-field effects are important and should be taken into account for a better quantitative understanding of the experiment.

It turns out that the dominant contribution to A_Q and B_Q comes from the nearest-neighbor positive ion. This is because the second and third neighbors [see Eqs. (5.19a) and (5.19b)] make contributions of opposite sign and almost equal (within 0.1%) magnitude to A_Q and B_Q. The fourth neighbor's contribution is $\lesssim 7\%$ of that of the nearest neighbor. For the quadrupolar contribution we find that

$$\delta_Q = B_Q(1 + \cdots)/A_Q(1 + \cdots) = B_Q/A_Q = -\sqrt{2/3} \; . \tag{6.3}$$

The large value of $|\delta_Q|$ compared to $|\delta_R|$ causes $C_{44} \to 0$ at a higher temperature than C_{11} if we consider the quadrupole contribution to the translational-rotational coupling alone. The above analysis concerning the competition between quadrupolar and repulsive forces in determining the effective rotation-translation coupling suggests that there should be interesting pressure effects because of the different volume dependences of A_R, B_R and A_Q, B_Q. Such a study is under present investigation.

C. Isothermal rotational susceptibility $\chi_{\alpha\beta}$

The temperature dependences of C_{11} and C_{44} are determined by $\chi_{\alpha\beta}(\vec{k})$. For the symmetry direction $\vec{k}=[0\,0\,k]$ that we are interested in, $\chi_{\alpha\beta}(\vec{k}) =\delta_{\alpha\beta}\chi_{\alpha\alpha}(\vec{k})$ and furthermore in the limit $k\rightarrow 0$, which is relevant for the calculation of elastic constants

$$\chi_{ii}(0)=\chi_{ii}^0/[1+D_{ii}(\vec{k}=0)\chi_{ii}^0]\,, \qquad (6.4)$$

where χ_{ii}^0 is defined in Eq. (4.13). As has been discussed in the first paragraph of this subsection, the T dependence of χ_{ii}^0 is determined by the single-site potential $V_0(\hat{n}_i)$. Because of cubic symmetry $\chi_{11}^0 =3\chi_{22}^0=\chi_{e_g}$ and $\chi_{33}^0=\chi_{44}^0=\chi_{55}^0=\chi_{t_{2g}}$ and the quantities $T\chi_{11}^0$ and $T\chi_{44}^0$ are given in Figs. 2(a) and 2(b). Our results differ from that of MN even if we use their C_1 and C_2 parameters and this difference is due to a factor of 2 error in the calculation of their $V_0(\hat{n}_i)$. In fact, their numerical values of $T\chi_{11}^0$ and $T\chi_{44}^0$ given in Figs. 1 and 2 are appropriate for a system for which $C_1\cong 2C_1^{\mathrm{MN}}$, a value much closer to that obtained from Tosi-Fumi parameters. However, for this stronger repulsion, A_R and B_R should be increased by a factor of 2. This will change their results on T dependence of C_{11} and C_{44} drastically and spoil the agreement with the experiment that they found.

In Figs. 2(a) and 2(b) we also give $R_1=\chi_{11}/\chi_{11}^0$ and $R_4=\chi_{44}/\chi_{44}^0$, χ_{11} and χ_{44} being the e_g and t_{2g} susceptibilities obtained in the presence of direct quadrupole-quadrupole interaction. Using the value of $Q=0.6Q_0$, we find that $D_{11}(\vec{k}=0) =-704$ K and $D_{44}(\vec{k}=0)=235$ K. From Eq. (6.4) we immediately see that $\chi_{11}/\chi_{11}^0>1$ and $\chi_{44}/\chi_{44}^0<1$ which indicates that direct intermolecular interaction enhances C_{11} softening and suppresses C_{44} softening. Over the temperature range of interest $100 \leq T<500$ K, $1.08<\chi_{11}/\chi_{11}^0<1.13$, and $0.6\leq\chi_{44}/\chi_{44}^0<0.9$. Thus effect of the direct interaction on elastic softening is quite important for C_{44} and not so for C_{11} which is essentially due to the fact that $\chi_{44}^0/\chi_{11}^0\approx 10$ in the temperature range of interest. From Eqs. (5.22) and (5.23) we see that the effect of direct molecular interaction is to decrease T_{44} and increase T_{11}, the actual amount of decrease will depend upon other parameters like C_{44}^0, C_{11}^0 and values of χ_{11}^0, χ_{44}^0. The maximum effect of direct interaction on T_{ii} in cyanides is found to be $\sim$20%.

D. Elastic constants C_{11} and C_{44} and transition temperature

Before presenting the results on the T dependence of $C_{11}(T)$ and $C_{44}(T)$ and the temperature where they approach zero, we would like to discuss the importance of anharmonic effects on C_{11} and C_{44}. It is well known[23] that anharmonic effects give rise to phonon-phonon interaction and renormalize the elastic constants, i.e.,

$$C_{ii}(T)=C_{ii}^0+\delta C_{ii}^{\mathrm{an}}(T)\,. \qquad (6.5)$$

At high temperatures $\delta C_{ii}^{\mathrm{an}}(T)=-\gamma_i T$. For alkali-halide crystals careful elastic constant measurements[35-37] have been made and it is found that $\gamma_1 \gg \gamma_4$. In order to incorporate anharmonicity effects in our calculation, we assume that

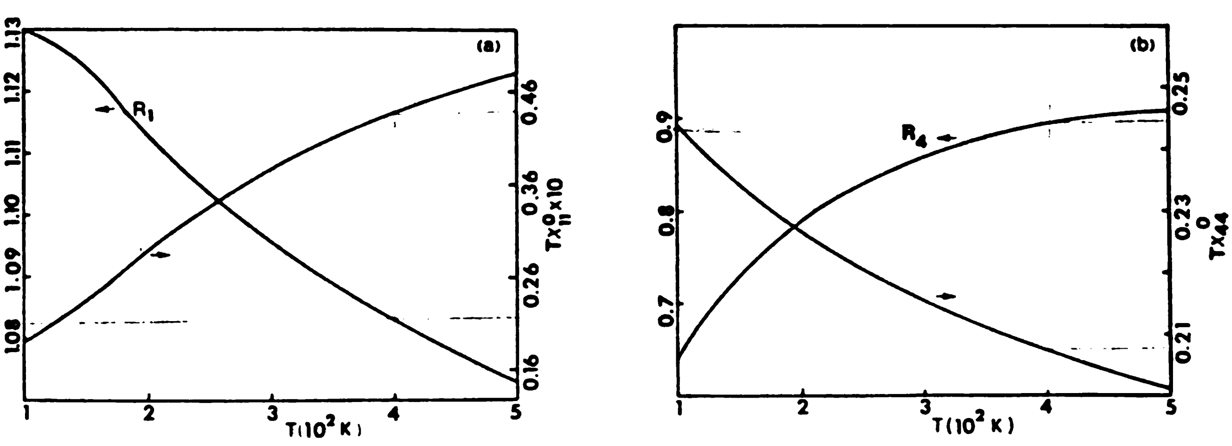

FIG. 2. Single-site susceptibility $\chi_{11}^0 T$ and enhancement factor $R_1=\chi_{11}(T)/\chi_{11}^0(T)$ for e_g symmetry (KCN). (b) Single-site susceptibility $\chi_{44}^0 T$ and enhancement factor $R_4=\chi_{44}(T)/\chi_{44}^0(T)$ for t_{2g} symmetry (KCN).

cyanides are equivalent to bromides[26] excepting for the nonzero translational-rotation coupling in the former and therefore use

$$\gamma_i(M\mathrm{CN})=\gamma_i(M\mathrm{Br}),\quad M=\mathrm{Na}\ ,\mathrm{K}\ ,\mathrm{Rb}\ . \qquad (6.6)$$

The values of γ_1 and γ_4 are given in Table V.

In the presence of both translational-rotational (tr-rot) coupling and anharmonicity effects, we then have

$$C_{ii}(T)=C_{ii}^{0}+\delta C_{ii}^{\mathrm{an}}(T)+\delta C_{ii}^{\mathrm{tr\text{-}rot}}(T)\ , \qquad (6.7)$$

where $\delta C_{ii}^{\mathrm{tr\text{-}rot}}(T)$ is given by Eqs. (5.22) and (5.23).

To calculate $C_{11}(T)$ and $C_{44}(T)$ we need to know the values of bare elastic constants C_{11}^{0} and C_{44}^{0}. In their calculation[16] MN obtained C_{11}^{0} and C_{44}^{0} by fitting to the experimental value of the transition temperatures T_{44} and T_{11}. Since the present theory is of mean-field nature and therefore does not include fluctuation effects, we have obtained C_{11}^{0} and C_{44}^{0} by fitting to the experimental values of C_{11} and C_{44} at temperatures T_{fit} far above the transition temperature T_c. The values of T_{fit} are given in Table V and those of T_c in Table I.

As has been pointed out earlier, the value of the quadrupole moment that we have used in our calculation is $0.6Q_0$ compared to $0.5Q_0$ used by Bound *et al.* in their MD study. In Fig. 3 we give $C_{44}(T)$ vs T for three values of Q, i.e., $Q=0.5Q_0$, $0.6Q_0$, $0.75Q_0$ in the absence of anharmonicity effects. We find that the temperature at which $C_{44}\rightarrow 0$ are <100, 200, 300, respectively. Inclusion of anharmonicity effects reduces the transition temperatures further although by only a few percent. Since our theory of phonon softening is of mean-field nature, we expect that inclusion of fluctuation effects will reduce the transition temperature still further for $Q=0.5Q_0$ (away from the experimental value $T^*=156$ K). The choice $Q=0.6Q_0$ gives $T^*_{\mathrm{theor}}\gtrsim T^*_{\mathrm{expt}}$ and a reasonable fit over the entire range of the experiment. For $Q=0.75Q_0$ the agreement between theory and experiment for $T \gg T^*$ is rather poor. For all the cyanides, instead of choosing different values of Q to obtain an optimum fit, we have chosen $Q=0.6Q_0$. The overall agreement between theory and experiment (to be discussed shortly) using this value is quite good.

TABLE V. Anharmonicity parameters (γ_1,γ_4) bare elastic constants (C_{11}^{0},C_{44}^{0}) and temperature T_{fit} where theoretical and experimental values are fitted.

	NaCN	KCN	RbCN
γ_1 (10^9 dyn/cm^{2}K)	0.26	0.27	0.28
γ_4 (10^9 dyn/cm^{2}K)	0.019	0.013	0.008
C_{11}^{0} (10^{11} dyn/cm^2)	5.749	5.115	4.022
C_{44}^{0} (10^{11} dyn/cm^2)	0.752	0.470	0.411
T_{fit} (K)	473	453	380

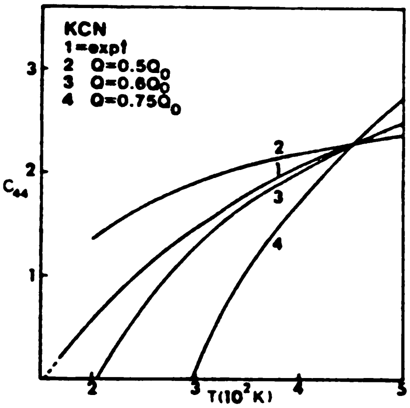

FIG. 3. T dependence of C_{44} (in units of 10^{11} dyn/cm^2) for KCN for different values of the (CN$^-$) quadrupole moment $Q=fQ_0$, where Q_0 is the free-ion value.

Before discussing individual systems separately we make a few general remarks. If we consider only the repulsion contribution to the translation-rotation coupling, i.e., $A_Q=B_Q=0$, then we find that $C_{11}\rightarrow 0$ at temperature T_{11} which is higher than T_{44} where $C_{44}\rightarrow 0$. Thus the repulsive forces tend to soften C_{11} much more than C_{44}. Since C_{11} couples to order parameter Y_1, one expects that $C_{11}\rightarrow 0$ will imply a nonzero $\langle Y_1\rangle$ in the ferroelastic phase. This corresponds to molecules orienting along the z axis with a concomitant tetragonal structure. Such a structure is not seen in the cyanides but in the superoxides. If on the other hand, we choose $A_R=B_R=0$ and $A_Q,B_Q\neq 0$, then we find that $T_{44}>T_{11}$ which is observed in the cyanides. Of course as can be seen from the Table IV, A_R, B_R, A_Q, and B_Q are all important for the cyanides. The fact that in these systems $T_{44}>T_{11}$ is due to the dominance of B_Q over B_R and a significant reduction in A_R caused by negative A_Q. Since the quadrupole moment of the O_2^- ion is about a factor of 2 smaller than that of (CN)$^-$ and since the short-range repulsion is stronger in the superoxides, we believe that the qualitative features of the ferroelastic instability in superoxides is determined by the short-range repulsive forces. However, for a quantitative understanding of the transition temperatures in superoxides, one has to include anisotropic (quadrupolar) electrostatic forces and the effect of orbital degen-

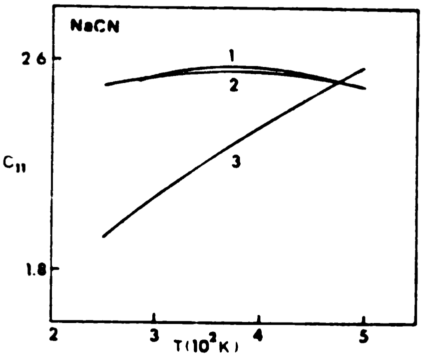

FIG. 4. T dependence of C_{11} (in units of 10^{11} dyn/cm^2) for NaCN. 1: experiment, 2: theory with anharmonicity, 3: theory without anharmonicity.

eracy of the superoxide ion.

In Figs. 4–9, we give the T dependence of C_{11} and C_{44} with and without the inclusion of anharmonicity effect and compare with the experimental result. For NaCN and KCN, the overall agreement appears to be very good. In particular the peak in $C_{11}(T)$ is understood in terms of a competition between the two contributions to the renormalization of the elastic constants δC_{11}^{an} and $\delta C_{11}^{tr\text{-}rot}$. For a proper understanding of the T dependence of C_{11} it is important to include the anharmonicity effect whereas for $C_{44}(T)$ this is not so. For RbCN, inclusion of anharmonicity effects in C_{11} gives a peak but at a much lower temperature than that seen experimentally. Our feeling is that although our calculations bring out the importance of various physical effects it is necessary to go beyond a simple mean-field theory for a complete understanding of the elastic softening in the orientationally disordered phases of molecular crystals. In this regard we propose to extend the work of Naudts and Mahanti[38] on spin-phonon systems and apply to molecular crystals.

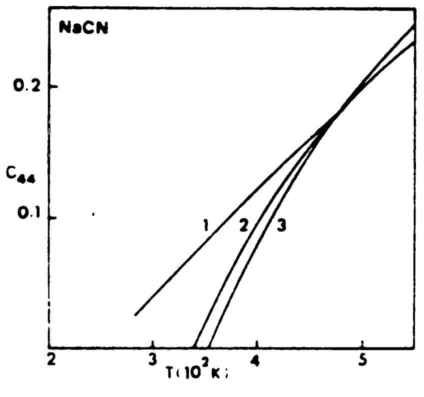

FIG. 5. T dependence of C_{44} (in units of 10^{11} dyn/cm^2) for NaCN. 1: experiment, 2: theory with anharmonicity, 3: theory without anharmonicity.

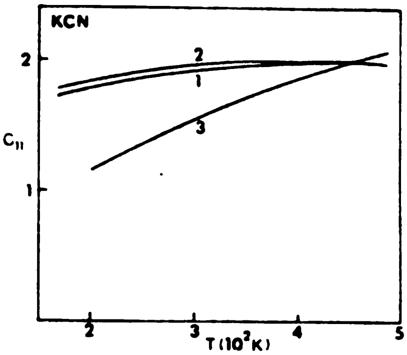

FIG. 6. T dependence of C_{11} (in units of 10^{11} dyn/cm^2) for KCN. 1: experiment, 2: theory with anharmonicity, 3: theory without anharmonicity.

The value of T_{44} is given in Table I. The effect of including anharmonicity is to reduce T_{44} by ~10 K. Comparing the theoretical values of T_{44} with T^* (see Table I), we see that the agreement is reasonably good in view of the mean-field nature of the present theory. Particularly remarkable is the trend in T_{44} in going from NaCN to RbCN. The T dependence of elastic constants in CsCN are not available but they will provide an additional test of the present microscopic theory.

E. Softening of phonons over the entire Brillouin zone

Strauch *et al.*[39] have used the translation-rotation (tr-rot) coupling model to calculate the phonon frequencies of NaCN and KNC at 300 K for the three symmetry directions [ζ00], [0$\zeta\zeta$], and [$\zeta\zeta\zeta$]. For the bare phonon frequencies which are determined by the dynamic matrix M^0, they have used a 10-parameter shell model. Translation-

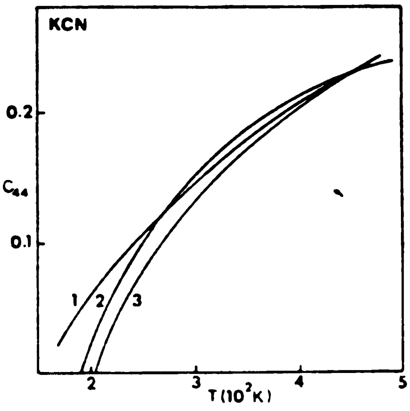

FIG. 7. T dependence of C_{44} (in units of 10^{11} dyn/cm^2) for KCN. 1: experiment, 2: theory with anharmonicity, 3: theory without anharmonicity.

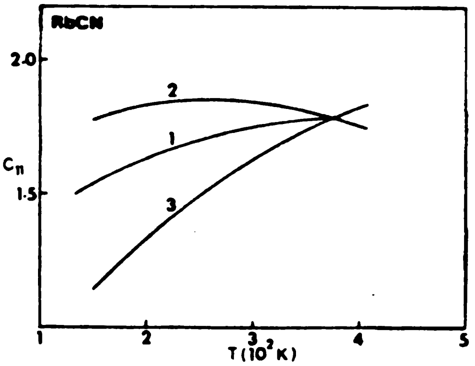

FIG. 8. T dependence of C_{11} (in units of 10^{11} dyn/cm^2) for RBCN. 1: experiment, 2: theory with anharmonicity, 3: theory without anharmonicity.

rotation coupling is incorporated by adding to M^0 a contribution δM given by

$$\delta M = \begin{bmatrix} \delta M_+ & 0 \\ 0 & 0 \end{bmatrix} , \tag{6.8}$$

where

$$\delta M_+ = -\upsilon \chi^0 \upsilon^\dagger , \tag{6.9}$$

where υ and χ^0 are the tr-rot coupling and rotational susceptibility matrices discussed in Sec. III of this paper. Only the nearest-neighbor contributions to υ, i.e., the interaction between a (CN)$^-$ ion and its nearest-neighbor M^+ ion was considered in Ref. 39 just as in Ref. 16. Strauch *et al.* did not include the direct interaction between the (CN)$^-$ molecules and therefore their renormalized phonon frequencies are the same as those given in Eq. (3.20) of this paper with $\chi_{\alpha\beta}(\vec{k},\omega)$ replaced by $\chi^0_{\alpha\beta}$, the single-site static susceptibility. Thus our results can be thought of as a generalization of their work.

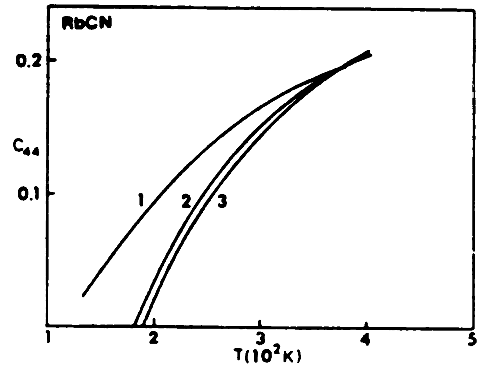

FIG. 9. T dependence of C_{44} (in units of 10^{11} dyn/cm^2) for RBCN. 1: experiment, 2: theory with anharmonicity, 3: theory without anharmonicity.

Since in the limit $\vec{k} \to 0$, δM_+ gives the renormalization of elastic constants, the latter completely determines δM_+ provided only nearest neighbors contribute to $\upsilon_{\alpha\mu}(\vec{k})$. Then knowing δC_{11} and δC_{44} at $T = 300$ K, one can calculate $\omega^2_{j\vec{k}} - \omega^{0^2}_{j\vec{k}}$ for all values of $j\vec{k}$ at this temperature. Strauch *et al.* had to use values of δC_{11} and δC_{44} different from those obtained by Michel and Naudts[16] to fit to the experimental data. In our analysis of the short-range repulsion and quadrupole contribution to $\upsilon^{\pm}_{\alpha\mu}(\vec{k})$ we found that because of near perfect cancellation between second- and third-neighbor contributions to $\upsilon_{\alpha\mu}(\vec{k})$, considering only the nearest-neighbor contribution to $\upsilon_{\alpha\mu}(\vec{k})$, is an excellent approximation. However, both the above mechanisms contribute to $\upsilon^{+}_{\alpha\mu}(\vec{k})$. As we discuss below our present calculations provide a microscopic justification of the values of δC_{11} and δC_{44} chosen by Strauch *et al.* to fit to the experiment. Since these authors, with their phenomenological choice of δC_{11} and δC_{44}, found excellent agreement with experiment we will use their calculated values of $\omega^2_{j\vec{k}} - \omega^{0^2}_{j\vec{k}}$ as an experimental measure of the phonon renormalization.

We define a quantity $\Gamma^{j\vec{k}} = (\omega^{0^2}_{jk} - \omega^2_{jk})^{1/2}/10^{13}$ cps which is a measure of phonon renormalization. We have calculated $\Gamma^{j\vec{k}}$ for phonons propagating along the $[00k]$ direction by using Eq. (3.20) and noting that the tr-rot coupling matrix (including both short-range and quadrupole contributions) has typically a form like Eq. (5.5) with $k_x = k_y = 0$ and $k_z = k$. In Table VI the results of our calculation of $\Gamma^{j\vec{k}}$ are given along with those obtained from the Fig. 1 of Ref. 39 where the phonon frequency $\nu = \omega/2\pi$ is given in units of THz. Using the appropriate polarization vectors of phonons given in Sec. V C it is easy to see that $\Gamma^{j\vec{k}}$ for the LA and TA phonons are determined by the rotational susceptibilities of e_g and t_{2g} symmetries, respectively. These susceptibilities in turn depend on the direct Q-Q interaction $D_{\alpha\beta}(\vec{k})$ through Eq. (4.10). We find that at $T \cong 300$ K inclusion of direct interaction affects LA phonon softening by about 7% whereas the TA phonons are affected by 5–25%. The TA phonons are influenced more strongly by direct interaction because at this temperature $\chi^0_{t_{2g}}/\chi^0_{e_g} \approx 10$, in spite of the fact that $D_{11}(k)$ is -704 K at $k=0$ and 1955 K at $k = k_{\text{BZ}}$ and that $D_{44}(k)$ is 235 K at $k=0$ and -652 K at $k = k_{\text{BZ}}$. As can be seen from Table VI, for LA modes our calculated values of $\Gamma^{j\vec{k}}$ are about 15–30% higher than experiment. This difference is due to the fact that for a proper calculation of phonon

TABLE VI. Renormalization of TA and LA phonons along [00k] direction; $\Gamma^i[(\omega_0^i)^2-(\omega^i)^2]^{1/2}/10^{13}$ cps; $i=\text{LA, TA}$.

$k/k_{\max}$	Γ^{TA} (present)	Γ^{TA} (Ref. 39)	Γ^{LA} (present)	Γ^{LA} (Ref. 39)
0	0	0	0	0
0.2	0.24	0.35(5)	0.71	0.61(5)
0.4	0.42	0.52	1.12	0.88
0.6	0.49	0.53	1.11	0.87
0.8	0.35	0.38(5)	0.71	0.56
1.0	0	0	0	0

softening one has to include the frequency dependence of $\chi_{\alpha\beta}(\vec{k},\omega)$. If one is far away from the phase transition temperature, i.e., $T>T_c$ (this may not be true for NaCN) then the frequency dependence of $\chi_{\alpha\beta}(\vec{k},\omega)$ is determined primarily by that of $\chi^0_{\alpha\beta}(\omega)$. The rotational dynamics at $T\cong 300$ K will be almost diffusive with a frequency scale $\Gamma_{\text{rot}}\sim 0.5\times 10^{13}$ cps, i.e.,

$$\chi(\vec{k},\omega)\sim\chi(\vec{k},0)\frac{\Gamma^2}{\Gamma^2+\omega^2}\ .$$

On physical grounds[40] one expects that for high-frequency phonons ($\omega>\omega_{\text{rot}},\Gamma_{\text{rot}}$) the effect of tr-rot coupling will be reduced from the values given in Table VI. This will improve agreement between theoretical and experimental values of $\omega_{\text{LA}}(\vec{k})$.

On the other hand, for TA phonons one finds from Table VI that our calculated values of $\Gamma^{j\vec{k}}$ are smaller than the experimental values by about $7-32\%$, the large discrepancy being in the low-k region. However, because of the direct interaction, the agreement with experiment ($\sim$ Strauch *et al.*'s work) is fairly good for large values of k. Therefore, for the low-frequency TA phonons, if one approximates the rotational dynamics by a resonant-type behavior, i.e., by

$$\chi(\vec{k},\omega)\sim\chi(\vec{k},0)\frac{\Gamma^2}{\Gamma^2+(\omega-\omega_{\text{rot}})^2}$$

with $\Gamma\sim\omega_{\text{rot}}$, then one can improve the agreement between experiment and present theory. There is some evidence of the behavior of the form given above from the MD calculation.[21] For the high-frequency TA phonons though, the quantity $\Gamma^{j\vec{k}}$ may depend sensitively on the values of $\chi^0_{t_{2g}}$, $D_{44}(\vec{k})$, and the frequency scales involved and the above-mentioned quantitative agreement should be reexamined carefully. A quantitative study of the phonon softening including the proper frequency dependence of $\chi_{\alpha\beta}(\vec{k},\omega)$ is beyond the scope of the present work.

F. Conclusion

In summary, we believe that the anomalous thermoelastic properties and softening of phonons in the orientationally disordered phase of the cyanides can be adequately described by the tr-rot coupling model.[16,17] The physics of these systems depends sensitively on the competition between the short-range repulsive and anisotropic electrostatic (predominantly quadrupole-EFG interaction) forces.[17] Furthermore, anharmonicity effects are also important for a proper understanding of the T dependence of C_{11}. For the phonons in general, it is necessary to include the retardation effects by considering the frequency dependence of the rotational susceptibility $\chi_{\alpha\beta}(\vec{k},\omega)$. Fluctuation effects not included in the present mean-field theory approach should be considered for a better quantitative understanding. We propose to extend our theory to CsCN which has a different high-T cubic structure and see if we can understand the large ferroelastic transtition temperature[41] $T_{\text{CsCN}}\simeq 200$ K. Finally for the alkali superoxides (which will be discussed in detail in a separate paper) short-range repulsion dominates over the quadrupole coupling and the orbital degeneracy of the superoxide ion plays an important role.

ACKNOWLEDGMENTS

We thank Dr. G. Kemeny and Dr. J. Naudts for helpful discussions. This work was partially supported by NSF Grant No. DMR 81-17297.

APPENDIX A: ROTATIONAL-TRANSLATIONAL COUPLING FROM QUADRUPOLE EFG INTERACTIONS

In this appendix we evaluate the coupling constant matrices arising from the contribution of various NN's to the electric field gradient. We explicitly consider the cases $\alpha=1$ and $\alpha=4$, other terms being readily obtainable from these by symmetry considerations.

1. First NN contribution

From (5.16), choosing the origin at $\vec{\mathrm{R}}_i^0$

$$U_{zz}(a\hat{z}) = -U_{zz}(-a\hat{z}) = -\frac{3|e|}{a^4} 2u_{jz}, \ldots \tag{A1}$$

We use (5.6), (5.15), (5.17), and (A1) and express the displacements $\vec{\mathrm{u}}_j$ in terms of their Fourier components and obtain for $\alpha=1$ [see Eq. (5.6) for the definition of S_x, C_x, etc.]. We have

$$\sum_i QY_1(\hat{n}_i)U_1^i = 2iA_Q \sum_{\vec{\mathrm{k}}} Y_1^\dagger(\vec{\mathrm{k}})[u_x(\vec{\mathrm{k}})S_x + u_y(\vec{\mathrm{k}})S_y - 2u_z(\vec{\mathrm{k}})S_z] , \tag{A2}$$

where

$$A_Q = \sqrt{9\pi/5}\frac{Q|e|}{a^4} \tag{A3}$$

so that

$$v_{1\mu}^{\mathrm{EFG}}(+|\vec{\mathrm{k}})_1 = 2A_Q \begin{bmatrix} S_x \\ S_y \\ -2S_z \end{bmatrix} . \tag{A4}$$

Similarly for $\alpha=4$,

$$U_{xz}(a\hat{z}) = -U_{xz}(-a\hat{z}) = \frac{3|e|}{a^4} u_{jx}, \ldots , \tag{A5}$$

$$\sum_i QY_4(\hat{n}_i)U_4^i = 2iB_Q \sum_{\vec{\mathrm{k}}} Y_4^\dagger(\vec{\mathrm{k}})[u_x(\vec{\mathrm{k}})S_z + u_z(\vec{\mathrm{k}})S_x] , \tag{A6}$$

where

$$B_Q = -\sqrt{2/3}A_Q , \tag{A7}$$

and therefore,

$$v_{4\mu}^{EFG}(+|\vec{\mathrm{k}})_1 = 2B_Q \begin{bmatrix} S_z \\ 0 \\ S_x \end{bmatrix} . \tag{A8}$$

Hence we obtain

$$v_{\alpha\mu}^{\mathrm{EFG}}(+|\vec{\mathrm{k}})_1 = 2 \begin{bmatrix} A_QS_x & -A_QS_x & B_QS_y & B_QS_z & 0 \\ A_QS_y & A_QS_y & B_QS_x & 0 & B_QS_z \\ -2A_QS_z & 0 & 0 & B_QS_x & B_QS_y \end{bmatrix} . \tag{A9}$$

2. Second NN contribution

From (5.16) we again obtain

$$\begin{aligned} U_{zz}(a\hat{x}+a\hat{y}) &= -U_{zz}(-a\hat{x}-a\hat{y}) \\ &= -\frac{3|e|}{2^{5/2}a^4}(u_{jx}+u_{jy}) , \end{aligned} \tag{A10}$$

$$\begin{aligned} U_{zz}(a\hat{x}-a\hat{y}) &= -U_{zz}(-a\hat{x}+a\hat{y}) \\ &= -\frac{3|e|}{2^{5/2}a^4}(u_{jx}-u_{jy}) , \end{aligned}$$

and

$$\begin{aligned} \sum_i QY_1(\hat{n}_i)U_1^i &= i2\bar{A}_Q \sum_{\vec{\mathrm{k}}} Y_1^\dagger(\vec{\mathrm{k}})[u_x(\vec{\mathrm{k}})S_x(3C_z-2C_y) \\ &\quad + u_y(\vec{\mathrm{k}})S_y(3C_z-2C_x) \\ &\quad + u_z(\vec{\mathrm{k}})S_z(C_x+C_y)] , \end{aligned} \tag{A11}$$

where

$$\bar{A}_Q = \frac{1}{4\sqrt{2}}A_Q \tag{A12}$$

so that

$$v_{1\mu}^{\mathrm{EFG}}(-|\vec{\mathrm{k}})_2 = 2\bar{A}_Q \begin{bmatrix} S_x(3C_z-2C_y) \\ S_y(3C_z-2C_x) \\ -S_z(C_x+C_y) \end{bmatrix} . \tag{A13}$$

Similarly with

$$\bar{B}_Q = \frac{1}{4\sqrt{2}}B_Q , \tag{A14}$$

we obtain

$$v_{2\mu}^{\mathrm{EFG}}(-|\vec{\mathrm{k}})_2 = \tfrac{2}{3}\bar{A}_Q \begin{bmatrix} S_x(C_z-4C_y) \\ S_y(4C_x-C_z) \\ 5S_z(C_x-C_y) \end{bmatrix} ,$$

$$v_{3\mu}^{\mathrm{EFG}}(-|\vec{\mathrm{k}})_2 = 2\bar{B}_Q \begin{bmatrix} S_y(3C_x-2C_z) \\ S_x(3C_y-2C_z) \\ 0 \end{bmatrix} , \tag{A15}$$

$$v_{4\mu}^{\mathrm{EFG}}(-\,|\,\vec{\mathrm{k}})_2=2\bar{B}_Q\begin{bmatrix} S_z(3C_x-2C_y) \\ 0 \\ S_x(3C_x-2C_y) \end{bmatrix},$$

and

$$v_{5\mu}^{\mathrm{EFG}}(-\,|\,\vec{\mathrm{k}})_2=2\bar{B}_Q\begin{bmatrix} 0 \\ S_z(3C_y-2C_x) \\ S_y(3C_z-2C_x) \end{bmatrix}.$$

3. Third NN contribution

Defining

$$\bar{\bar{A}}=-\frac{8}{27\sqrt{3}}A_Q\,, \tag{A16}$$

$$\bar{\bar{B}}=-\frac{8}{27\sqrt{3}}B_Q\,, \tag{A17}$$

we obtain the following terms for the coupling constant matrix:

$$v_{1\mu}^{\mathrm{EFG}}(+\,|\,\vec{\mathrm{k}})_3=2\bar{\bar{A}}_Q\begin{bmatrix} S_xC_yC_z \\ S_yC_xC_z \\ -2S_zC_xC_y \end{bmatrix},$$

$$v_{2\mu}^{\mathrm{EFG}}(+\,|\,\vec{\mathrm{k}})_3=2\bar{\bar{A}}_Q\begin{bmatrix} -S_xC_yC_z \\ S_yC_zC_x \\ 0 \end{bmatrix},$$

$$v_{3\mu}^{\mathrm{EFG}}(+\,|\,\vec{\mathrm{k}})_3=2\bar{\bar{B}}_Q\begin{bmatrix} S_yC_zC_x \\ S_xC_yC_z \\ -\frac{5}{2}S_xS_yS_z \end{bmatrix}, \tag{A18}$$

$$v_{4\mu}^{\mathrm{EFG}}(+\,|\,\vec{\mathrm{k}})_3=2\bar{\bar{B}}_Q\begin{bmatrix} S_zC_xC_y \\ -\frac{5}{2}S_xS_yS_z \\ S_xC_yC_z \end{bmatrix},$$

$$v_{5\mu}^{\mathrm{EFG}}(+\,|\,\vec{\mathrm{k}})_3=2\bar{\bar{B}}_Q\begin{bmatrix} -\frac{5}{2}S_xS_yS_z \\ S_zC_xC_y \\ S_yC_zC_x \end{bmatrix}.$$

APPENDIX B: ROTATIONAL-TRANSLATIONAL COUPLING FROM SHORT-RANGE REPULSION

Equations (A13) and (A15) of Ref. 16 are correct. There is an error of a factor of $1/\sqrt{2}$ in Eq. (A14) where $B_R\equiv B$ is expressed in terms of $\vec{\mathrm{P}}^{(1)}(a_z;\Omega)$, but the other equations are correct. The parameters A and B (which are A_R and B_R in the present paper) are

$$A_R\equiv A=\sqrt{5\pi}C_1C_2(d^2+a^2)^{-1/2}\times[a(3f_2-f_0)+d(f_1-3f_3)]\,, \tag{B1}$$

$$B_R\equiv B=-\sqrt{30\pi}C_1C_2(d^2+a^2)^{-1/2}d(f_1-f_3)\,, \tag{B2}$$

where

$$f_n=g^{-(n+1)}\int_{\sqrt{1-g}}^{\sqrt{1+g}}(1-y^2)^n e^{-hy}dy \tag{B3}$$

and

$$h=C_2(d^2+a^2)^{1/2}\,, \tag{B4}$$

$$g=2da/(d^2+a^2)\,. \tag{B5}$$

In the above equations C_1,C_2 are the repulsion parameters discussed in Sec. VI A of the text, $2d$ is the internuclear separation, and a is the distance between the (CN)$^-$ ion and its nearest M^+ ion.

---

[1] S. Haussühl, J. Eckstein, K. Recker, and F. Wallrafen, Acta Crystallogr. A 33, 847 (1977)

[2] S. Haussühl, Solid State Commun. 13, 147 (1973).

[3] S. Haussühl, Solid State Commun. 32, 181 (1979).

[4] J. M. Rowe, J. J. Rush, N. J. Chesser, K. H. Michel, and J. Naudts, Phys. Rev. Lett. 40, 455 (1978).

[5] Y. Kondo, D. Schoemaker, and F. Lüty, Phys. Rev. B 19, 4210 (1979).

[6] H. D. Hochheimer, W. F. Love, and C. T. Walker, Phys. Rev. Lett. 38, 832 (1977).

[7] H. T. Stokes, T. A. Case, and D. C. Ailion, Phys. Rev. Lett. 47, 268 (1981).

[8] V. M. Ziegler, M. Rosenfeld, W. Känzig, and P. Fischer, Helv. Phys. Acta 49, 57 (1976).

[9] W. Känzig and M. Labhart, J. Phys. (Paris) Colloq. 7, 39 (1976).

[10] M. Rosenfeld, M. Ziegler, and W. Känzig, Helv. Phys. Acta 51, 298 (1978).

[11] J. C. Raich and A. Hüller, J. Chem. Phys. 70, 3669 (1979).

[12] J. J. Rush, L. A. de Graaf, and R. C. Livingston, J. Chem. Phys. 58, 3439 (1973). See also H. Bleif and H. Dachs, Acta Crystallogr. Sect. A 31, S188 (1975) for the case of sodium hydroxide.

[13] K. D. Ehrhardt and K. H. Michel, Phys. Rev. Lett. 46, 291 (1981).

[14] In NaO_2, the transition is from an disordered to a four-sublattice antiferroelastic phase and there are no accompanying elastic anomalies.

[15] There is some evidence that in RbCN, the molecular orientations in the ordered phase is along [111] direction (see also Ref. 41).

[16] K. H. Michel and J. Naudts, Phys. Rev. Lett. 39, 212 (1977); J. Chem. Phys. 67, 547 (1977).

[17] S. D. Mahanti and D. Sahu, Phys. Rev. Lett. 48, 936 (1982).

[18] In their work on structural phase transition in NaN_3, Raich and Huller (see Ref. 11) took into account the quadrupole and hexadecapole moment of the N_3^- ion and found that $C_{44} \to 0$ at T_c. However, owing to the complicated nature of the system, they did not study the effect of competition between short-range repulsion and anistropic electrostatic effects on the elastic softening.

[19] M. A. Bösch, M. E. Lines, and M. Labhart, Phys. Rev. Lett. 45, 140 (1980); M. E. Lines and M. A. Bösch, Phys. Rev. B 23, 263 (1981); M. E. Lines, *ibid.* 24, 5248 (1981).

[20] S. D. Mahanti and G. Kemeny, Phys. Rev. B 20, 2105 (1979); the sign of Q given in Table II should be negative.

[21] D. G. Bounds, M. L. Klein, and I. R. McDonald, Phys. Rev. Lett. 46, 1682 (1981); Chem. Phys. Lett. 78, 383 (1981); Phys. Rev. B 24, 3568 (1981).

[22] J. Naudts, Z. Phys. B 42, 323 (1981).

[23] H. B. Huntington, in *Solid State Physics*, edited by F. Seitz, D. Turnbull, and H. Ehrenreich (Academic, New York, 1958), Vol. 7, p. 214; G. Leibfried and W. Ludwig, in *Solid State Physics*, edited by F. Seitz and D. Turnbull (Academic, New York, 1961), Vol. 12, p. 276.

[24] F. G. Fumi and M. P. Tosi, J. Phys. Chem. Solids 25, 31 (1964).

[25] F. L. Hirshfeld and K. Mirsky, Acta Crystallog. Sect. A 35, 366 (1979).

[26] B. deRaedt, K. Binder, and K. H. Michel, J. Chem. Phys. 75, 2977 (1981).

[27] B. C. Kohin, J. Chem. Phys. 33, 882 (1960).

[28] D. A. Goodings and M. Henkelman, Can. J. Phys. 49, 2898 (1971).

[29] P. V. Dunmore, Can. J. Phys. 55, 554 (1977).

[30] D. N. Zubarev, Usp. Fiz. Nauk 71, 71 (1960) [Sov. Phys—Usp. 3, 320 (1960)].

[31] When the time scales of rotational motion is fast compared to the translational motion (valid for elastic response), the effects of modes other than the particular one under investigation $(j\vec{k})$ can be included by carrying out a canonical transformation. This leads to a correction to the direct intermolecular interaction and to the single-site susceptibility. However, in the limit $\vec{k} \to 0$, the modification of the direct interaction is only through optical phonons and hence very small. Quantitative effects of this mode-mode coupling on the elastic softening will be discussed elsewhere [S. D. Mahanti and D. Sahu (unpublished)].

[32] R. Kubo, J. Phys. Soc. Jpn. 12, 570 (1957).

[33] M. H. Cohen and F. Reif, in *Solid State Physics*, edited by F. Seitz and D. Turnbull (Academic, New York, 1957), Vol. 5, p. 322.

[34] C. Kittel, *Introduction to Solid State Physics* (Wiley, New York, 1967). p. 120.

[35] M. H. Norwood and C. V. Briscoe, Phys. Rev. 112, 45 (1958).

[36] M. Ghafelehbashi, D. P. Dandekar, and A. L. Ruoff, J. Appl. Phys. 41, 652 (1970).

[37] W. C. Overton, Jr. and R. T. Swim, Phys. Rev. 84, 758 (1951).

[38] J. Naudts and S. D. Mahanti, Phys. Rev. B 25, 5875 (1982).

[39] D. Strauch, U. Schroder, and W. Bauernfeind, Solid State Commun. 30, 559 (1979).

[40] A careful study of the coupled translation-rotation dynamics has been made by K. H. Michel and J. Naudts [J. Chem. Phys. 68, 216 (1978)] when $\omega_{\mathrm{phonon}} \sim \not\omega_{\mathrm{rotation}} \sim \Gamma_{\mathrm{rot}}$ using Mori's projection operator tecnhique.

[41] F. Lüty, paper presented at International Conference on Defects on Insulating Crystals, Riga, 1981 (private communication).

LIST OF REFERENCES

LIST OF REFERENCES

Bij 40 J.M.Bijvoet and J.A.Lely; Recl. Trav. Chim. Pays. Bas.,59,908(1940).

Boi 78 M.Boissier, R.Vacher, D.Fontaine and R.M.Pick; J.de Physique, 39, 205(1978).

Boi 80 M.Boissier, R.Vacher, D.Fontaine and R.M.Pick; J. de Physique, 41,1437(1980).

Bou 81 D.G.Bounds, M.L.Klein and I.R.McDonald; Phys. Rev. Lett. 46,1682(1981).

Coh 57 M.H.Cohen and F.Reif; in *Solid State Physics*, edited by F.Seitz and D.Turnbull(Academic, N.Y. 1957) vol.5, p. 322.

Cou 76 E.Courtens; J. de Physique Lett., 37,L-21(1976).

Cow 81 R.A.Cowley in *Structural Phase Transitions*, by A.D.Bruce and R.A.Cowley (Taylor and Francis, London, 1981), p.106.

deB 42 J.de Boer; Physica, 9,363(1942).

deR 81 B.DeRadet, K.Binder and K.H.Michel; J. Chem. Phys. 75,2977(1981).

Dun 77 P.V.Dunmore; Can. J. Phys. 55,554(1980).

Ehr 80 K.D.Ehrhardt, W.Press, J.Lefebvre and S.Haussuhl; Solid State Commun., 34,591(1980).

Ehr 83 K.D.Ehrhardt, W.Press and J.Lefebvre; J. Chem. Phys. 78,1476(1983).

Feh 76 W.R.Fehlner and S.H.Vosko; Can. J. Phys., 54,2159(1976).

Fis 79 M.E.Fisher in Proceedings of the 23rd Robert

A.Welch Foundation Conferences on Chemical Research, Modern Structural Methods (Houston, Nov.12-14,1979), p.75. I am grateful to Dr. M.E.Fisher for giving me this refernce.

Fle 81 P.A.Fleury, Science,**211**,125(1981).

Fum 64 F.G.Fumi and M.P.Tosi; J. Phys. Chem. Solids, **25**,31(1964).

Geh 75 G.A.Gehring and K.A.Gehring; Rep. Prog. Phys.,**38**,1(1975).

Gha 70 M.Ghafelebashi, D.P.Dandekar and A.L.Ruoff; J. Appl. Phys., **41**,652(1970).

Goo 71 D.A.Goodings and M.Henkelman; Can. J. Phys.,**49**,2898(1971).

Har 79 J.R.Hardy and A.M.Karo; *Lattice Dynamics and Statics of Alkali Halide Crystals*, (Plenum, N.Y.,1979).

Hau 73 S.Haussuhl; Solid State Commun., **13**,147(1973).

Hau 77 S.Haussuhl; J.Eckstein, K.Recker and F.Wallrafen; Acta Crystallog. A **33**,847(1977).

Hau 79 S.Haussuhl; Solid State Commun., **32**,181(1979)

Hir 79 F.L,Hirshfeld and K.Mirsky; Acta Crystallog. A, **35**,366(1979).

Hub 68 A.Huber in *Mathematical Methods in Solid State and Superfluid Theory*, edited by R.C.Clark and G.H.Derrick (Plenum,N.Y.,1968).

Koh 60 B.C.Kohin; J. Chem. Phys., **33**,882(1960)

Kon 79 Y.Kondo, D.Schoemaker and F.Luty; Phys. Rev. B, **19**,4210(1979)

Kle 81 M.L.Klein and I.R.McDonald; Chem. Phys. Letts., **78**,383(1981)

Kle 82 M.L.Klein, Y.Ozaki and I.R.McDonald; J. Phys. C, Solid State, **15**,4993(1982).

Kra 79 W.Krasser, B.Janik, K.D.Ehrhardt and S.Haussuhl; Solid State Commun., **30**,33(1979).

Lel 42 J.A.Lely; Dissertation, Utrecht(1942).

LeS 82 R.LeSar and R.G.Gordon; J. Chem. Phys., 77,3682(1982).

Loi 80a A.Loidl, K.Knorr, J.I.Kjems and S.Haussuhl; J. Phys. C, Solid State, 13,L349(1980).

Loi 80b A.Loidl, K.Knorr, J.Daubert, W.Dultz, and W.J.Fitzgerald; Z.Physik B, 38,153(1980).

Loi 83 A.Loidl, S.Haussuhl and J.K.Kjems; Z. Physik B,50,187(1983) .

Lut 81 F.Luty, paper presented at International Conference on Defects in Insulating Crystals, Riga, 1981 (private communication).

Lut 83 F.Luty and J. Ortiz-Lopez; Phys. Rev. Lett.,50,1289(1983).

Lyn 83 R.M.Lynden-Bell, I.R.McDonald and M.L.Klein; (preprint)

Mah 79 S.D.Mahanti and G.Kemeny; Phys. Rev. B, 20,2105,(1979).

Mah 82 S.D.Mahanti and D.Sahu; Phys. Rev. Lett., 48,936(1982).

Mic 77a K.H.Michel and J.Naudts; J.Chem. Phys., 67,547(1977).

Mic 77b K.H.Michel and J.Naudts; Phys. Rev. Lett., 39,212(1977).

Mic 78 K.H.Michel and J.Naudts; J. Chem. Phys., 68,216(1978).

Muh 81 C.Muhlhausen and R.G.Gordon; Phys. Rev. B, 23,900(1981).

Nor 58 M.H.Norwood and C.V.Briscoe; Phys. Rev.,112,45(1958).

Ove 51 W.C.Overton,Jr. and R.T.Swim; Phys. Rev., 84,758(1951)

Rai 79 J.C.Raich and A.Huller; J.Chem. Phys., 70,3669(1970).

Reh 77 W.Rehwald, J.R.Sandercock and M.Rossinelli; Phys. Stat. Sol.(a), 42,699(1977).

Rei 61 K.Reinitz; Phys. Rev., 123,1615(1961).

Row 75 J.M.Rowe, J.J.Rush, N.Vagelatos, D.L.Price, D.J.Hinks and S.Susman; J.Chem. Phys.,62,4551(1975).

Row 82 J.M.Rowe; Private communication (1982).

Sah 82 D.Sahu and S.D.Mahanti; Phys. Rev. B, 26,2981(1982).

Sah 83a D.Sahu and S.D.Mahanti; Solid State Commun.,47,203(1983).

Sah 83b D.Sahu and S.D.Mahanti; preprint,(1983).

Sat 77 S.K.Satija and C.H.Wang; J. Chem. Phys., 66,2221(1977).

Sch 79 P.C.Schmidt, A.Weiss and T.P.Das; Phys. Rev. B,19,5525(1979).

Sto 81 H.T.Stokes, T.A.Case and and D.C.Ailion; Phys. Rev. Lett., 47,268(1981).

Str 79 D.Strauch, U.Schroder and W.Bauernfeind; Solid State Commun., 30,559(1979).

Sug 68 M.Sugisaki, T.Matsuo, H.Suga and S.Seki; Bull. Chem. Soc. Japn., 41,1747(1968)

Ver 38 H.J.Verweel and J.M.Bijvoet; Z.Kristallogr. Kristallgeom. Kristallphys. Kristallchem.,100,201(1938).

Zub 60 D.N.Zubarev; Usp. Fiz. Nauk, 71,71(1960) [Sov. Phys- Usp. 3,320(1960)].